MEASURING TECHNIQUES FOR THE CALIBRATION OF STANDARD GAIN HORN ANTENNAS

Errol K. English

The Ohio State University

The Ohio State University

ElectroScience Laboratory

Department of Electrical Engineering
Columbus, Ohio 43212

Technical Report 711587-3

Contract N00014-76-A-0039-RZ01

March 1980

2750th Air Base Wing/PMR
Specialized Procurement Branch
Building 1, Area C
Wright-Patterson Air Force Base, Ohio 45433

NOTICES

When Government drawings, specifications, or other data are used for any purpose other than in connection with a definitely related Government procurement operation, the United States Government thereby incurs no responsibility nor any obligation whatsoever, and the fact that the Government may have formulated, furnished, or in any way supplied the said drawings, specifications, or other data, is not to be regarded by implication or otherwise as in any manner licensing the holder or any other person or corporation, or conveying any rights or permission to manufacture, use, or sell any patented invention that may in any way be related thereto.

SECURITY CLASSIFICATION OF THIS PAGE *(When Data Entered)*

REPORT DOCUMENTATION PAGE

READ INSTRUCTIONS BEFORE COMPLETING FORM

1. REPORT NUMBER	2. GOVT ACCESSION NO. ADA 084574
3. RECIPIENT'S CATALOG NUMBER	
4. TITLE *(and Subtitle)* Measuring Techniques for the Calibration of Standard Gain Horn Antennas	5. TYPE OF REPORT & PERIOD COVERED Technical Report
	6. PERFORMING ORG. REPORT NUMBER ESL 711587-3
7. AUTHOR(s) Errol K. English	8. CONTRACT OR GRANT NUMBER(s) N00014-76-A-0039-RZ01
9. PERFORMING ORGANIZATION NAME AND ADDRESS The Ohio State University ElectroScience Laboratory, Department of Electrical Engineering, Columbus, Ohio 43212	10. PROGRAM ELEMENT, PROJECT, TASK AREA & WORK UNIT NUMBERS Project F692SB8187-0001 & 0002
11. CONTROLLING OFFICE NAME AND ADDRESS 2750th Air Base Wing/PMR Specialized Procurement Branch Building 1, Area C, WPAFB, OH 45433	12. REPORT DATE March 1980
	13. NUMBER OF PAGES 80
14. MONITORING AGENCY NAME & ADDRESS*(if different from Controlling Office)*	15. SECURITY CLASS. *(of this report)* Unclassified
	15a. DECLASSIFICATION/DOWNGRADING SCHEDULE

16. DISTRIBUTION STATEMENT *(of this Report)*

APPROVED FOR PUBLIC RELEASE:
DISTRIBUTION IS UNLIMITED

17. DISTRIBUTION STATEMENT *(of the abstract entered in Block 20, if different from Report)*

18. SUPPLEMENTARY NOTES

The material presented in this report was also used as a thesis presented to The Ohio State University as partial fulfillment for the degree Master of Science.

19. KEY WORDS *(Continue on reverse side if necessary and identify by block number)*

Horn antennas
Antenna gain
Measurement instrumentation
Antenna patterns

20. ABSTRACT *(Continue on reverse side if necessary and identify by block number)*

The main objective of this study is to accurately determine the far-field gain of microwave horn antennas from measured, on-axis, near-field coupling. In order to determine the gain, it is important to first locate the amplitude center of each horn antenna. Two methods of determining far-field horn antenna gain are presented. Both involve determining the amplitude center location. The first method involves only simple calculations based on measured coupling and Friis' transmission formula. The second method is more complicated but results

DD FORM 1 JAN 73 1473 EDITION OF 1 NOV 65 IS OBSOLETE

SECURITY CLASSIFICATION OF THIS PAGE *(When Data Entered)*

20.

in more accurate gain calculations, especially for larger horns. This second method is based on measured coupling, Friis' transmission formula, and theoretical near-field corrections. Included is a chapter on accurate coupling measurement techniques as well as a chapter on principal plane radiation patterns of horn antennas.

ACKNOWLEDGMENT

The author would like to express his appreciation to Dr. Roger Rudduck for the supervision of the research. Dr. Roger Rudduck as well as Dr. W. D. Burnside have been very helpful in reviewing the manuscript. Also, many thanks are extended to Ross Caldecott for his many hours of assistance in developing the computer software associated with the automated antenna coupling measurements.

TABLE OF CONTENTS

CHAPTER I
INTRODUCTION

The main objective of this study is to accurately determine the far-field gain of microwave horn antennas. The focus will be on laboratory measurements and the interpretation of the measurements. But these measurements and interpretations will be compared to theory as well. This objective necessitates an investigation into the fundamental radiation properties of horn antennas. Some of the major investigations discussed here are:

1) on-axis antenna coupling,
2) antenna interaction,
3) the location of the antenna's amplitude center, and
4) principal-plane radiation patterns.

There are several methods of determining antenna gain from coupling measurements. These methods include:

1) comparison of the horn under test to a standard gain horn and, using Friis' transmission formula, to calculate gain;

$$\frac{P_r}{P_t} = G_t G_r \left(\frac{\lambda}{4\pi R}\right)^2 \qquad (1)$$

2) measurement of the on-axis antenna coupling as a continuous function of R and using Equation (1) to extract the gain as well as the location of the amplitude center;

3) a theoretical calculation of the location of the amplitude center and a modification of Equation (1) to account for errors due to the near-field measurement of on-axis coupling.

The first method mentioned above is probably the most widely used. Two horns, one transmitting and one receiving, are placed facing each other with coincident main-beam axes. One horn is a standard gain horn and the other is the horn in question. The antennas are separated by a fixed distance R. The antennas must not be placed too close together. Jakes [1] implies that $R_{min} = 2b^2/\lambda$, where b is the larger dimension of the antenna aperture, has been previously accepted as the minimum antenna separation for gain measurements. Measuring P_r and knowing P_t, R, and the gain of the standard

horn, Equation (1) may be solved for the gain of the antenna under test. As will be apparent later, the accuracy of gain calculated in this manner is questionable.

The second method is an extension and a considerable improvement of the first method. As before, the two antennas are placed facing each other with coincident main beam axes. The two horns are assumed to be identical and not necessarily standard gain horns. Instead of measuring P_r at a fixed separation distance, P_r is measured as a continuous function of antenna aperture separation. Horn antenna aperture separation will be denoted by Z_{AA} in the remainder of this paper. A continuous function of P_r/P_t versus Z_{AA} allows an investigation into the effect of antenna interaction which appears as a ripple superimposed on the P_r/P_t curve predicted by Equation (1). It also allows one to determine the amount of received multipath signal. Both interaction and multipath can lead to some error in the gain as calculated by the first method. But the greatest advantage in having a continuous coupling curve is in defining R in Equation (1) which has been very loosely defined as antenna separation. At this point we shall define R, as it appears in Equation (1), as the separation between the horns' amplitude centers, where Z_{AA} is the separation of the apertures of the two horns (see Figure 1). The ampli-

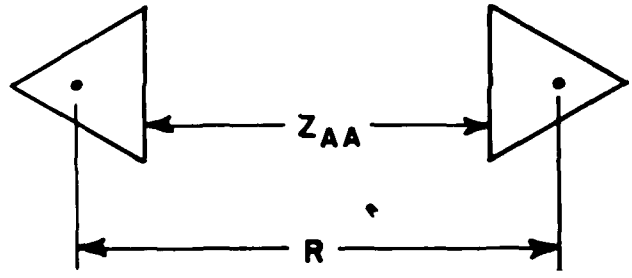

Figure 1. Relation between Z_{AA} and R.

tude center of a horn is the on-axis point inside the horn (between aperture and apex) from which the on-axis radiated power decays as $1/R^2$. The location of this amplitude center is a function of frequency and horn geometry and is found by experiment. A continuous coupling curve allows us to find the location of the horn's amplitude center. As Jakes [1] has pointed out, if $2b^2/\lambda$ is taken as Z_{AA} and is used in Equation (1) as R, gain errors on the order of 1 dB result. Therefore, if the amplitude center separation instead of aperture separation is used in Equation (1) the accuracy of gain calculations improves significantly. The exact mechanics of extracting gain and amplitude center information from the P_r/P_t versus Z_{AA} curve will be presented later.

The third method is similar to the second because horn coupling is measured as a continuous function of horn separation. But instead of extracting the amplitude center from the measured coupling, it is obtained form a theoretical calculation based on horn geometry and frequency. Also, it has been shown that the far-field gain of a horn can not be accurately determined from near-field coupling measurements without a near-field correction. Therefore, a theoretical calculation of near-field correction factors has been developed. A computer program has been developed which provides a simple and systematic method of calculating horn antenna gain from measured coupling [2]. This method represents the major effort in this study.

CHAPTER II
EQUIPMENT SET-UP

On-axis horn antenna coupling was measured in an anechoic chamber with respect to antenna aperture separation. All measurements were made at X-band. The transmitting equipment consisted of:

1.) 1 H.P. model 8690A X-band sweep generator;
2.) 1 H.P. model 8694A plug-in unit;
3.) 1 Autohet model 331 frequency counter;
4.) 1 tuning fork, square wave oscillator (1 KHz);
5.) 1 H.P. model 7779D 20 dB, coaxial directional coupler;
6.) 1 H.P. model 8734B PIN modulator;
7.) 1 FXR model X157A isolator;
8.) 1 H.P. model X752A, 3 dB, waveguide directional coupler;
9.) 2 H.P. model X382A rotary vane attenuators;
10.) 2 H.P. model X375A card-type variable attenuator;
11.) 1 H.P. model 8482A power sensor;
12.) 1 H.P. model 435A power meter;
13.) RG9 coaxial cable;
14.) RG52 waveguide; and
15.) 1 X-Band horn antenna.

Figure 2 shows how the equipment was connected. The equipment was arranged on a large table equipped with wheels for easy positioning (see Figure 3).

The receiving equipment consisted of:

1.) 1 X-band horn antenna;
2.) RG52 waveguide;
3.) 1 FXR model X157A isolator;
4.) 1 H.P. model X485B tunable detector mount;
5.) 1 Sylvania model 1N23B crystal detector;and
6.) 1 Scientific Atlanta model 1520 chart recorder.

The entire measuring procedure was controlled and monitored by a Digital Equipment Corporation PDP11/03 minicomputer. The receiving antenna, crystal detector, and associated waveguide were rigidly mounted on a computer-controlled movable platform (see Figure 5). The platform was capable of linear motion over a 16-inch range. Figure 4 shows a schematic block diagram of the receiving equipment and computer.

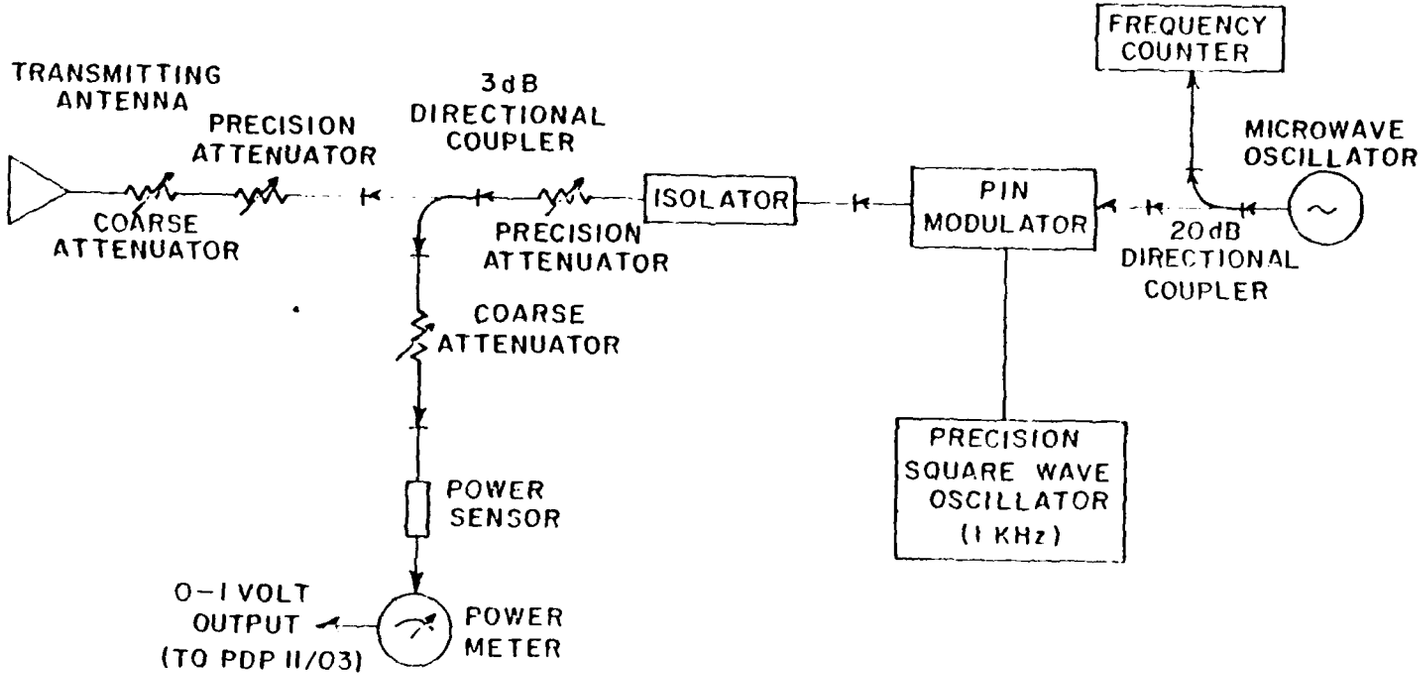

Figure 2. Transmitting equipment.

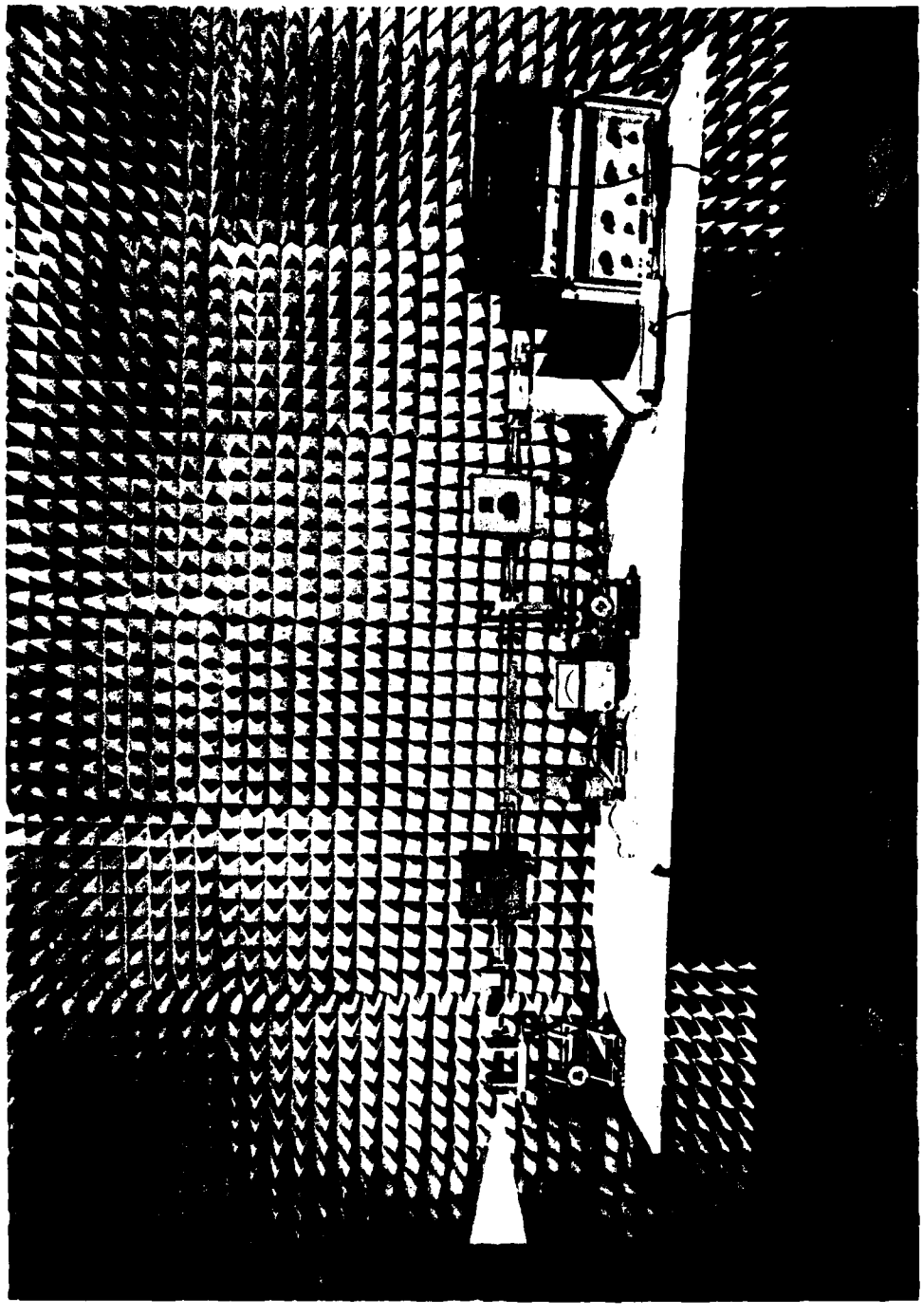

Figure 3. Transmitting Equipment.

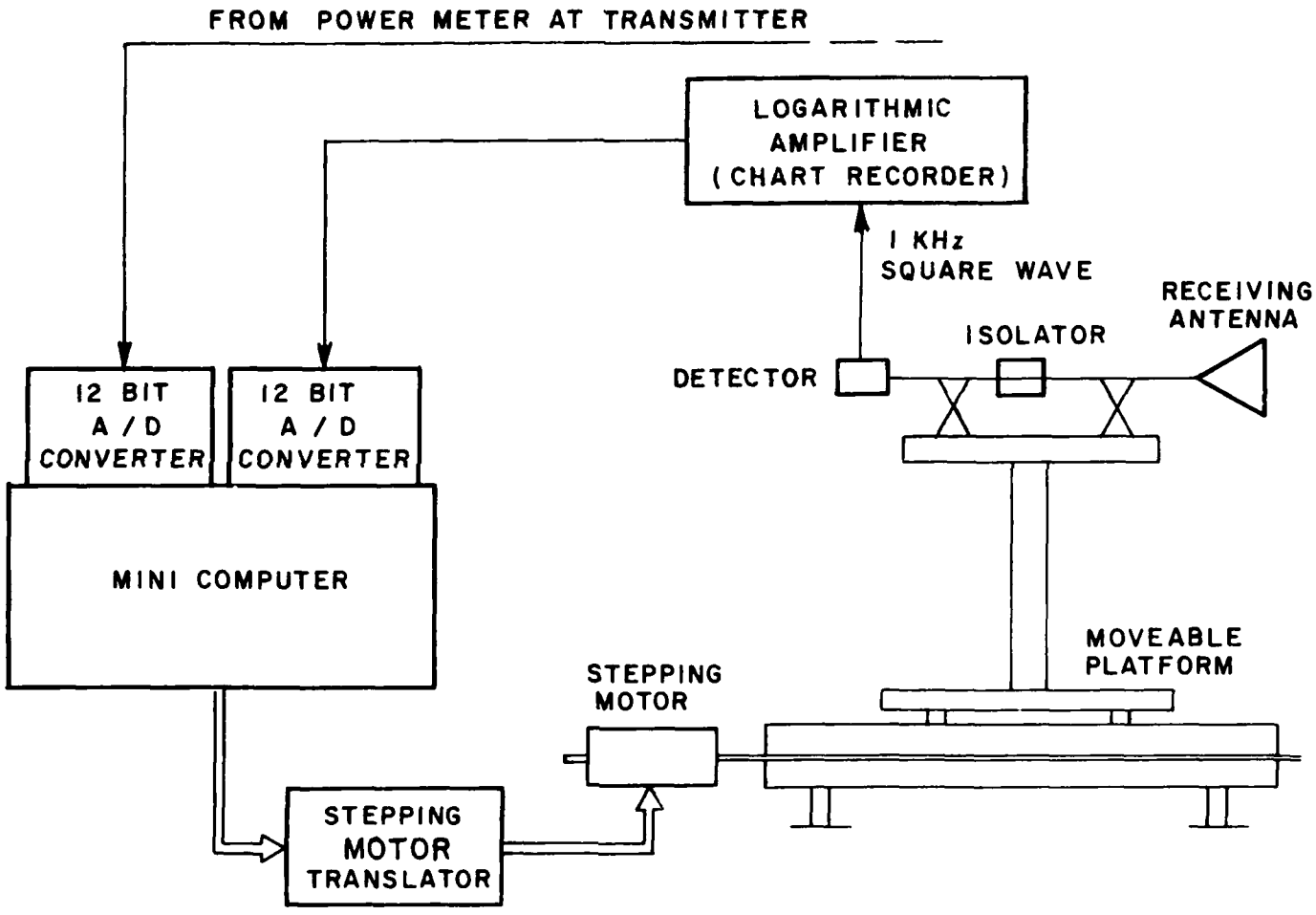

Figure 4. Receiving equipment.

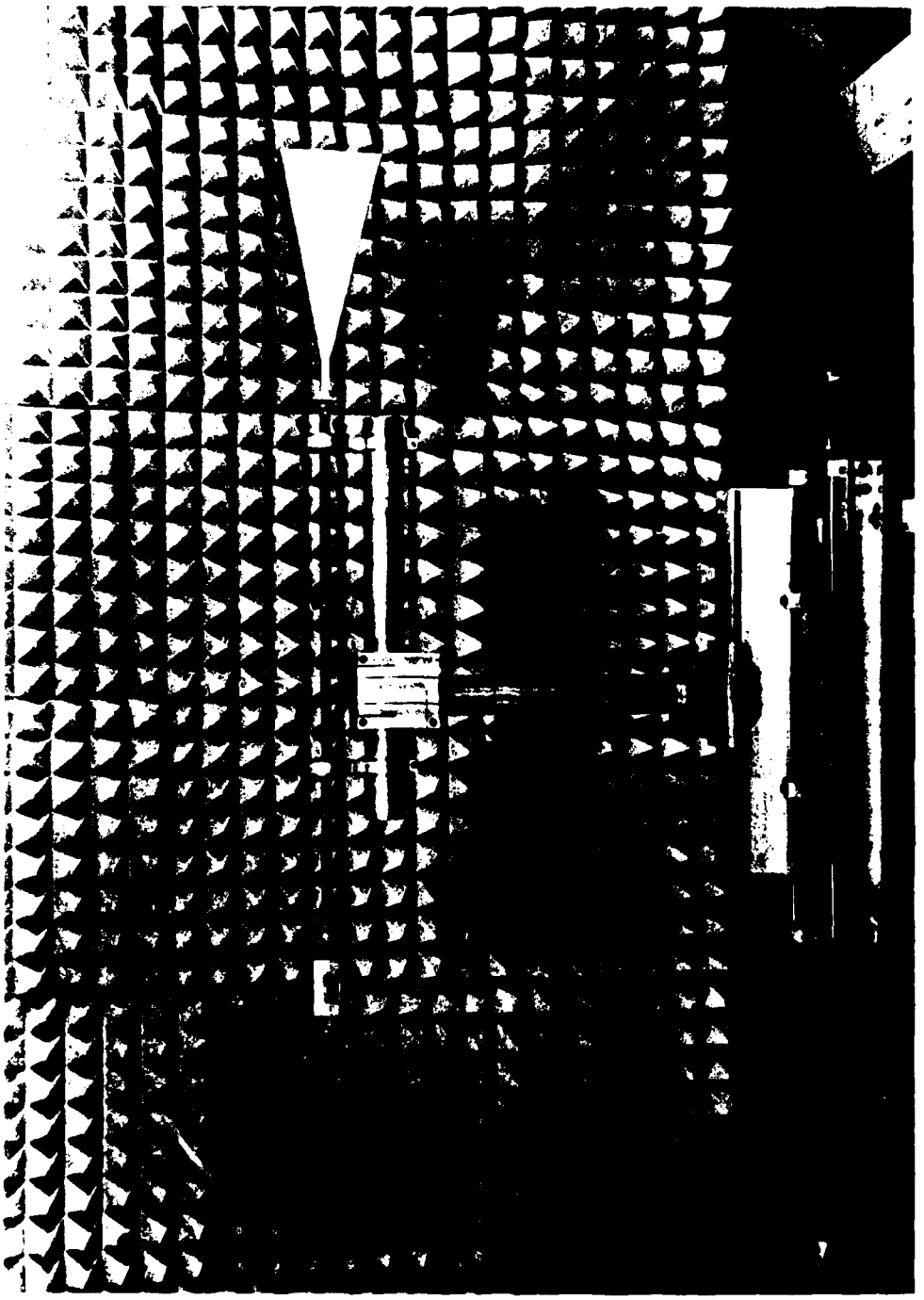

Figure 5. Receiving antenna and movable platform.

The detected signal, a 1 KHz square wave, was fed to the Scientific Atlanta 1520 chart recorder. The chart recorder was used as a logarithmic amplifier. Its output was an analog voltage proportional to received power in dB. This signal was fed to the computer where it was converted into digital form and recorded on a floppy disc. The typical measuring procedure was as follows:

A. System Calibration

The horn antennas were removed and the transmitting and receiving waveguides were bolted together. The transmitter gain was reduced by 20 dB (via one of the H.P. rotary vane attenuators at the transmitter), and the corresponding received signal was read by the computer 20 times with a 1/120 second time delay between readings. These 20 readings were averaged. This average was stored and established a -20 dB reference power level.

The transmitter gain was then restored to its original 0 dB setting. As before, the computer read and averaged 20 readings of the Scientific Atlanta chart recorder output. This average value was stored and established a 0 dB reference power level. Immediately following this the computer stored a 20-reading average of the HP435A power meter output. The power meter, attached to the transmitter through a directional coupler, monitored the transmitter power throughout the coupling measurement (see Figure 2).

The system calibration was then completed. The waveguide junction between transmitter and receiver was disconnected and the two horn antennas under test were then bolted to the waveguides.

B. Antenna Coupling Measurements

The mobile table with the transmitting equipment was positioned for an initial aperture separation. Care was taken to ensure that the two antennas were facing each other with coincident main beam axes. With the transmitter arrangement in position, the computer was instructed to record the received power (referenced to 0 dB transmitted power) as the receiving antenna was automatically moved away from the transmitter.

The computer first read the transmitter power via the H.P. 435A power meter (an average of 20 readings was stored as before). This value was compared to the original power meter reading obtained during calibration. The computer calculated the amount of transmitter power drift, ΔP in dB, since calibration. The computer then read the received power via the Scientific Atlanta chart recorder (an average of 20 readings). This value was corrected by adding ΔP (in dB) to

it. This value of corrected power was stored as the first point of received power versus aperture separation. The computer then instructed the stepping motor to move the receiving antenna away from the transmitting antenna (typically .07 inches). At this point there was a short time delay on the order of 1 second to allow for damping of mechanical vibrations.

The above procedure was repeated 201 times typically. This resulted in 201 data points of corrected received power (referenced to 0 dB transmitted power) versus aperture separation over a 14-inch range of aperture separation. Continuous monitoring of transmitter power and correction of received power minimized the effects of transmitter power drift.

CHAPTER III
MEASURED DATA: ANALYSIS AND RESULTS

A. Gain Calculations Based on Measured Coupling and Friis' Transmission Formula

Horn antenna coupling was measured for aperture separations of 100 to 500 centimeters. Scientific Atlanta 12-8.2, Narda 640, and Ladar Systems CX-20 horn antennas were used for most of the measurements. Coupling measurements at various frequencies and aperture separations were repeated numerous times to ensure data reliability. A typical coupling plot for two Scientific Atlanta 12-8.2 horns at 10 GHz is shown in Figure 6.

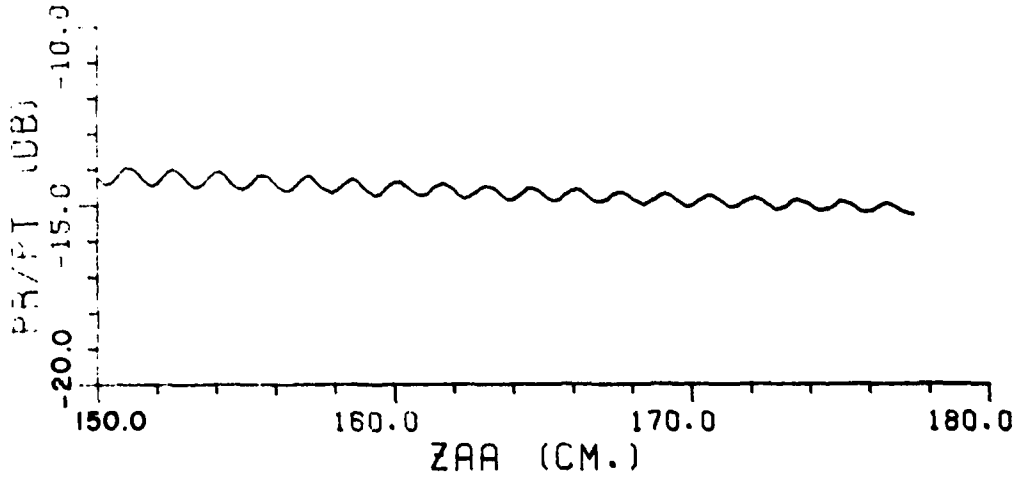

Figure 6. Typical coupling.

The object of the data analysis is to accurately compute the far-field gain of the antenna under test. The familiar formula,

$$\frac{P_r}{P_t} = G_r G_t \left(\frac{\lambda}{4\pi R}\right)^2 \qquad (2)$$

where P_r = received power

P_t = transmitted power

G_t = gain of transmitting horn

G_r = gain of receiving horn

λ = free-space wavelength

R = antenna separation

if used with caution, will give good results for horn gain measurements. The major problem is in defining R, the antenna separation. If the horns are very far apart, R may be taken as the aperture separation or the throat separation with negligible difference in the respective gain calculations. But, it is usually not practical to measure horn coupling at extremely large separations. Smaller separations will reduce room effects such as multipath. Smaller separations will also enable more accurate on-axis placement of the two horns.

To minimize error, R should be measured between the amplitude centers of the two horns (see Figure 7). The amplitude center is

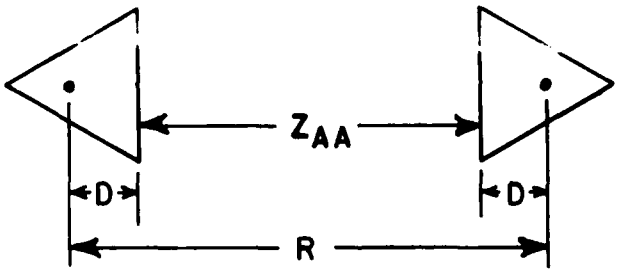

Figure 7. Relation between Z_{AA}, R and D.

the on-axis point inside the horn from which the on-axis radiation decays as $1/R^2$. This point has been theoretically determined in Reference [2] and has been found to be approximately half way between the E-plane and H-plane phase centers of the horn.

Another method of locating the amplitude center is to determine it from measurements as follows. This argument assumes identical transmitting and receiving horns. Referring to Figure 8, the horns are positioned for an initial aperture separation Z_{AA1}, and a corresponding received power P_{r1} is measured. Next, the aperture separation is increased to Z_{AA2}, and a corresponding received power P_{r2} is measured. From Figure 8, the following relations are obtained:

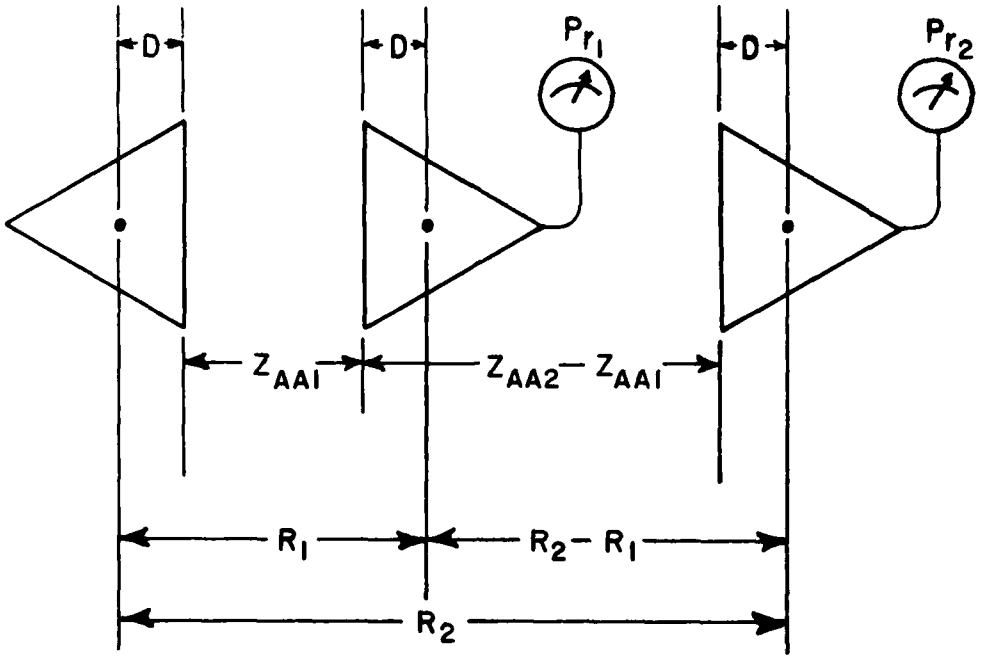

Figure 8. Horn arrangement for locating the amplitude center.

$$2D = R_1 - Z_{AA1} = R_2 - Z_{AA2} \tag{3}$$

$$Z_{AA2} - Z_{AA1} = R_2 - R_1 \tag{4}$$

Equation (2) is of the form

$$P_r = K \frac{1}{R^2} \tag{5}$$

where K is a constant. Therefore,

$$P_{r1} = K \frac{1}{R_1^2} \tag{6}$$

and

$$P_{r2} = K \frac{1}{R_2^2} \tag{7}$$

Dividing, we obtain

$$\frac{P_{r_1}}{P_{r_2}} = \left(\frac{R_2}{R_1}\right)^2 \tag{8}$$

$$10 \log\left(\frac{P_{r_1}}{P_{r_2}}\right) = 20 \log\left(\frac{R_2}{R_1}\right) \tag{9}$$

$$P_{r1}(dB) - P_{r2}(dB) = 20 \log\left(\frac{R_2}{R_1}\right) \tag{10}$$

or

$$10^{\left(\frac{P_{r1}(dB)-P_{r2}(dB)}{20}\right)} = \frac{R_2}{R_1} \tag{11}$$

therefore,

$$R_2 = R_1 \, 10^{\left(\frac{P_{r1}(dB)-P_{r2}(dB)}{20}\right)} \tag{12}$$

Substituting Equation (12) into Equation (4) we obtain

$$Z_{AA2}-Z_{AA1} = R_1\left(10^{\left(\frac{P_{r1}(dB)-P_{r2}(dB)}{20}\right)} - 1\right) \qquad (13)$$

Solving Equation (13) for R_1 and substituting into Equation (3) and solving for D, we obtain

$$D = \frac{Z_{AA2} - Z_{AA1}}{2\left[10^{\left(\frac{P_{r1}(dB)-P_{r2}(dB)}{20}\right)} - 1\right]} - \frac{Z_{AA1}}{2} \qquad (14)$$

D should be calculated for various combinations of Z_{AA1} and Z_{AA2}. Ideally, D should be independent of the choice of Z_{AA1} and Z_{AA2}; but this is not true. The difficulty arises because of horn interaction. Referring to Figure 6, it is obvious that the coupling is not simply a $1/R^2$ curve. Superimposed on this is a ripple due to interaction (standing wave) which decays with increasing aperture separation. If Z_{AA1} and Z_{AA2} are chosen with discretion, a fairly tight distribution of values for D may be obtained. Z_{AA1} and Z_{AA2} should be chosen such that P_{r1} and P_{r2} lie half way between the coupling maxima and minima (see Figure 9). Also, it should be noted that the calculation of D is very sensitive to errors in the measurement of Z_{AA} and P_R.

The following is an example of determining D as described above. Two identical horns, described in Figure 10, were measured at 10 GHz. Received power (referenced to 0 dB transmitted power) versus Z_{AA} is shown in Table 1. As described above, these points were chosen to minimize the effect of horn interaction.

Equation (14) was used for sixteen arbitrary combinations of Z_{AA1} (and P_{r1}) and Z_{AA2} (and P_{r2}) to calculate D (see Table 2). The average value of D is 2.31 wavelengths. A computer program was used to calculate D for every possible combination of Z_{AA1} and Z_{AA2}, resulting in an average D of 2.35 wavelengths. Figure 11 shows the distribution of the 16 values of D. D is measured from the aperture, and the location of the E-plane and H-plane apexes are also shown for perspective.

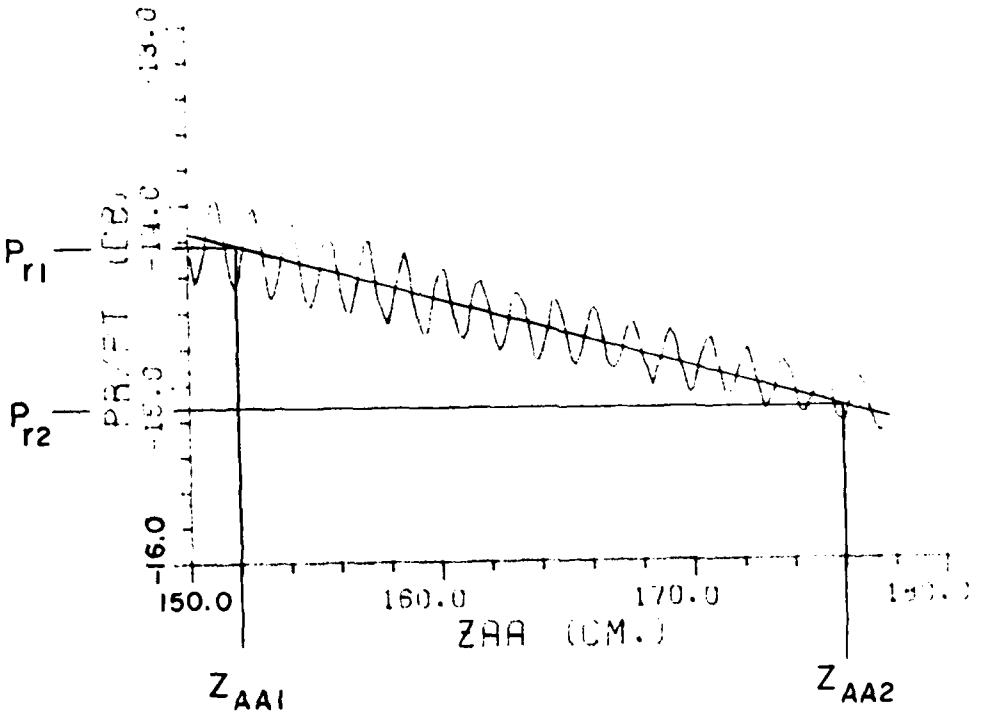

Figure 9. Selection of P_r for a given Z_{AA}.

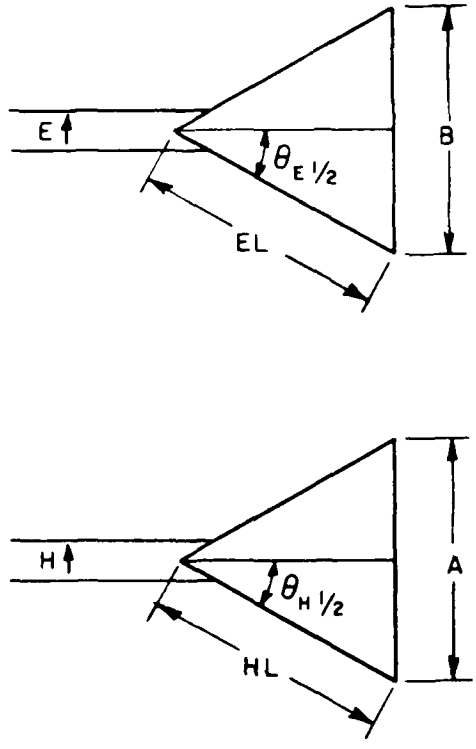

B = 7.65 cm

EL = 13.67 cm

$\theta_{E\,1/2}$ = 16.25°

A = 9.68 cm

HL = 15.06 cm

$\theta_{H\,1/2}$ = 18.75°

Figure 10. Horn geometry

Table 1
Measured Coupling at 10.0 GHz

Z_{AA} (cm)	(P_r/P_t) (dB)
31.2	- 8.96
39.22	-10.27
46.13	-11.30
55.12	-12.51
63.43	-13.56
75.38	-14.86
85.90	-15.79
99.45	-16.91
111.43	-16.91
130.18	-19.05
152.83	-20.15

Table 2
Calculation of Amplitude Center D at 10.0 GHz:
Average D=2.31λ (6.93 cm)

Z_{AA1} (cm)	Z_{AA2} (cm)	$(P_r/P_t)_1$ (dB)	$(P_r/P_t)_2$ (dB)	D (λ's)
31.2	46.13	- 8.96	-11.30	2.84
46.13	99.45	-11.30	-16.91	2.10
55.12	111.43	-12.51	-17.81	1.97
39.22	152.83	-10.27	-20.15	2.40
75.38	130.18	-14.86	-19.05	2.17
63.42	99.45	-13.56	-16.91	2.19
85.90	152.83	-15.79	-20.15	2.79
31.20	75.38	- 8.96	-14.86	2.37
39.22	99.45	-10.27	-16.91	2.21
85.90	130.18	-15.79	-19.05	1.88
31.20	111.43	- 8.96	-17.81	2.35
39.22	111.43	-10.27	-17.81	2.17
31.20	152.83	- 8.96	-20.15	2.51
46.13	130.18	-11.30	-19.05	2.03
55.12	152.83	-12.51	-20.15	2.36
63.42	152.83	-13.56	-20.15	2.55

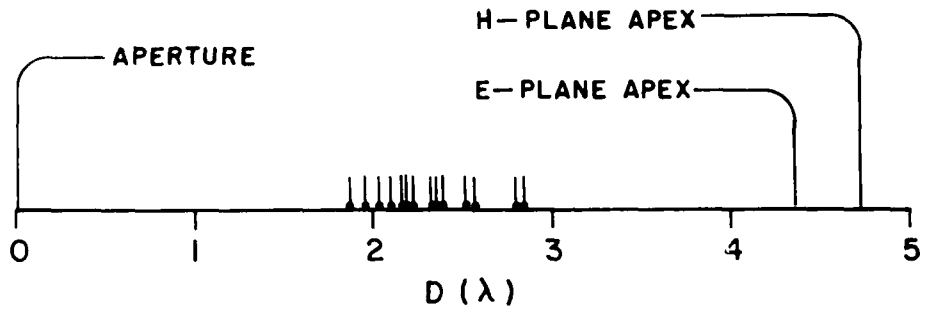

Figure 11. Amplitude center distribution.

With this reasonable approximation of D (D average), a more accurate value of horn gain may be computed. Substituting $R = Z_{AA}+2D$ into Equation (2) we obtain

$$\frac{P_r}{P_t} = G_r G_t \left(\frac{\lambda}{4\pi(Z_{AA}+2D)} \right)^2 \qquad (15)$$

Figure 12 shows P_r/P_t versus Z_{AA} (curve A) and P_r/P_t versus R (curve B) just as Jakes has shown. It is apparent that curve B has a constant slope of -6 dB per octave (as predicted by Equations (2)). Also, note that as Z_{AA} becomes very large, curve A asymptotically approaches curve B.

Table 3 compares gain calculations using a.) $R = Z_{AA}$ in Equation (2) and b.) $R = Z_{AA} + 2D$ in equation (2).

Table 3
Far-Field Gain Calculation (G_{FF})

(P_r/P_r) (dB)	Z_{AA} (cm)	R (cm)	$G_{FF}(R=Z_{AA})$ (dB)	$G_{FF}(R=Z_{AA}+2D)$ (dB)
- 8.96	31.2	45.06	16.68	18.28
-10.27	39.22	53.08	17.02	18.34
-11.30	46.13	59.99	17.21	18.35
-12.51	55.12	68.98	17.38	18.35
-13.56	63.43	77.29	17.46	18.32
-14.86	75.38	89.24	17.56	18.30
-15.79	85.90	99.76	17.67	18.32
-16.91	99.45	113.31	17.74	18.31
-17.81	111.43	125.29	17.79	18.30
-19.05	130.18	144.04	17.84	18.18
-20.15	152.83	166.66	17.99	18.36

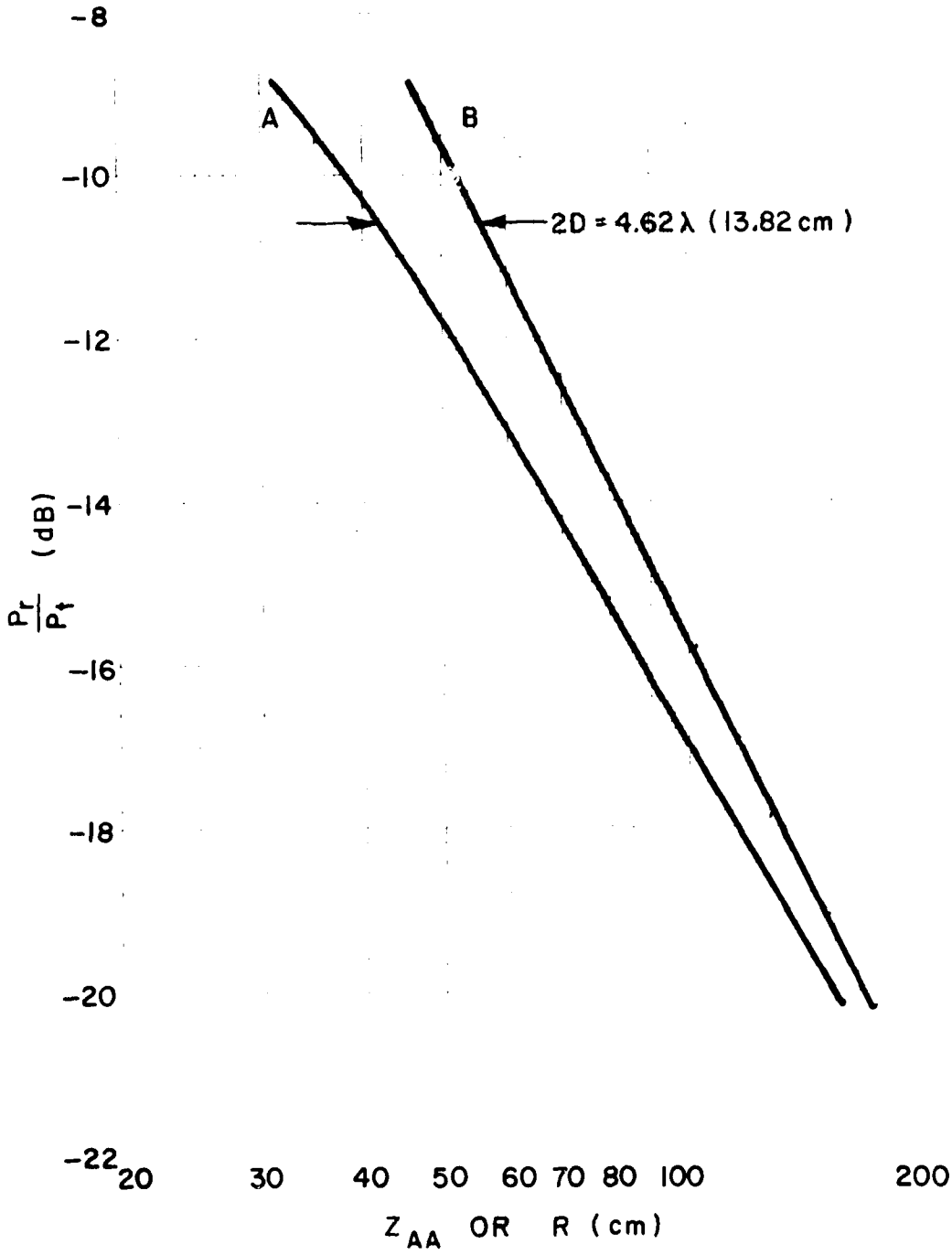

Figure 12. Horn coupling.
(a) P_r/P_t versus Z_{AA}
(b) P_r/P_t versus R

Note that even at $Z_{AA} = \frac{2b^2}{\lambda} \cong 63$ cm (where b is the larger dimension of the horn aperture) the calculated gain using aperture separation in Equation (1) is in error by approximately .85 dB.

Therefore, it is essential that the separation between amplitude centers be used in Equation (2) if accurate gain calculations are to be made from relatively close-range coupling measurements.

The data used in the above example were not measured by the previously described computer-controlled equipment. They were measured manually, early in the course of the research, before the automated version of the measurement equipment had been developed.

Presented in the same format as the above example, the following three sets of figures and tables are the results of three similar experiments using:

1.) two Scientific Atlanta 12-8.2 horn antennas
2.) two Narda 640 horn antennas
3.) two Ladar Systems CX-20 horn antennas

Figures 13, 16 and 19 show photographs and the dimensions for the above horns. Tables 4, 7 and 10 show coupling versus aperture separation Z_{AA} for the above horns. Tables 5, 8 and 11 present the calculation of the amplitude center location D for the above horns. Figures 14, 17 and 20 show distributions of D values for each horn listed above. Tables 6, 9 and 12 show gain versus Z_{AA} for each horn. Finally, Figures 15, 18 and 21 show coupling versus Z_{AA} and coupling versus R for each horn tested.

1. Scientific Atlanta 12-8.2

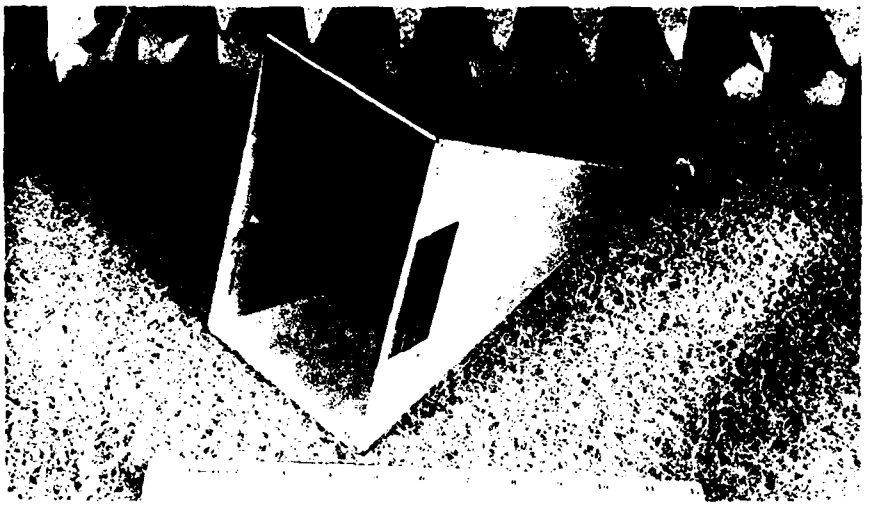

(a)

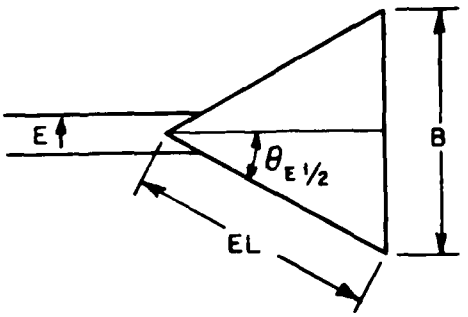

B = 14.402 cm

EL = 32.004 cm

$\theta_{E\,1/2}$ = 13.0°

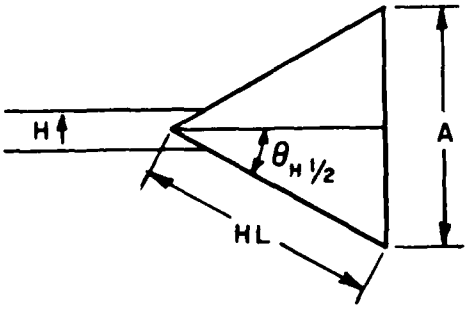

A = 19.431 cm

HL = 34.29 cm

$\theta_{H\,1/2}$ = 16.46°

(b)

Figure 13. Scientific Atlanta 12-8.2 horn geometry.
a) Photograph b) Dimensions

Table 4
Measured Coupling for Scientific Atlanta
Model 12-8.0 at 10.0 GHz

Z_{AA} (cm)	(P_r/P_t) (dB)
149.86	-14.13
200.00	-15.97
220.00	-16.60
300.00	-18.75
500.00	-22.65

Table 5
Calculation of Amplitude Center Location D for
Scientific Atlanta Model 12-8.2 at 10.0 GHz:
Average D=10.29λ (30.86 cm)

Z_{AA1} (cm)	Z_{AA2} (cm)	$(P_r/P_t)_1$ (dB)	$(P_r/P_t)_2$ (dB)	D (λ)
149.86	200.0	-14.13	-15.97	10.51
149.86	220.0	-14.13	-16.60	10.61
149.86	300.0	-14.13	-18.75	10.69
149.86	500.0	-14.13	-22.65	10.05
200.00	220.0	-15.97	-16.60	10.98
200.00	300.0	-15.97	-18.75	10.85
200.00	500.0	-15.97	-22.65	9.85
220.00	300.0	-16.60	-18.75	10.81
220.00	500.0	-16.60	-22.65	9.69
300.00	500.0	-18.75	-22.65	8.81

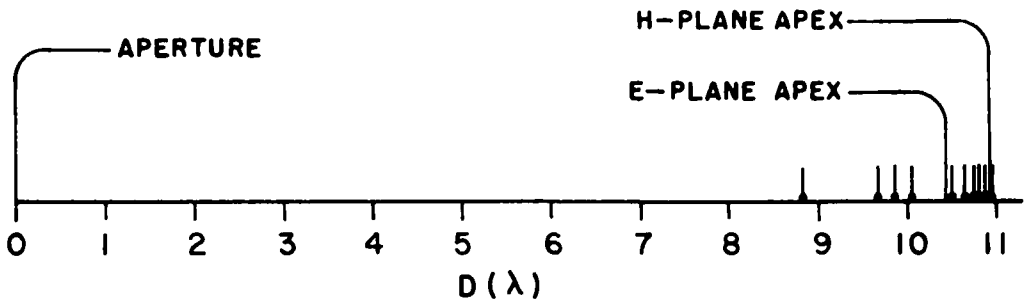

Figure 14. Amplitude center distribution.

Table 6
Far-Field Gain Calculation (G_{FF})

(P_r/P_t) (dB)	Z_{AA} (cm)	R (cm)	$G_{FF}(R=Z_{AA})$ (dB)	$G_{FF}(R=Z_{AA}+2D)$ (dB)
-14.13	149.86	211.57	20.91	22.41
-15.97	200.0	261.71	21.25	22.41
-16.60	220.0	281.71	21.35	22.42
-18.75	300.0	361.71	21.62	22.43
-22.65	500.0	561.71	21.89	22.39

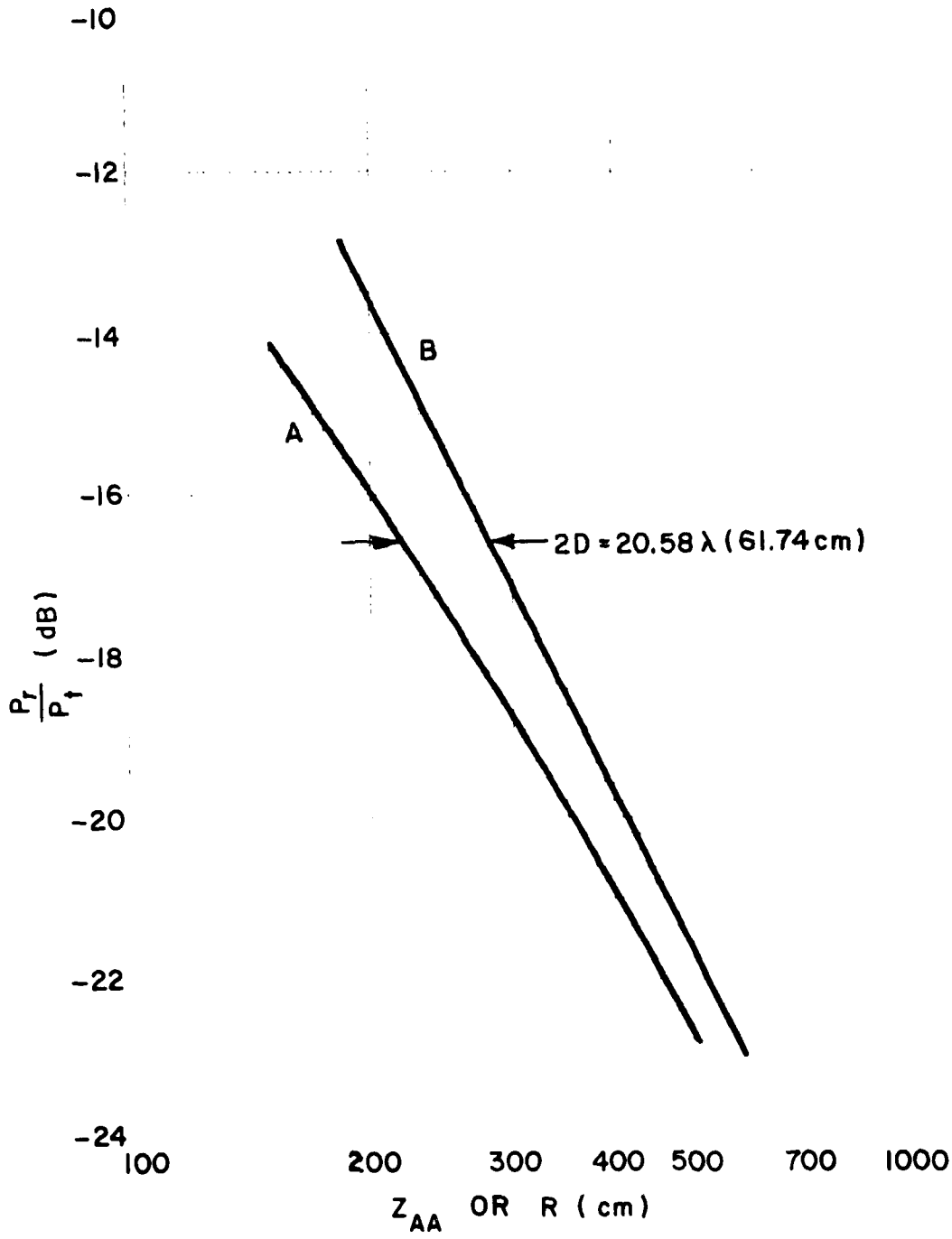

Figure 15. Scientific Atlanta 12-8.2 coupling.
(a) P_r/P_t versus Z_{AA}
(b) P_r/P_t versus R

2. Narda 640

(a)

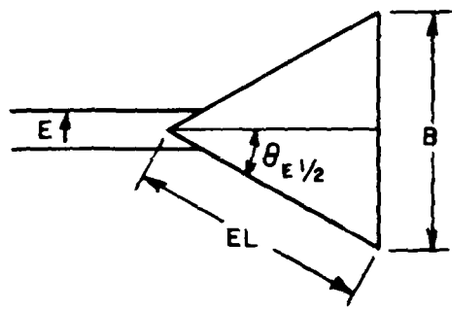

B = 5.954 cm

EL = 12.751 cm

$\theta_{E\,1/2}$ = 13.5°

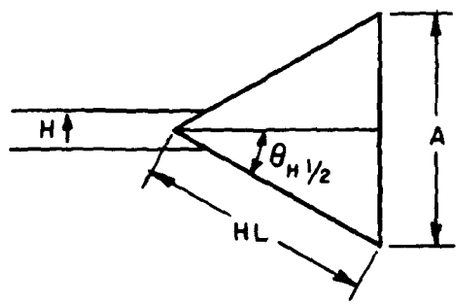

A = 7.859 cm

HL = 14.254 cm

$\theta_{H\,1/2}$ = 16.0°

(b)

Figure 16. Narda 640 horn geometry.
a) Photograph b) Dimensions

Table 7
Measured Coupling for Narda 640 at 10.0 GHz

Z_{AA} (cm)	(P_r/P_t) (dB)
150	-23.4
160	-24.0
200	-25.9
220	-26.8
300	-29.35

Table 8
Calculation of Amplitude Center Location D for Narda 640 at 10.0 GHz; Average D=-.05λ (-.15 cm)

Z_{AA1} (cm)	Z_{AA2} (cm)	(P_r/P_t) (dB)	(P_r/P_t) (dB)	D (λ)
150	160	-23.4	-24.0	- .17
150	200	-23.4	-25.9	0.0
150	220	-23.4	-26.8	- .65
150	300	-23.4	-29.35	.41
160	200	-24.0	-25.9	.60
160	220	-24.0	-26.8	- .38
160	300	-24.0	-29.35	.74
200	220	-25.9	-26.8	-2.8
200	300	-25.9	-29.35	.84
220	300	-26.8	-29.35	2.41

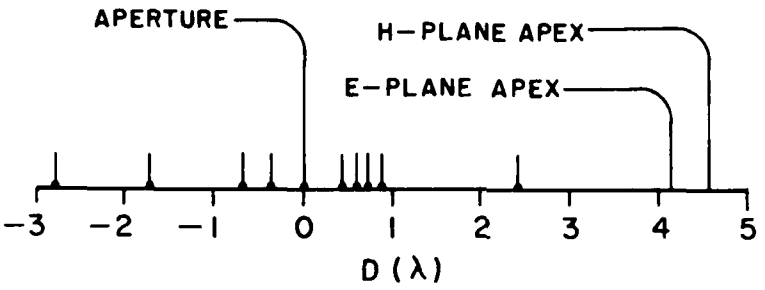

Figure 17. Amplitude center distribution

Table 9
Far-Field Gain Calculation (G_{FF})
Note: $Z_{AA} \leq R$

(P_r/P_t) (dB)	Z_{AA} (cm)	$G_{FF}(R=Z_{AA})$ (dB)
-23.4	150	16.28
-24.0	160	16.26
-25.9	200	16.28
-26.8	220	16.25
-29.35	300	16.32

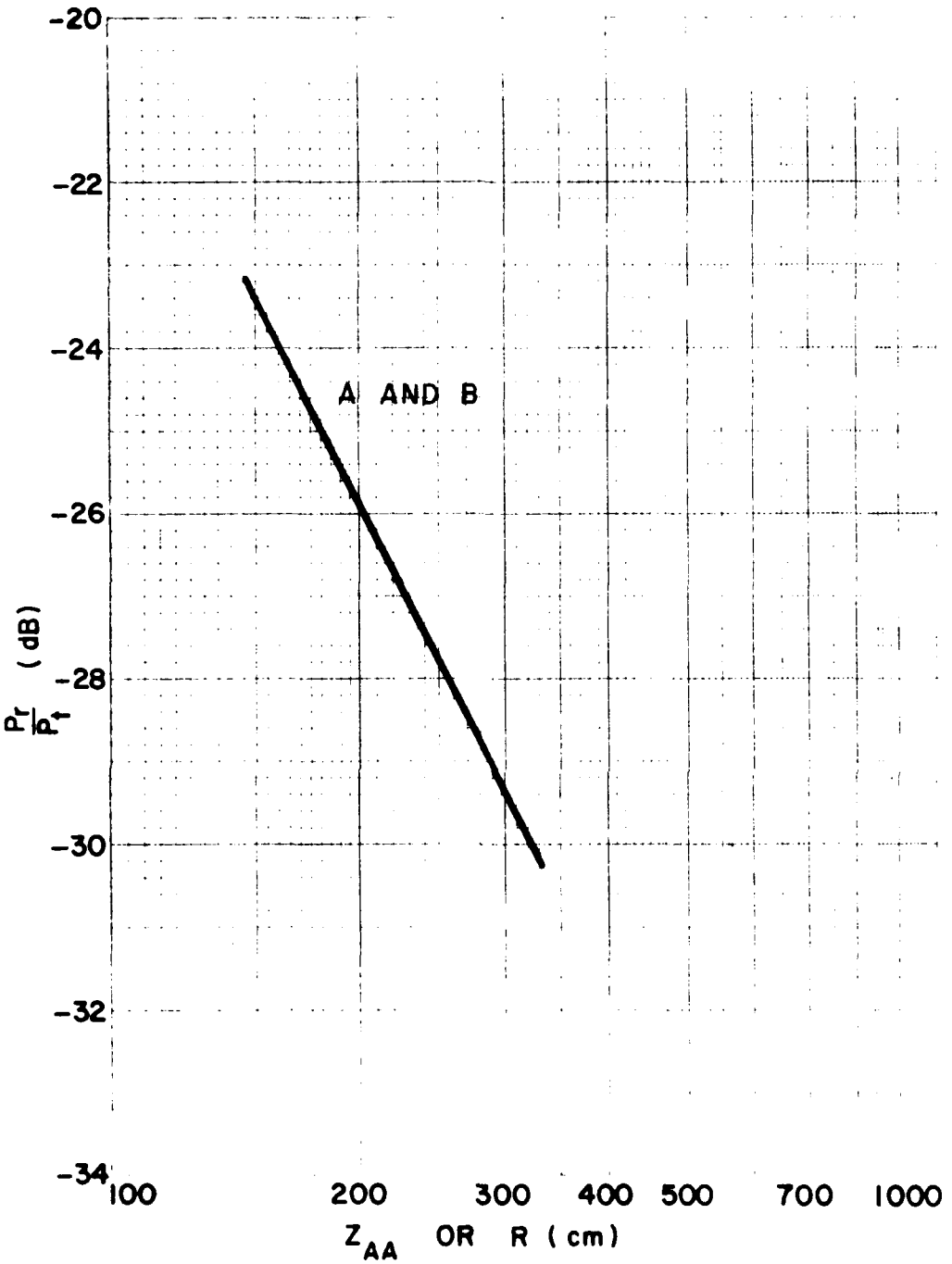

Figure 18. Narda 640 coupling.
a) P_r/P_t versus Z_{AA}
b) P_r/P_t versus R

3. Ladar Systems CX-20

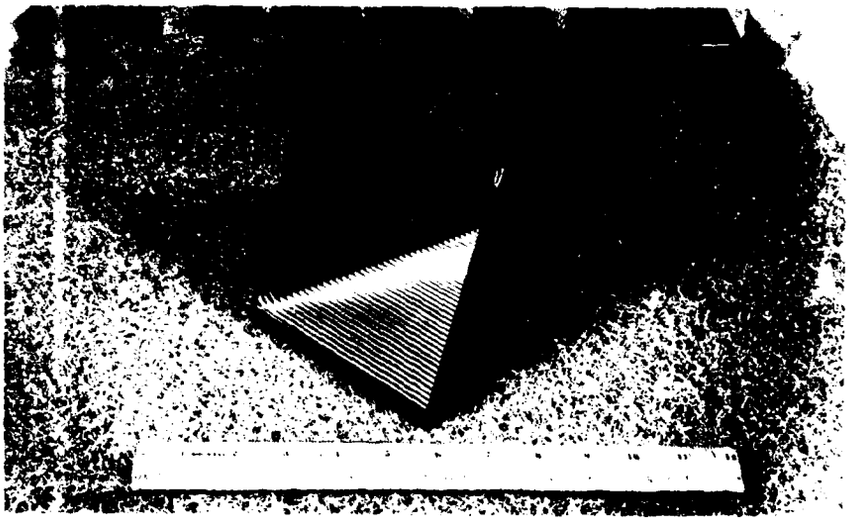

(a)

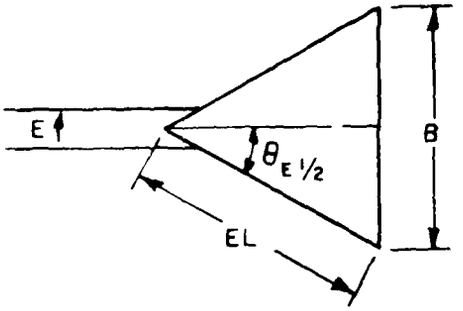

B = 12.65 cm

EL = 22.6 cm

$\theta_{E\,1/2}$ = 16.25°

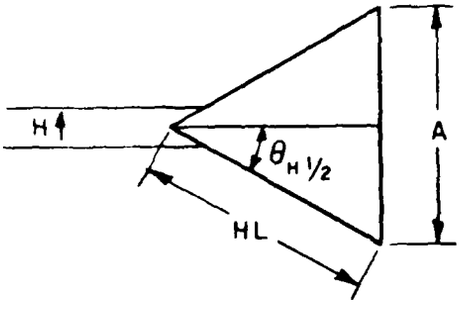

A = 12.65 cm

HL = 24.84 cm

$\theta_{H\,1/2}$ = 14.75°

(b)

Figure 19. Ladar Systems CX-20 horn geometry.
a) Photograph b) Dimensions

Table 10
Measured Coupling for Ladar Systems
CX-20 at 10.0 GHz

Z_{AA} (cm)	(P_r/P_t) (dB)
300	-21.28
330	-22.09
490	-25.43
520	-25.98

Table 11
Calculation of Amplitude Center Location D for
Ladar Systems CX-20 at 10.0 GHz
Average D=1.37λ (4.11 cm)

Z_{AA1} (cm)	Z_{AA2} (cm)	(P_r/P_t) (dB)	(P_r/P_t) (dB)	D (λ)
300	330	-21.28	-22.09	1.16
300	490	-21.28	-25.43	1.70
300	520	-21.28	-25.98	1.07
330	490	-22.09	-25.43	1.87
330	520	-22.09	-25.98	1.05
490	520	-25.43	-25.98	-5.18

Note: last point (D=-5.18λ) not included in average

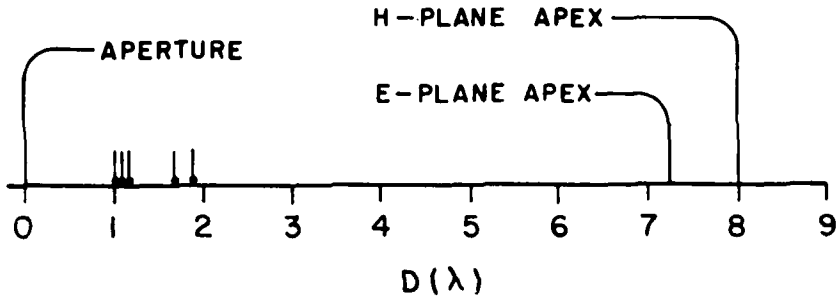

Figure 20. Amplitude center distribution.

Table 12
Far-Field Gain Calculation (G_{FF})

(P_r/P_t) (dB)	Z_{AA} (cm)	R (cm)	$G_{FF}(R=Z_{AA})$ (dB)	$G_{FF}(R=Z_{AA}+2D)$ (dB)
-21.28	300	308.22	20.35	20.47
-22.09	330	338.22	20.36	20.47
-25.43	490	498.22	20.41	20.48
-25.98	520	528.22	20.39	20.46

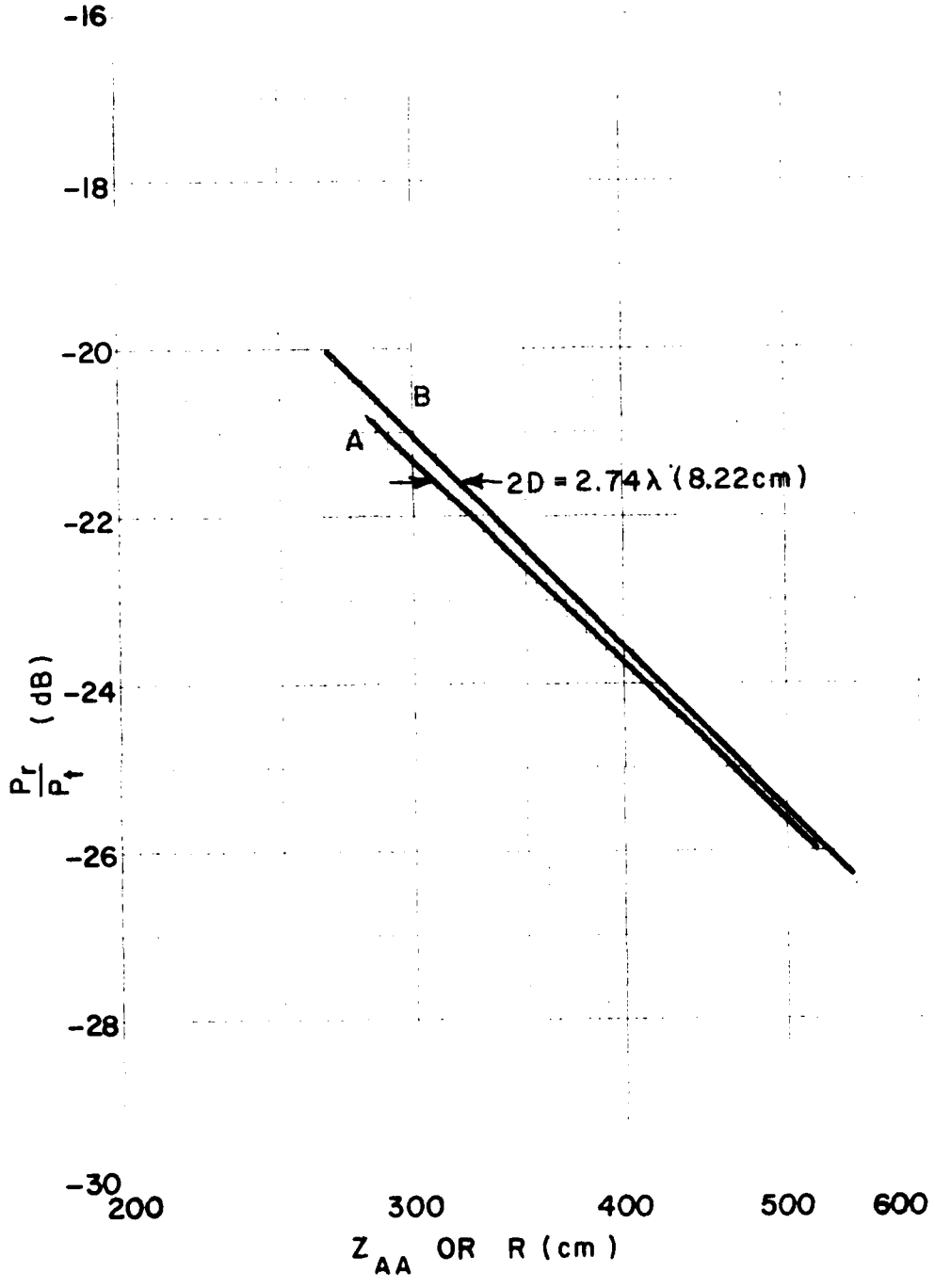

Figure 21. Ladar Systems CX-20 coupling.
a) P_r/P_t versus Z_{AA}
b) P_r/P_t versus R

B. Gain Calculations Based on Measured Coupling, Friis' Transmission Formula, and Theoretical Corrections

It is desirable to have a simple and systematic method of determining the far-field gain from the measured coupling. The basic formula, assuming identical horns, is:

$$\frac{P_r}{P_t} = G^2(R)\left(\frac{\lambda}{4\pi R}\right)^2 \quad . \tag{16}$$

This formula assumes that each horn radiates a uniform spherical wave. If the two horns are separated by a large distance, the transmitted wave at the receiving horn is almost spherical and uniform over the extent of the receiving horn aperture. But, at normal coupling measurement separations, Equation (16) should be modified. This equation is:

$$\frac{P_r}{P_t} = G^2(R)\left(\frac{\lambda}{4\pi R}\right)^2 \frac{1}{\sqrt{1 + T_E^2}} \frac{1}{\sqrt{1 + T_H^2}} \tag{16a}$$

where G(R) is the near-field gain. The factors involving T_E and T_H, which account for the antennas' patterns, are derived in [2]. Also, it has been determined that the gain is not a constant, but is a function of amplitude-center separation R [2]. We define a gain ratio:

$$R_g = \frac{G(R)}{G(\infty)} = \frac{\text{near-field gain}}{\text{far-field gain}} \quad . \tag{17}$$

This ratio may be less than or greater than unity depending on frequency, horn geometry, and antenna separation R. The gain ratio quickly approaches unity as R increases. Solving Equation (17) for G(R) and substituting into Equation (16a), we obtain

$$\frac{P_r}{P_t} = (R_g G(\infty))^2 \left(\frac{\lambda}{4\pi R}\right)^2 \frac{1}{\sqrt{(1+T_E^2)(1+T_H^2)}} \tag{18}$$

where R_g is a function of amplitude-center separation R.

Rearranging Equation (18) we obtain

$$\left(\frac{P_r}{P_t}\right) \frac{\sqrt{(1+T_E^2)(1+T_H^2)}}{R_g^2} = G^2(\infty) \left(\frac{\lambda}{4\pi R}\right)^2 \qquad (19)$$

where the right-hand side has the same form as Equation (2). Therefore, we define the left side of Equation (19) as modified coupling:

$$\left(\frac{P_r}{P_t}\right)^{mod.} = \left(\frac{P_r}{P_t}\right) \frac{\sqrt{(1+T_E^2)(1+T_H^2)}}{R_g^2} \qquad (20)$$

If we repeat the experiment in Chapter III, Section A1 (calculation of the location of the amplitude center of the Scientific Atlanta 12-8.2 horn), using modified coupling instead of actual coupling, calculated values of D agree very well with the theoretical value of D (6.58λ) obtained in [2]. A computer program has been written that calculates the factor by which the coupling is modified in Equation (20). Presented in the same format as the examples in Section A of this chapter, the following tables are the gain and amplitude center results of the Scientific Atlanta 12-8.2 horn at 10 GHz using modified coupling instead of actual coupling. Table 13 shows the modified coupling versus Z_{AA}. Table 14 shows the calculation of D. Figure 22 shows the distribution of D values and the improved agreement with the theoretical value. Table 15 shows the gain calculations. Finally, Figure 23 shows modified coupling versus Z_{AA} and modified coupling versus R.

Table 13
Modified Coupling for Scientific Atlanta Model 12-8.2 at 10.0 GHz

Z_{AA} (cm)	P_r/P_t (dB)	$\frac{\sqrt{(1+T_E^2)(1+T_H^2)}}{R_g^2}$ (dB)	$(P_r/P_t)^{mod}$ (dB)
150.0	-14.13	.584	-13.55
200.0	-15.97	.344	-15.63
220.0	-16.60	.284	-16.31
300.0	-18.75	.152	-18.60
500.0	-22.65	.044	-22.61

Table 14
Calculation of the Amplitude Center Location D Using Modified Coupling for Scientific Atlanta Model 12-8.2 at 10.0 GHz: Average D=6.93λ (20.79 cm), Theoretical D=6.58λ (19.74 cm)

Z_{AA1} (cm)	Z_{AA2} (cm)	$(P_r/P_t)_1^{mod}$ (dB)	$(P_r/P_t)_2^{mod}$ (dB)	D (λ)
150	200	-13.55	-15.63	5.8
150	220	-13.55	-16.31	6.19
150	300	-13.55	-18.60	6.70
150	500	-13.55	-22.61	6.74
200	220	-15.63	-16.31	7.60
200	300	-15.63	-18.60	7.55
200	500	-15.63	-22.61	7.20
220	300	-16.31	-18.60	7.53
220	500	-16.31	-22.61	7.14
300	500	-18.60	-22.61	6.81

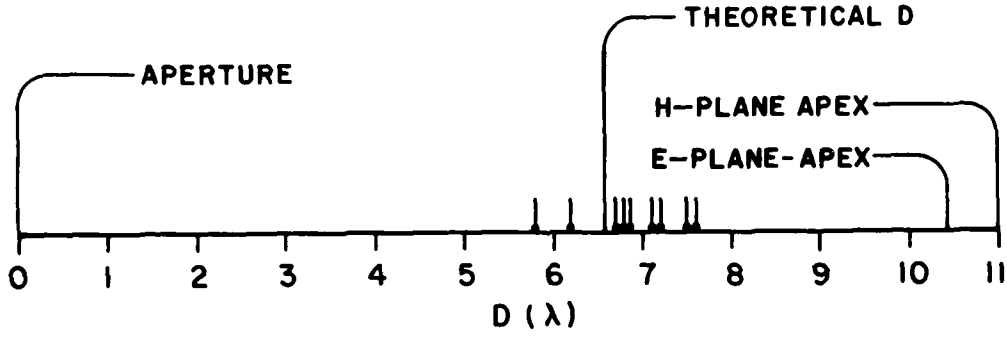

Figure 22. Amplitude center distribution.

Table 15
Far-Field Gain Calculation (G_{FF})

$(P_r/P_t)^{mod}$ (dB)	Z_{AA} (cm)	R (cm)	$G_{FF}(R=Z_{AA})$ (dB)	$G_{FF}(R=Z_{AA}+2D)$ (dB)
-13.55	150	191.56	21.21	22.27
-15.63	200	241.56	21.42	22.24
-16.31	220	261.56	21.49	22.24
-18.60	300	341.56	21.69	22.26
-22.61	500	541.56	21.91	22.25

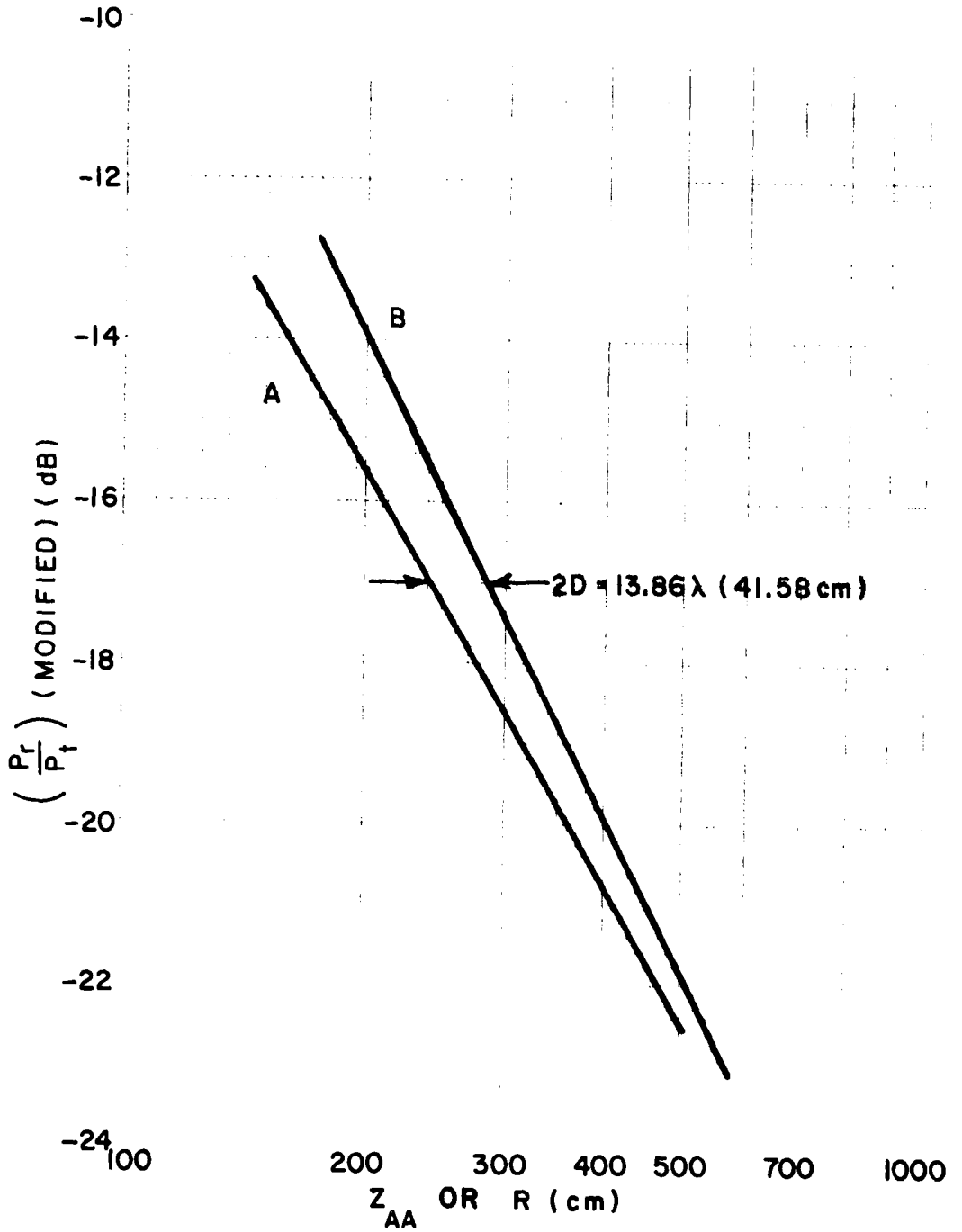

Figure 23. Scientific Atlanta 12-8.2 modified coupling
a) $(P_r/P_t)^{mod}$ versus Z_{AA}
b) $(P_r/P_t)^{mod}$ versus R

The gain and amplitude center location just presented agree with other methods of calculation better than that presented in Section A1 of this chapter. However, modification of the coupling for the Narda 640 and the Ladar Systems CX-20 do not significantly change the results. This is because the coupling modification factor in Equation (20) is close to unity in the range of aperture separations used for these horns. The Scientific Atlanta 12-8.2 has a rather large aperture which requires a larger aperture separation to approach far-field conditions. Table 16 is a comparison of D values using the previously described methods.

Table 16
Summary of Amplitude Center Location Calculation (f=10 GHz)

Horn	D(λ) (1)	(2)	(3)
Scientific Atlanta 12-8.2	6.58	10.29	6.93
Narda 640	.44	- .15	-
Ladar Systems CX-20	2.07	1.37	-

(1) theoretical, from [2].
(2) calculated from measured coupling (P_r/P_t) as in Chapter III Section A.
(3) calculated from modified measured coupling $(P_r/P_t)^{mod}$ instead of actual measured coupling (P_r/P_t).

Note that column 2 in Table 16 agrees fairly well with theoretical values (excluding the Scientific Atlanta). Although D for the Narda is negative (which can never be true for any horn), it differs by less than a wavelength from the theoretical value. Also, note the improved agreement of columns 1 and 3 for the Scientific Atlanta horn due to coupling modification.

Returning to the original criterion of having a simple and systematic method of determining far-field gain from near-field measured coupling, we solve Equation (18) for $G(\infty)$ and obtain:

$$G(\infty) = \frac{4\pi R}{\lambda R_g}\sqrt{\frac{P_r}{P_t}}\left[(1+T_E^2)(1+T_H^2)\right]^{1/4} \qquad (21)$$

and in dB:

$$G_{dB}(\infty) = 10\ \log\left[\frac{4\pi R}{\lambda R_g}\left((1+T_E^2)(1+T_H^2)\right)^{1/4}\right] + 1/2\left(\frac{P_r}{P_t}\right)_{dB} \qquad (22)$$

We define

$$RGC_{(dB)} = 10\ \log\left[\frac{4\pi R}{\lambda R_g}\left((1+T_E^2)(1+T_H^2)\right)^{1/4}\right] \quad . \qquad (23)$$

A computer program has been written which calculates D, T_E, T_H, R_g and subsequently R and RGC as a function of Z_{AA} for a horn of given dimensions at a given frequency [2]. Therefore, assuming we have a list of RGC and P_r/P_t values as a function of Z_{AA}, we have a simple formula for calculating the far-field gain of horn antennas.

$$G_{dB}(\infty) = RGC_{dB} + 1/2\left(\frac{P_r}{P_t}\right)_{dB} \quad . \qquad (24)$$

The actual measured coupling and the far-field gain results are presented graphically in the following figures for the three horn models:

1.) Scientific Atlanta Model 12-8.2,
2.) Narda Model 640, and
3.) Ladar Systems Model CX-20 (corrugated).

Coupling was measured using all six possible transmitter-receiver combinations

Transmitter	Receiver
Scientific Atlanta	Scientific Atlanta
Narda	Narda
Ladar Systems	Ladar Systems
Scientific Atlanta	Narda
Scientific Atlanta	Ladar Systems
Narda	Ladar Systems

Figures 24 through 38 show typical coupling and gain curves. The actual gain is obtained by drawing a straight line through the center of the ripple of the following gain curves.

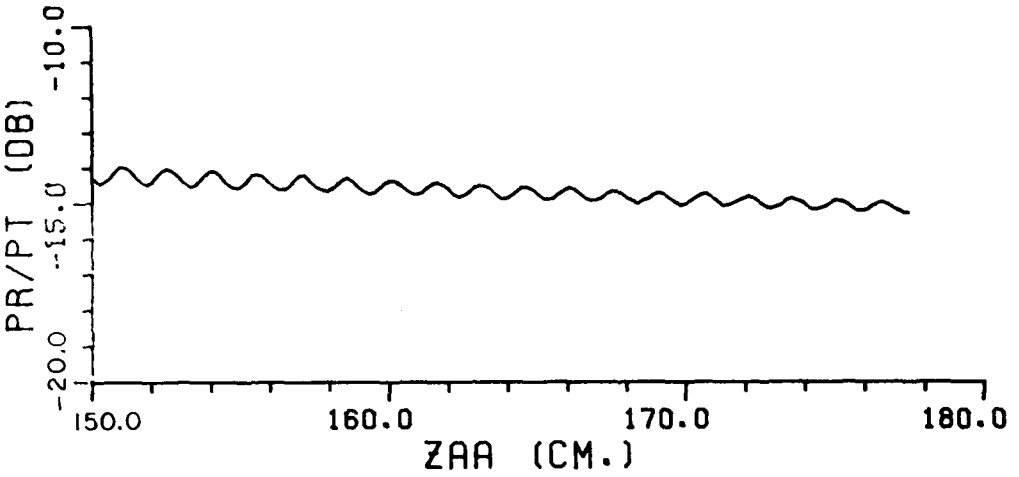

(a)

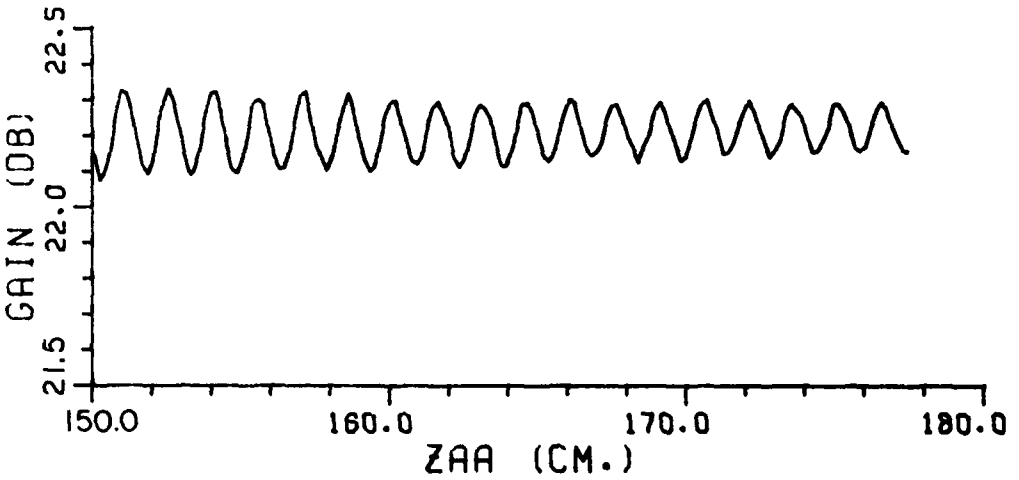

(b)

Transmitting Antenna:	Scientific Atlanta 12-8.2, Serial #1329
Receiving Antenna:	Scientific Atlanta 12-8.2, Serial #1331
Frequency:	10 GHz
Aperture Separation Range:	Z_{AA} = 150.0 to 180.0 cm.
Theoretical D:	D = 19.75 cm.
Average Gain:	22.21 dB.
Date Measured:	9/10/79

Figure 24. (a) Measured coupling.
(b) Gain: $G=RGC+1/2(P_r/P_t)$.

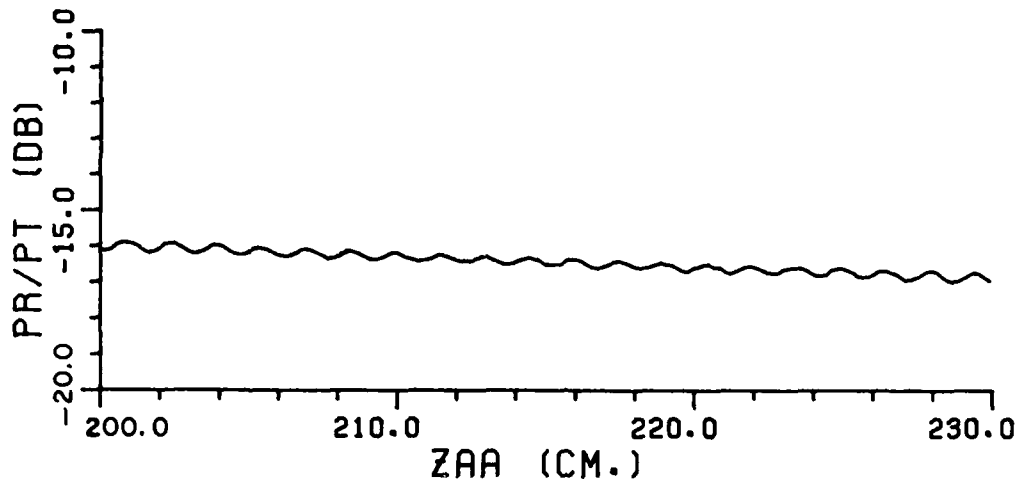

(a)

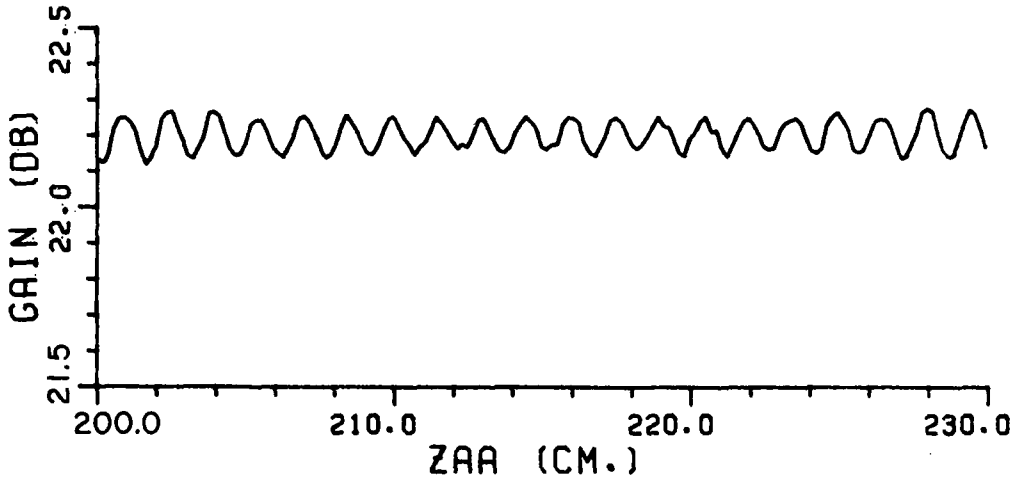

(b)

Transmitting Antenna:	Scientific Atlanta 12-8.2, Serial #1329
Receiving Antenna:	Scientific Atlanta 12-8.2, Serial #1331
Frequency:	10 GHz
Aperture Separation Range:	Z_{AA} = 200.0 to 230.0 cm.
Theoretical D:	D = 19.75 cm.
Average Gain:	22.21 dB.
Date Measured:	9/10/79

Figure 25. (a) Measured coupling.
(b) Gain: $G=RGC+1/2(P_r/P_t)$.

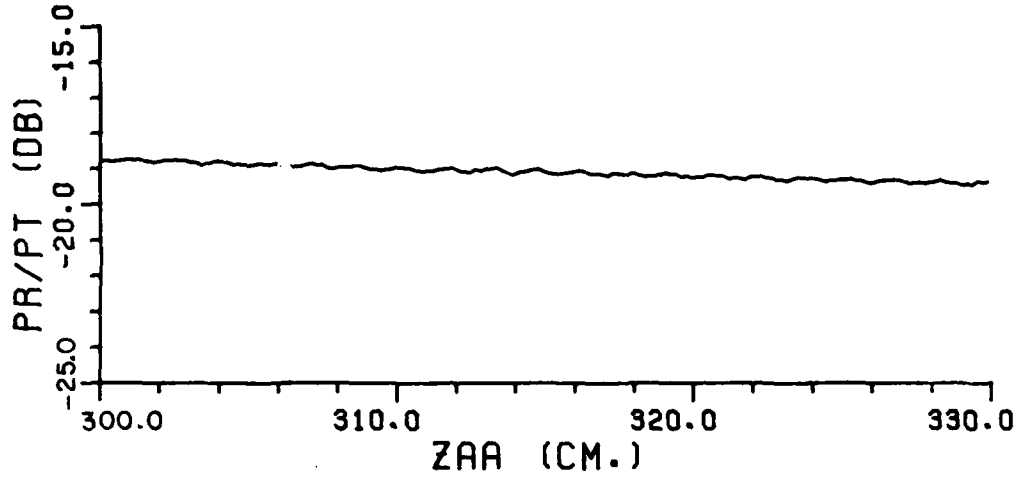

(a)

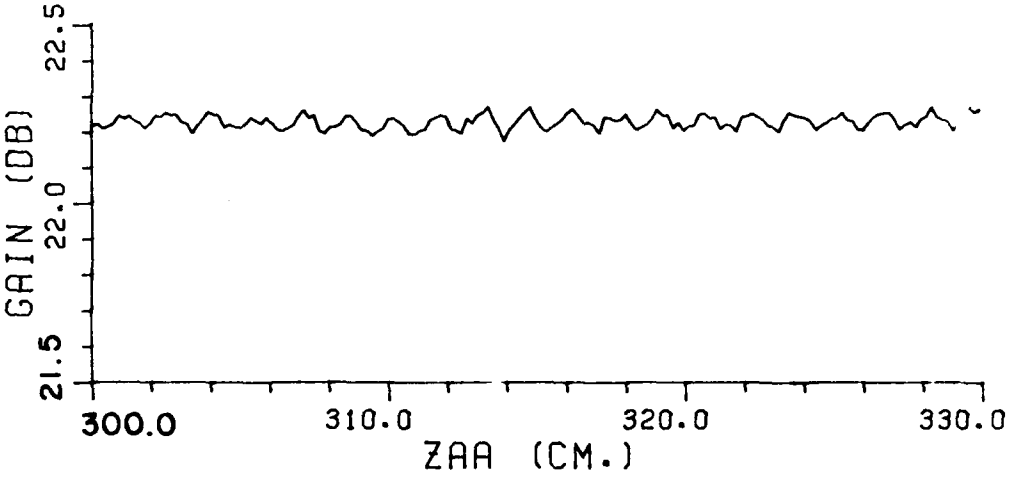

(b)

Transmitting Antenna:	Scientific Atlanta 12-8.2, Serial #1329
Receiving Antenna:	Scientific Atlanta 12-8.2, Serial #1331
Frequency:	10 GHz
Aperture Separation Range:	Z_{AA} = 300.0 to 330.0 cm.
Theoretical D:	D = 19.75 cm.
Average Gain:	22.22 dB.
Date Measured:	0/10/79

Figure 26. (a) Measured coupling.
(b) Gain: $G=RGC+1/2(P_r/P_t)$.

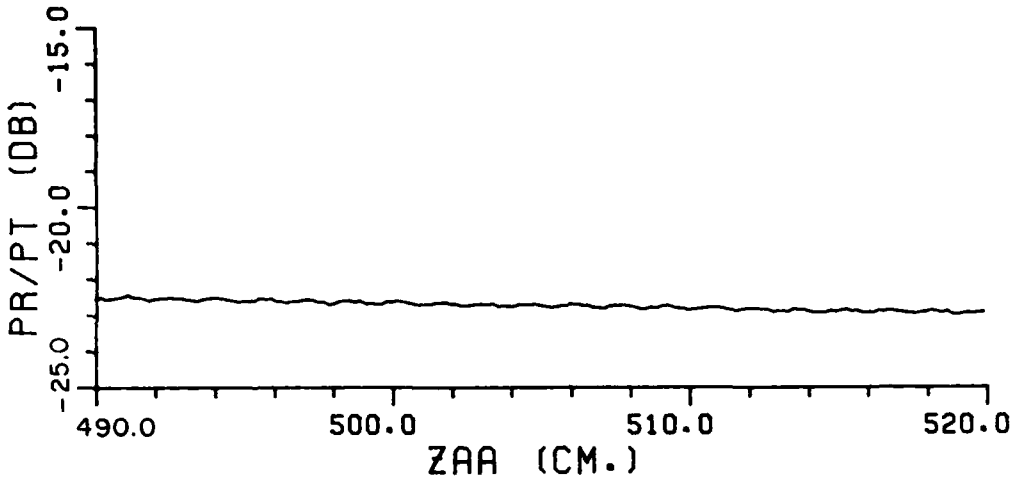

(a)

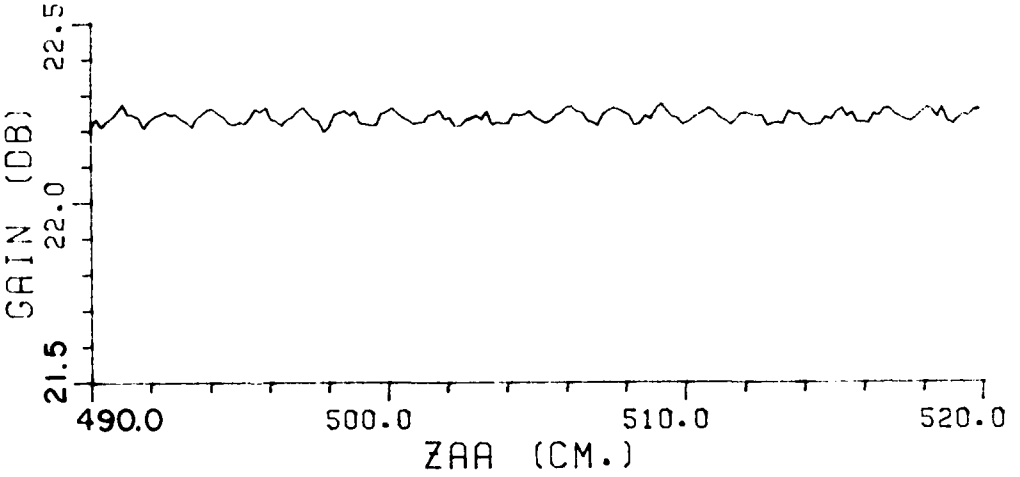

(b)

Transmitting Antenna:	Scientific Atlanta 12-8.2, Serial #1329
Receiving Antenna:	Scientific Atlanta 12-8.2, Serial #1331
Frequency:	10 GHz
Aperture Separation Range:	Z_{AA} = 490.0 to 520.0 cm.
Theoretical D:	D = 19.75 cm.
Average Gain:	22.24 dB.
Date Measured:	9/10/79

Figure 27. (a) Measured coupling.
(b) Gain: $G=RGC+1/2(P_r/P_t)$.

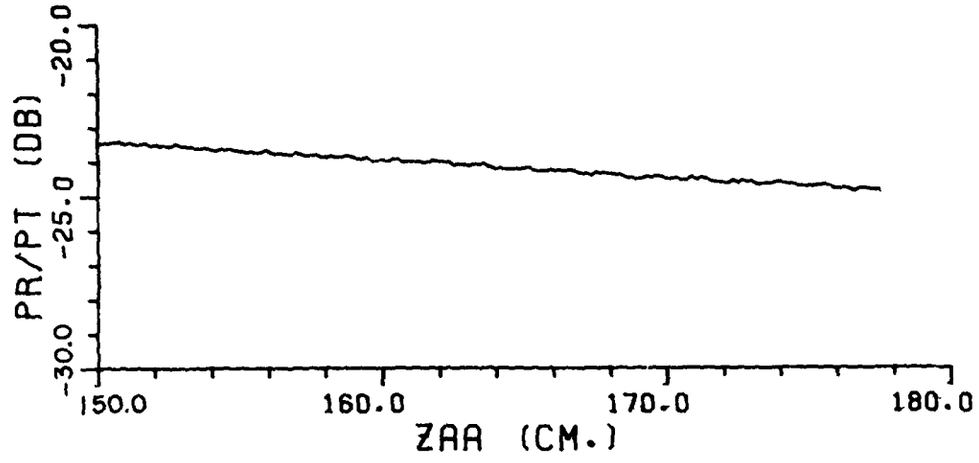

(a)

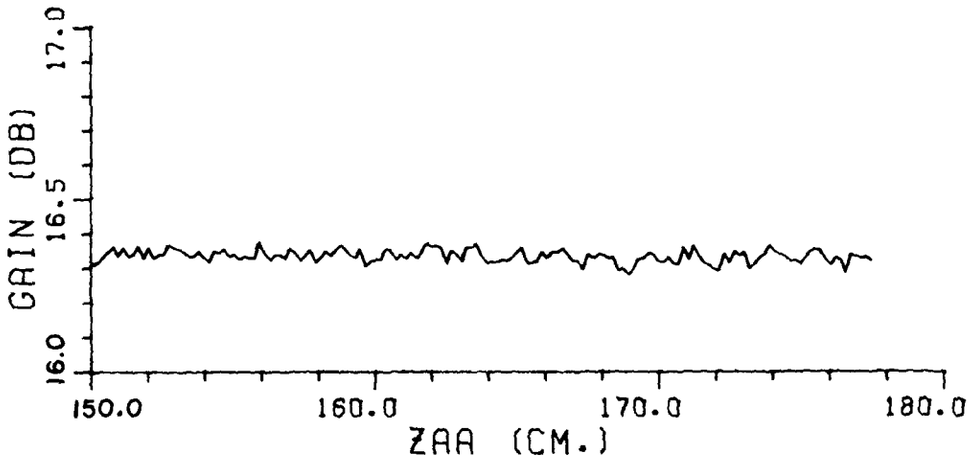

(b)

Transmitting Antenna:	Narda 640, Serial #115
Receiving Antenna:	Narda 640, Serial #114
Frequency:	10 GHz
Aperture Separation Range:	Z_{AA} = 150.0 to 180.0 cm.
Theoretical D:	D = 1.32 cm.
Average Gain:	16.33 dB.
Date Measured:	7/15/79

Figure 28. (a) Measured Coupling.
(b) Gain: $G=RGC+1/2(P_r/P_t)$.

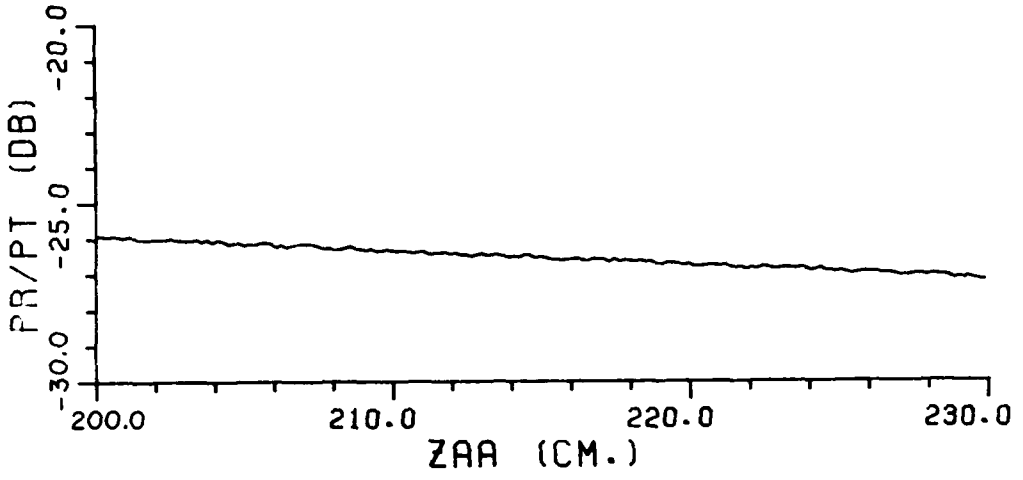

(a)

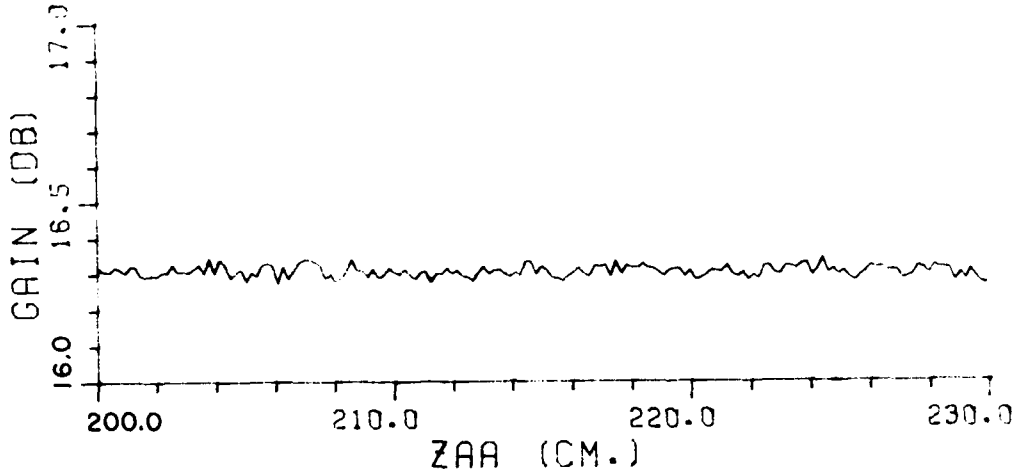

(b)

Transmitting Antenna:	Narda 640, Serial #115
Receiving Antenna:	Narda 640, Serial #114
Frequency:	10 GHz
Aperture Separation Range:	Z_{AA} = 200.0 to 230.0 cm.
Theoretical D:	D = 1.32 cm.
Average Gain:	16.30 dB.
Date Measured:	7/15/79

Figure 29. (a) Measured Coupling.
(b) Gain: $G=RGC+1/2(P_r/P_t)$.

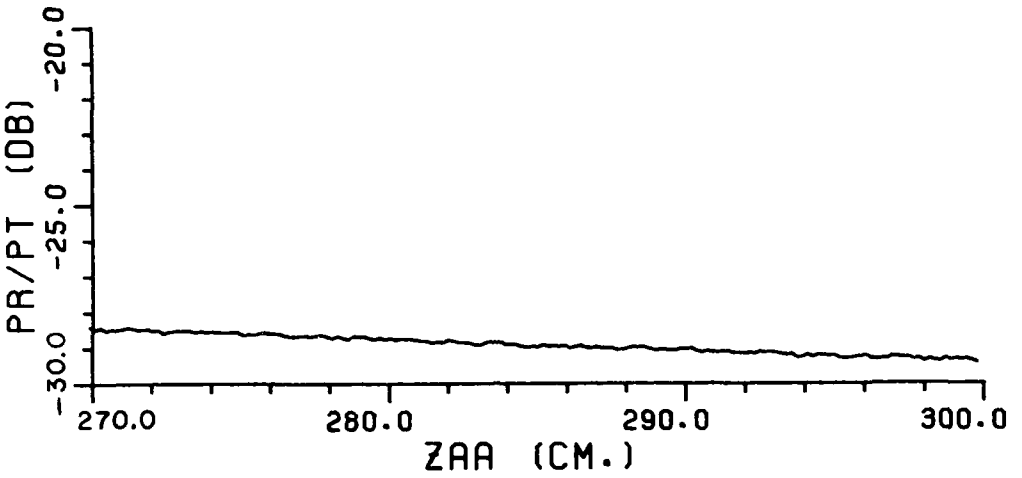

(a)

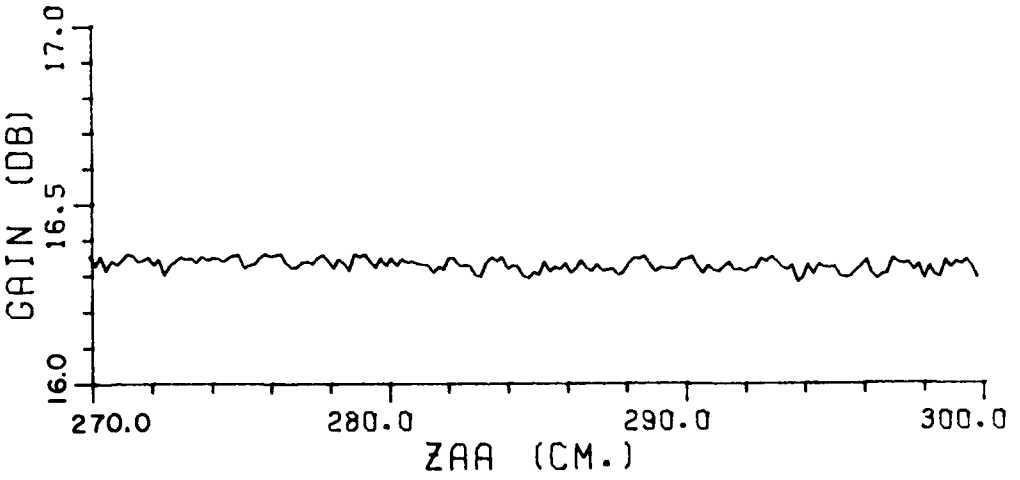

(b)

Transmitting Antenna:	Narda 640, Serial #115
Receiving Antenna:	Narda 640, Serial #114
Frequency:	10 GHz
Aperture Separation Range:	Z_{AA} = 270.0 to 300.0 cm.
Theoretical D:	D = 1.32 cm.
Average Gain:	16.33 dB.
Date Measured:	7/15/79

Figure 30. (a) Measured Coupling.
(b) Gain: $G=RGC+1/2(P_r/P_t)$.

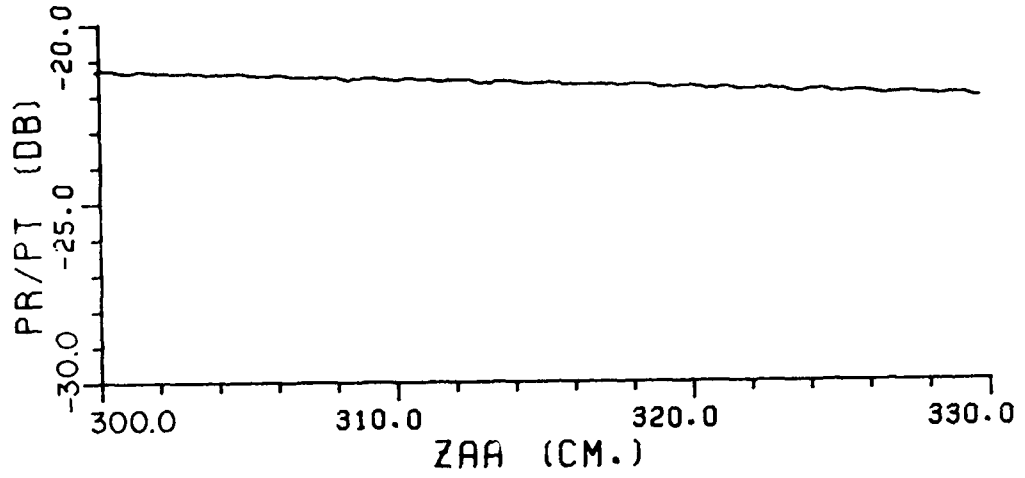

(a)

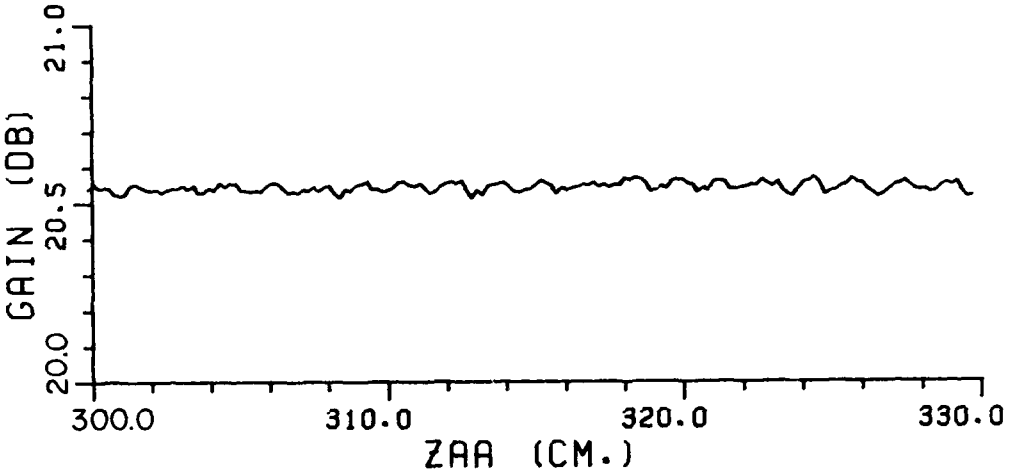

(b)

Transmitting Antenna:	Ladar Systems CX-20, Serial #43
Receiving Antenna:	Ladar Systems CX-20, Serial #41
Frequency:	10 GHz
Aperture Separation Range:	Z_{AA} = 300.0 to 330.0 cm
Theoretical D:	D=6.21 cm.
Average Gain:	20.54 dB
Date Measured:	12/11/79

Figure 31. (a) Measured Coupling.
(b) Gain: $G=RGC+1/2(P_r/P_t)$.

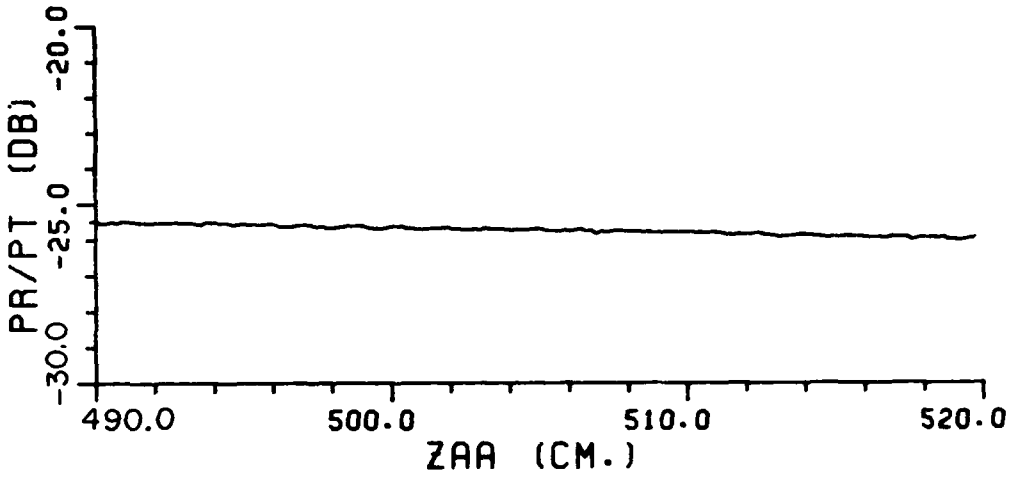

(a)

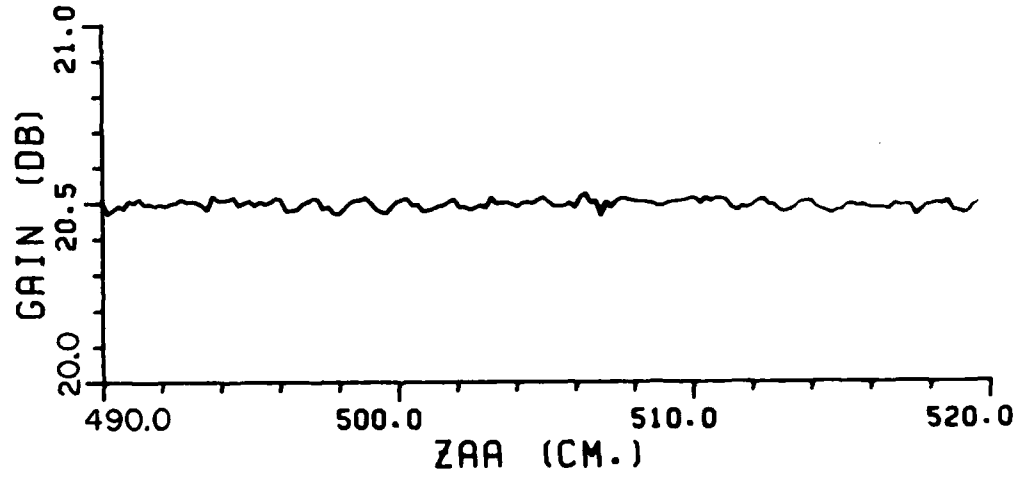

(b)

Transmitting Antenna:	Ladar Systems CX-20, Serial #43
Receiving Antenna:	Ladar Systems CX-20, Serial #4
Frequency:	10 GHz
Aperture Separation Range:	Z_{AA} = 490.0 to 520.0 cm
Theoretical D:	D=6.21 cm
Average Gain:	20.49 dB
Date Measured:	12/11/79

Figure 32. (a) Measured Coupling.
(b) Gain: $G=RGC+1/2(P_r/P_t)$.

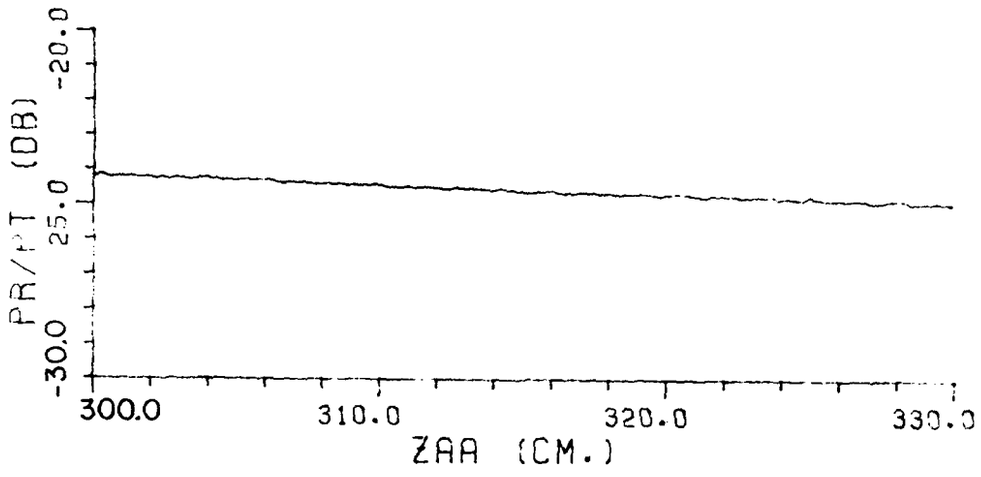

(a)

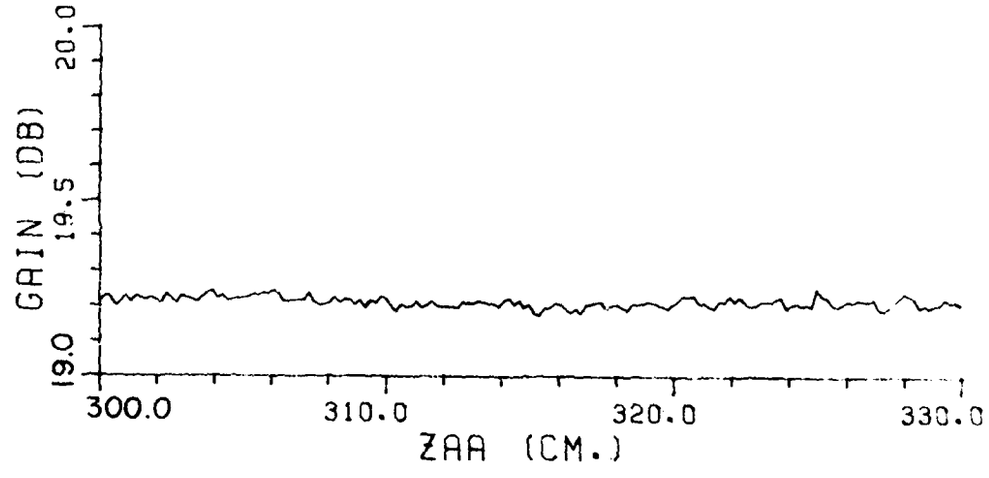

(b)

Transmitting Antenna:	Narda 640, Serial #114
Receiving Antenna:	Scientific Atlanta 12-8.2, Serial #1331
Frequency:	10 GHz
Aperture Separation Range:	Z_{AA} = 300.0 to 330.0 cm.
Theoretical D:	D(ave.) = 10.53 cm.
Average Gain:	19.21 dB
Date Measured:	12/14/79

Figure 33. (a) Measured Coupling.
(b) Gain: $G=RGC+1/2(P_r/P_t)$.

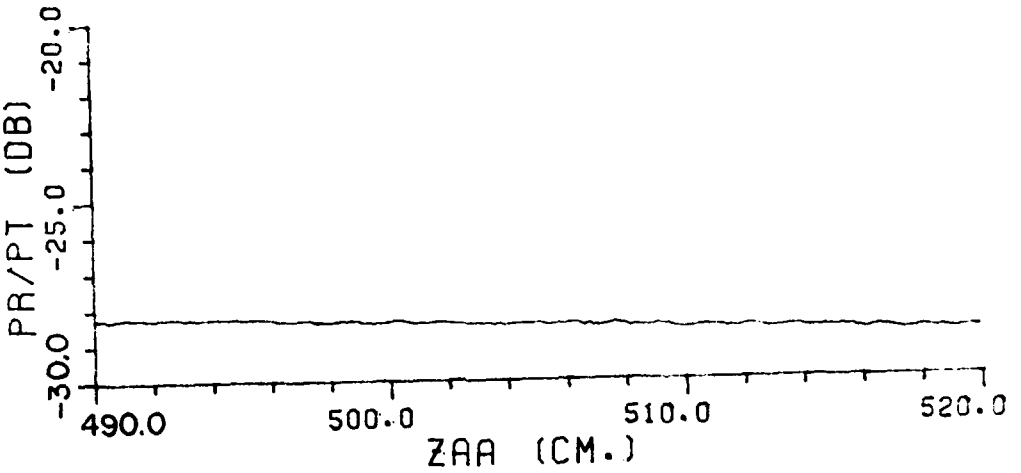

(a)

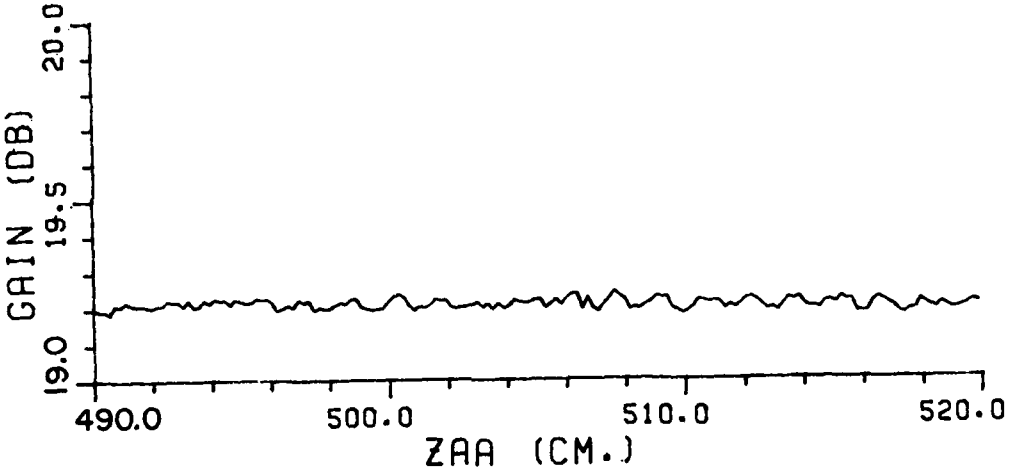

(b)

Transmitting Antenna:	Narda 640, Serial #114
Receiving Antenna:	Scientific Atlanta 12-8.2, Serial #1331
Frequency:	10 GHz
Aperture Separation Range:	Z_{AA} = 490.0 to 520.0 cm.
Theoretical D:	D(ave.) = 10.53 cm.
Average Gain:	19.21 dB
Date Measured:	12/14/79

Figure 34. (a) Measured Coupling.
(b) Gain: $G=RGC+1/2(P_r/P_t)$.

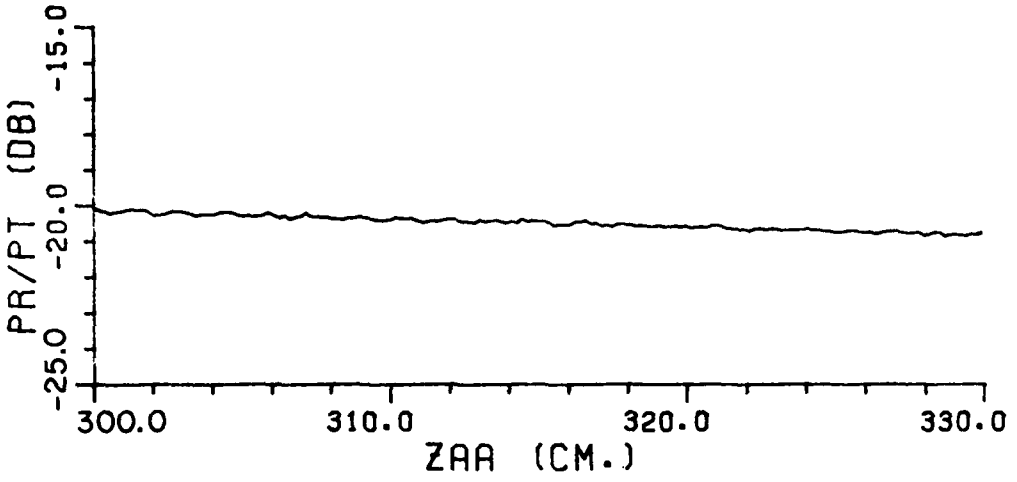

(a)

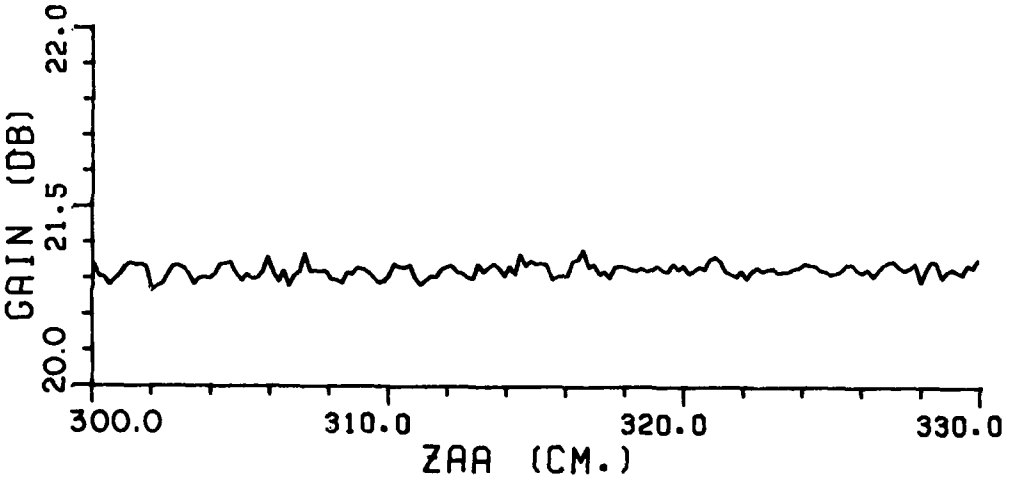

(b)

Transmitting Antenna:	Scientific Atlanta 12-8.2, Serial #1331
Receiving Antenna:	Ladar Systems CX-20, Serial #41
Frequency:	10 GHz
Aperture Separation Range:	Z_{AA} = 300.0 to 330.0 cm.
Theoretical D:	D(ave.) = 12.98 cm.
Average Gain:	21.32 dB.
Date Measured:	12/13/79

Figure 35. (a) Measured Coupling.
(b) Gain: $G=RGC+1/2(P_r/P_t)$.

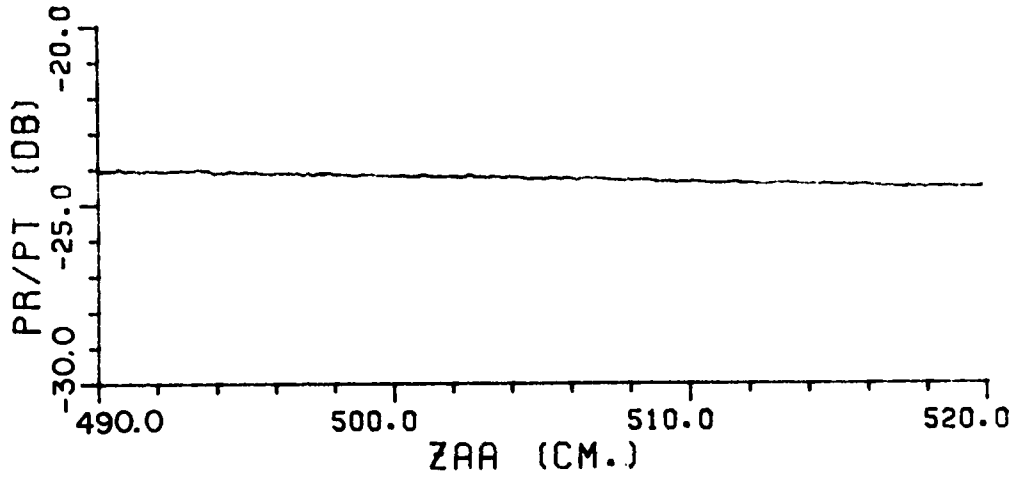

(a)

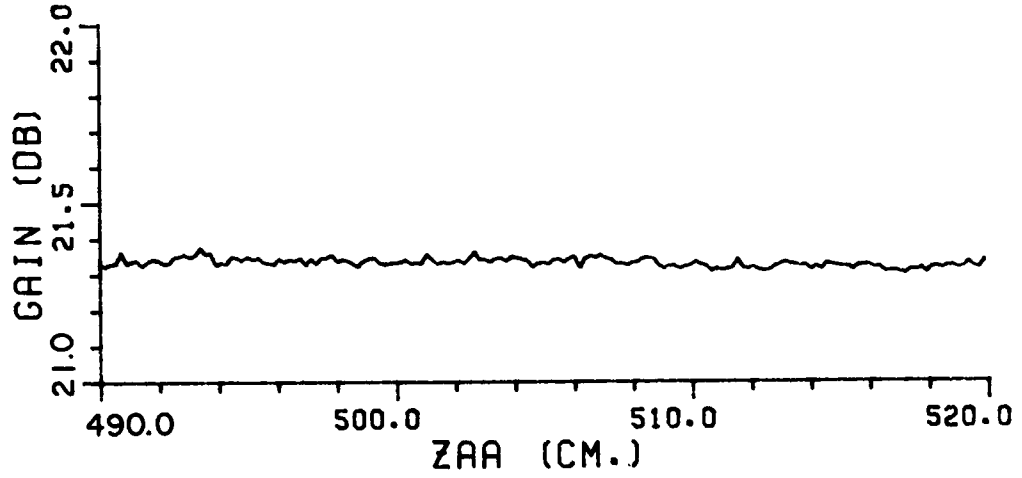

(b)

Transmitting Antenna:	Scientific Atlanta 12-8.2, Serial #1331
Receiving Antenna:	Ladar Systems CX-20, Serial #41
Frequency:	10 GHz
Aperture Separation Range:	Z_{AA} = 490.0 to 520.0 cm.
Theoretical D:	D(ave.) = 12.98 cm.
Average Gain:	21.33 dB.
Date Measured:	12/13/79

Figure 36. (a) Measured Coupling.
(b) Gain: $G=RGC+1/2(P_r/P_t)$.

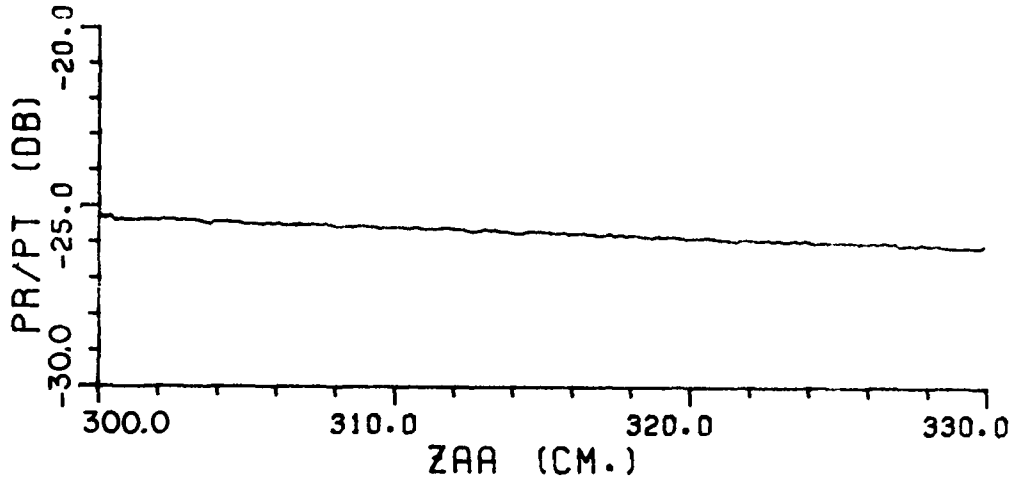

(a)

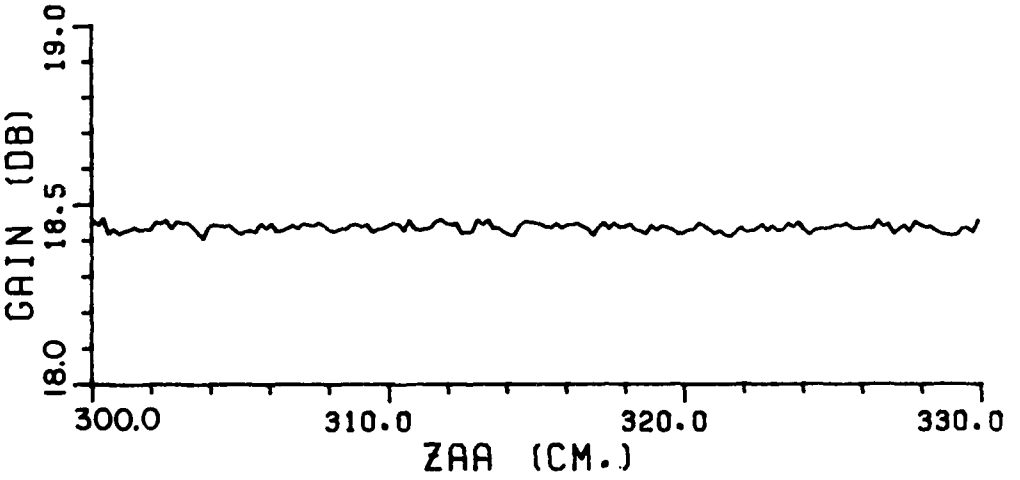

(b)

Transmitting Antenna:	Narda 640, Serial #114
Receiving Antenna:	Ladar Systems CX-20, Serial #41
Frequency:	10 GHz
Aperture Separation Range:	Z_{AA} = 300.0 to 330.0 cm.
Theoretical D:	D(ave.) = 3.77 cm.
Average Gain:	18.45 dB
Date Measured:	12/14/79

Figure 37. (a) Measured Coupling.
(b) Gain: $G=RGC+1/2(P_r/P_t)$.

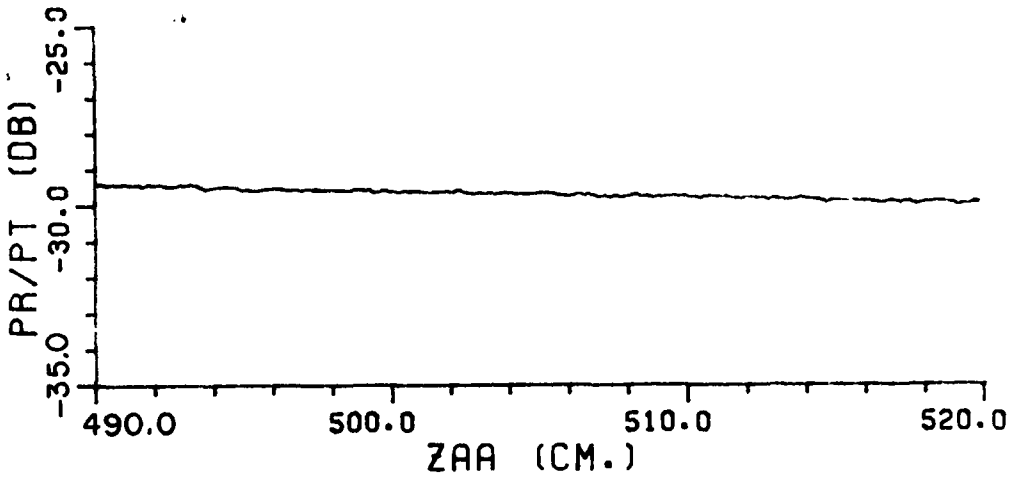

(a)

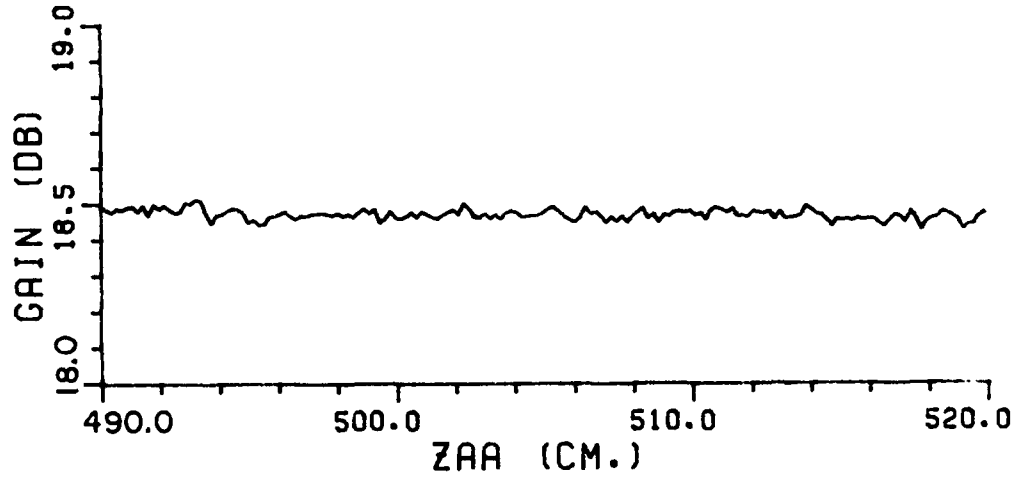

(b)

Transmitting Antenna:	Narda 640, Serial #114
Receiving Antenna:	Ladar Systems CX-20, Serial #41
Frequency:	10 GHz
Aperture Separation Range:	Z_{AA} = 490.0 to 520.0 cm.
Theoretical D:	D(ave.) = 3.77 cm.
Average Gain:	18.47 dB
Date Measured:	12/14/79

Figure 38. (a) Measured Coupling.
(b) Gain: $G=RGC+1/2(P_r/P_t)$.

CHAPTER IV
RADIATION PATTERNS OF STANDARD GAIN HORNS

This chapter is an evaluation of horn antennas intended for general purpose laboratory use, as well as precision gain standards. The emphasis here is on the radiation patterns in the principal planes. In most cases a general purpose laboratory horn should have low side and back lobes. This is true regardless of whether or not it is used as a highly calibrated gain standard. Even in situations where high precision measurements are being made that do not require a highly calibrated standard gain horn, multipath, due to high side and back lobes, can be a problem in many anechoic chambers. The measured E-plane and H-plane radiation patterns of three different horn antennas (Scientific Atlanta 12-8.2, Narda 640, and Ladar Systems CX-20) are shown in Figure 39 through Figure 56.

The Ladar systems CX-20 horn has reduced side and back lobes in the E-plane due to its corrugated walls. These corrugations cause the E-plane energy distribution in the aperture to be approximately sinusoidal, similar to the H-plane distribution. Therefore, the energy at the E-plane edges, which is diffracted in the side and back directions, is greatly reduced relative to a non-corrugated horn. Complete details of the corrugated horn are available in the literature [3].

Figure 57 shows the improved E-plane pattern of the corrugated horn relative to the same horn without corrugated walls. Curve A is an actual measured pattern of the corrugated horn, whereas curve B is a calculation based on the Geometrical Theory of Diffraction (GTD) [4]. A calculated pattern is shown here because a noncorrugated horn of the same dimensions as the CX-20 was not available for measurements. But the GTD method of pattern calculation generally agrees very well with measurements (see Figures 58 and 59).

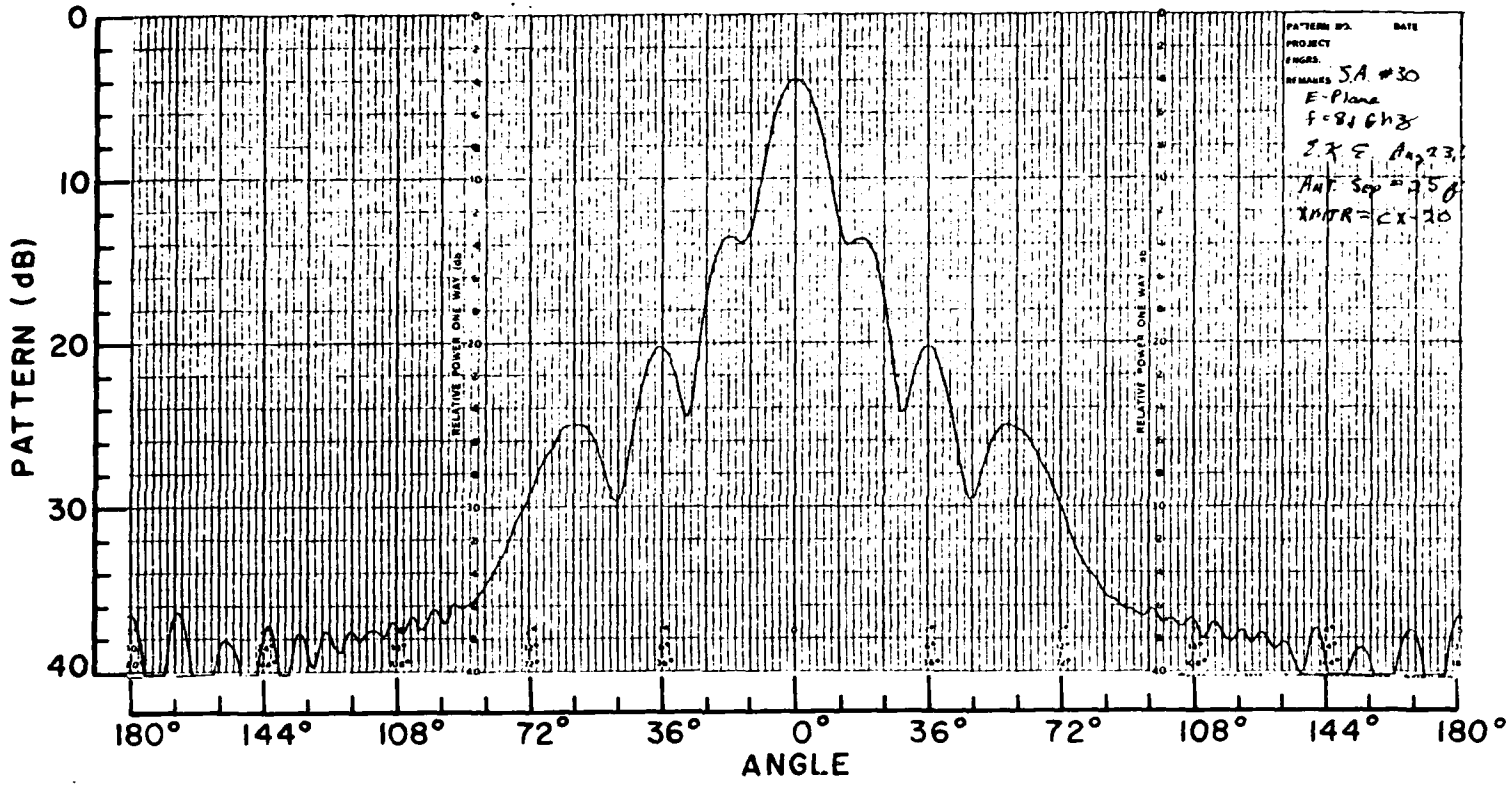

Figure 39. Scientific Atlanta 12-8.2.
E-Plane
f = 8.1 GHz

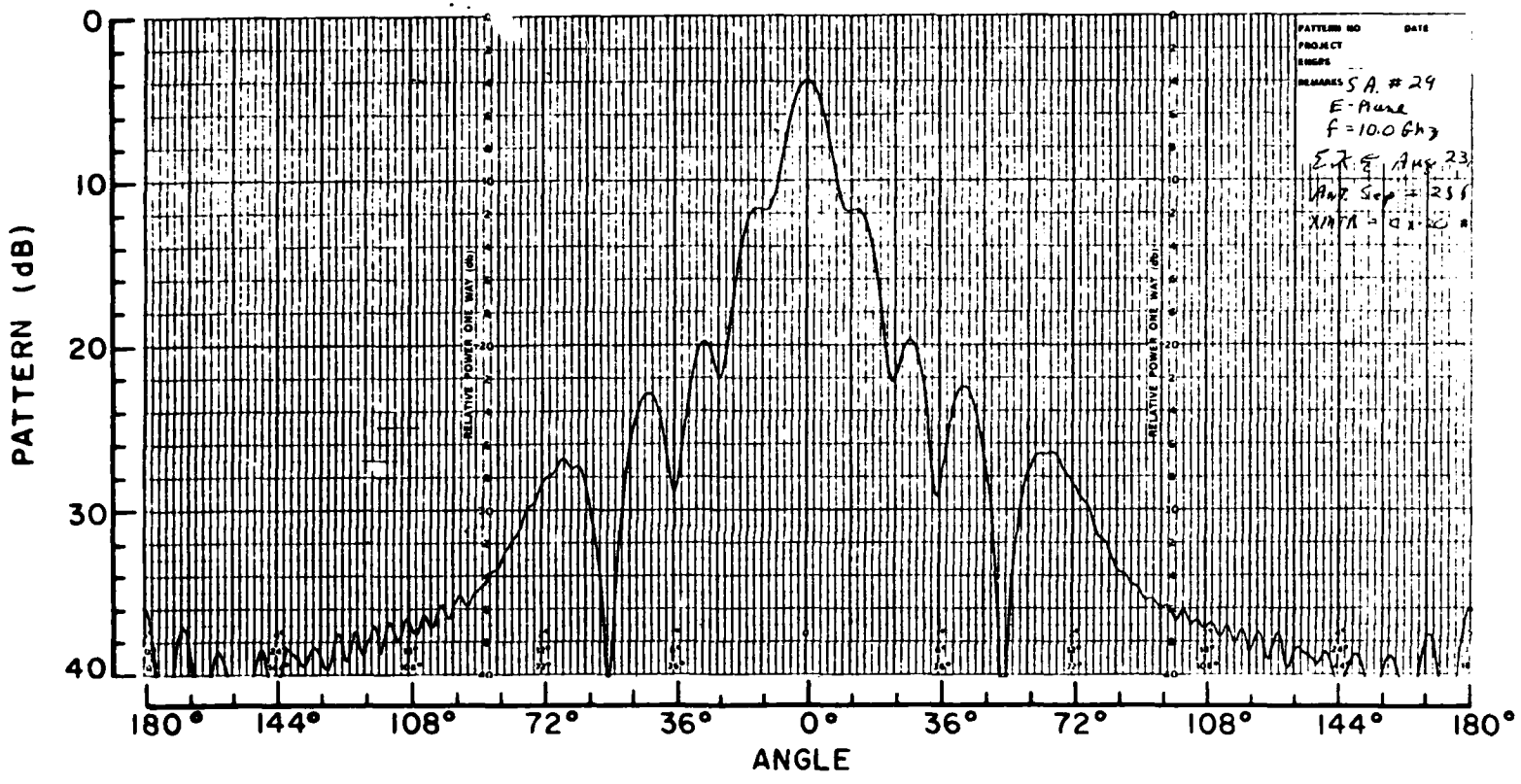

Figure 40. Scientific Atlanta 12-8.2.
E-Plane
f = 10.0 GHz

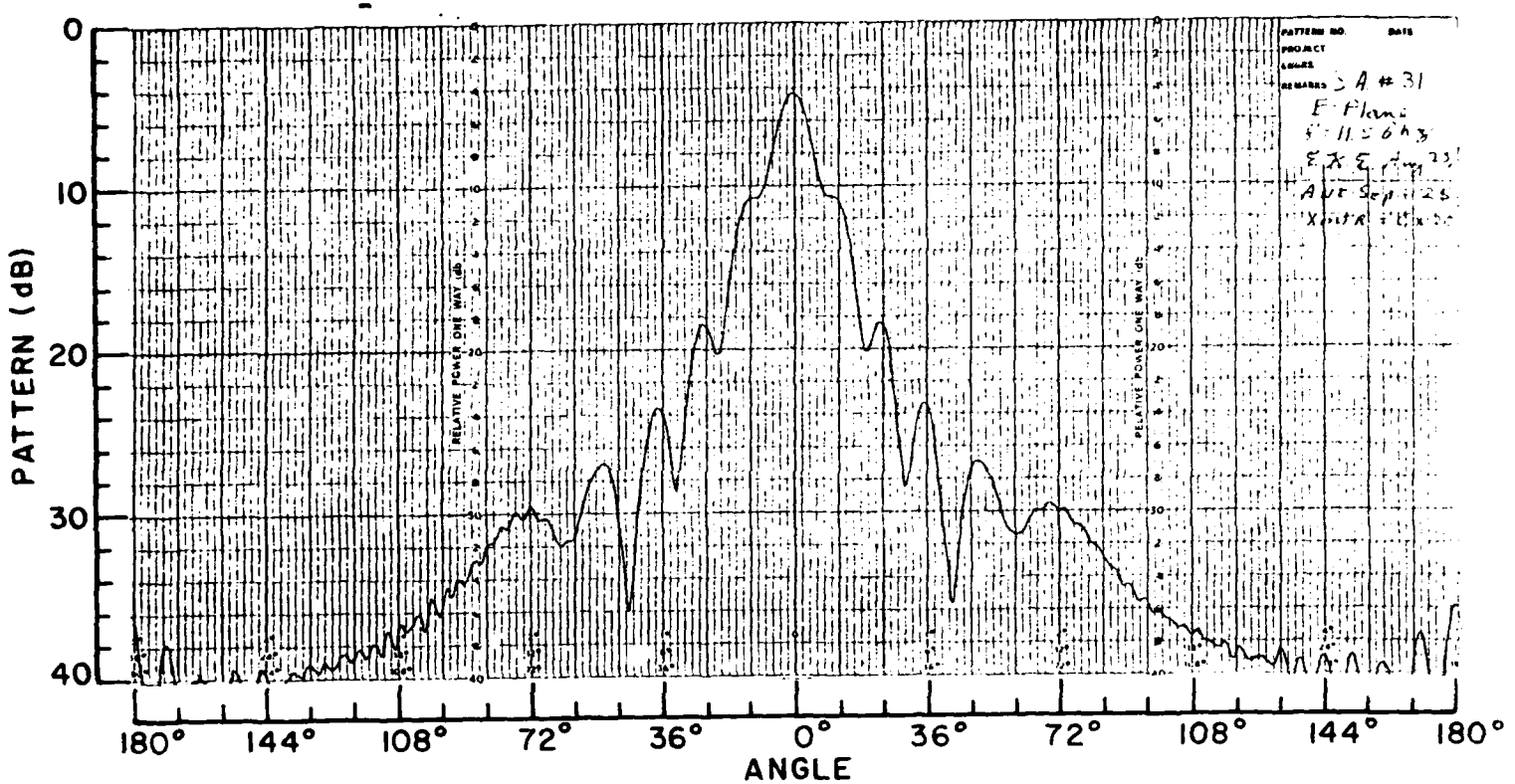

Figure 41. Scientific Atlanta 12-8.2.
E-Plane
f = 11.5 GHz

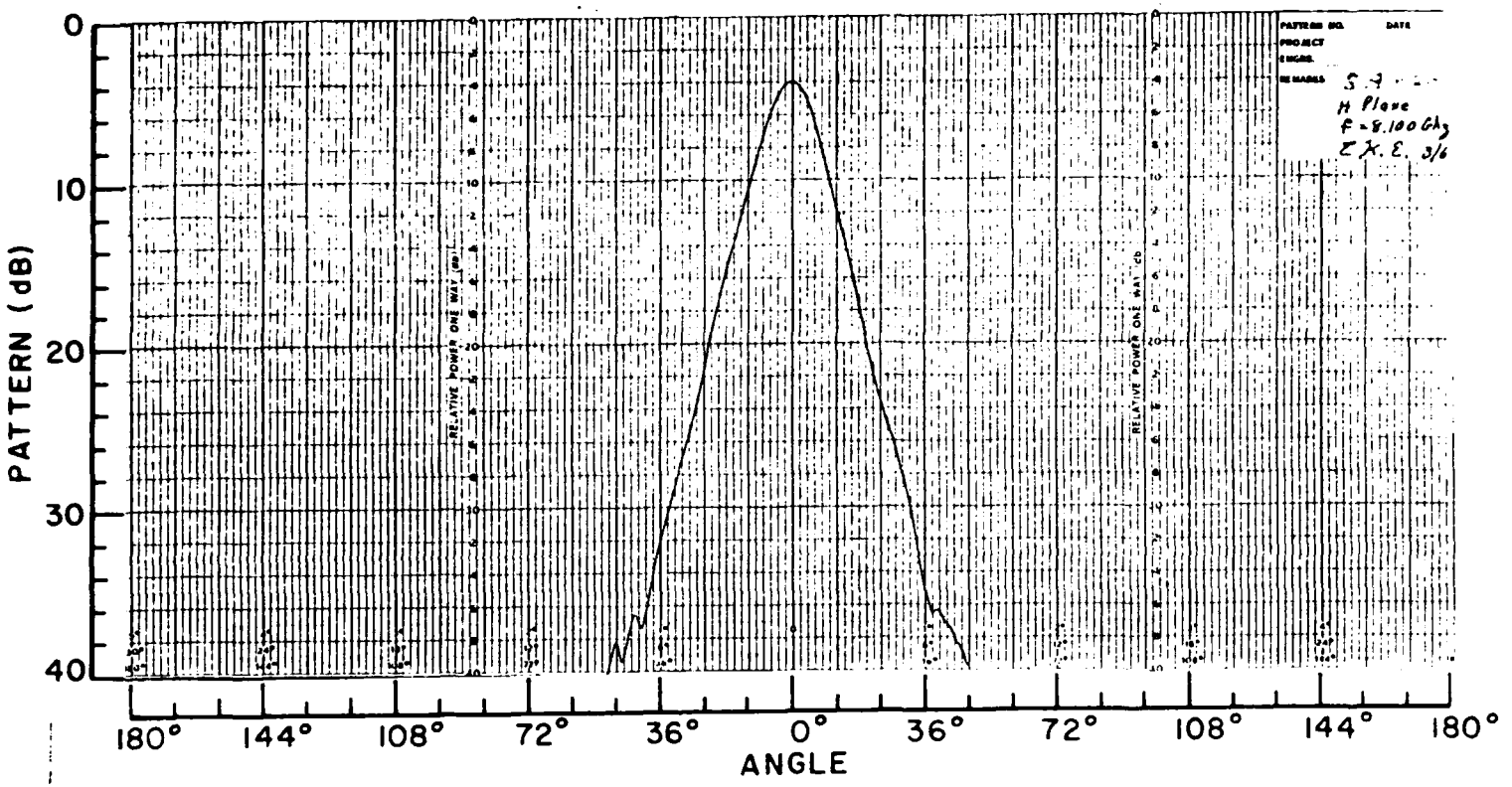

Figure 42. Scientific Atlanta 12-8.2.
H-Plane
f = 8.1 GHz

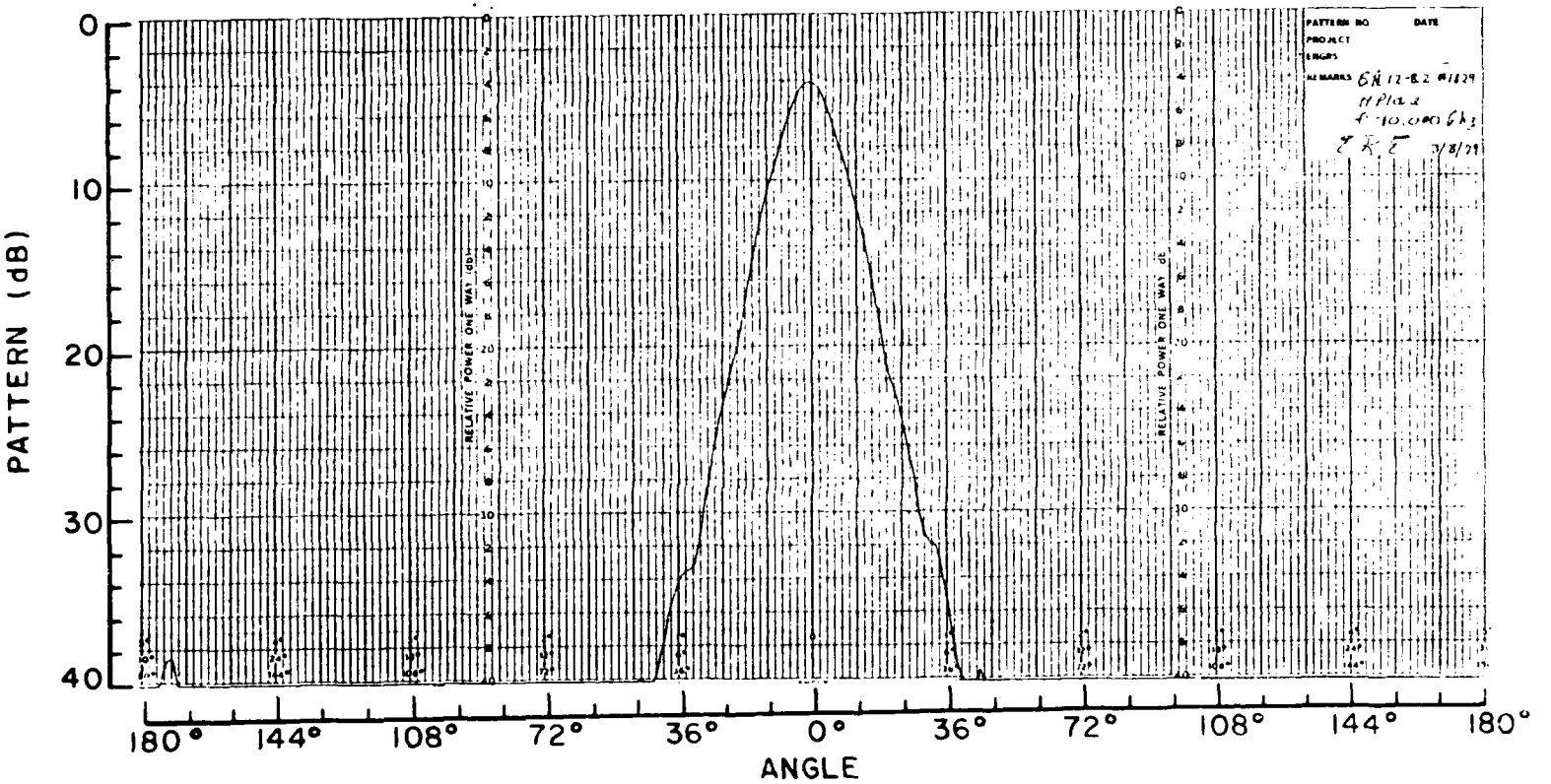

Figure 43. Scientific Atlanta 12-8.2.
H-Plane
f = 10.0 GHz

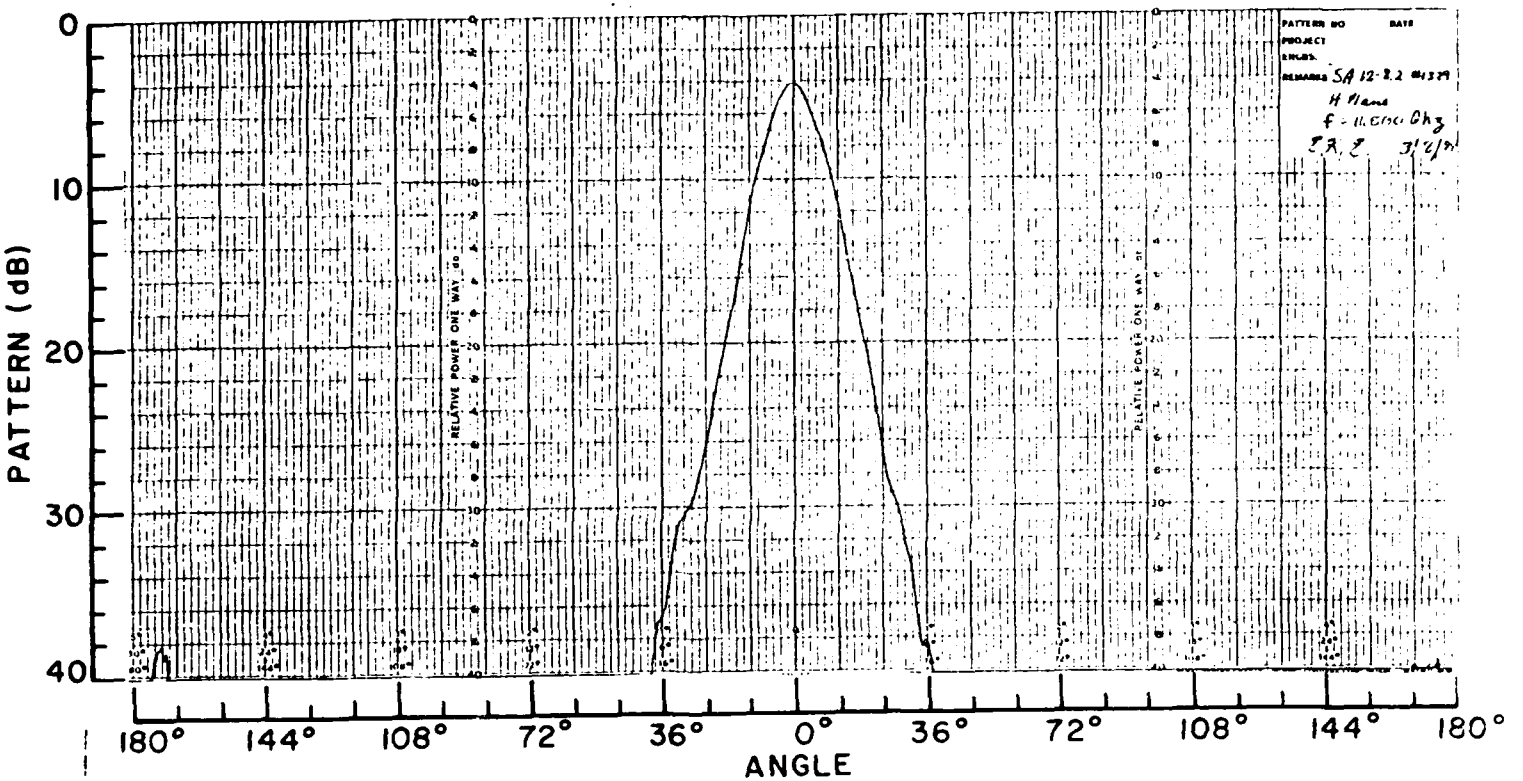

Figure 44. Scientific Atlanta 12-8.2.
H-Plane
f = 11.5 GHz

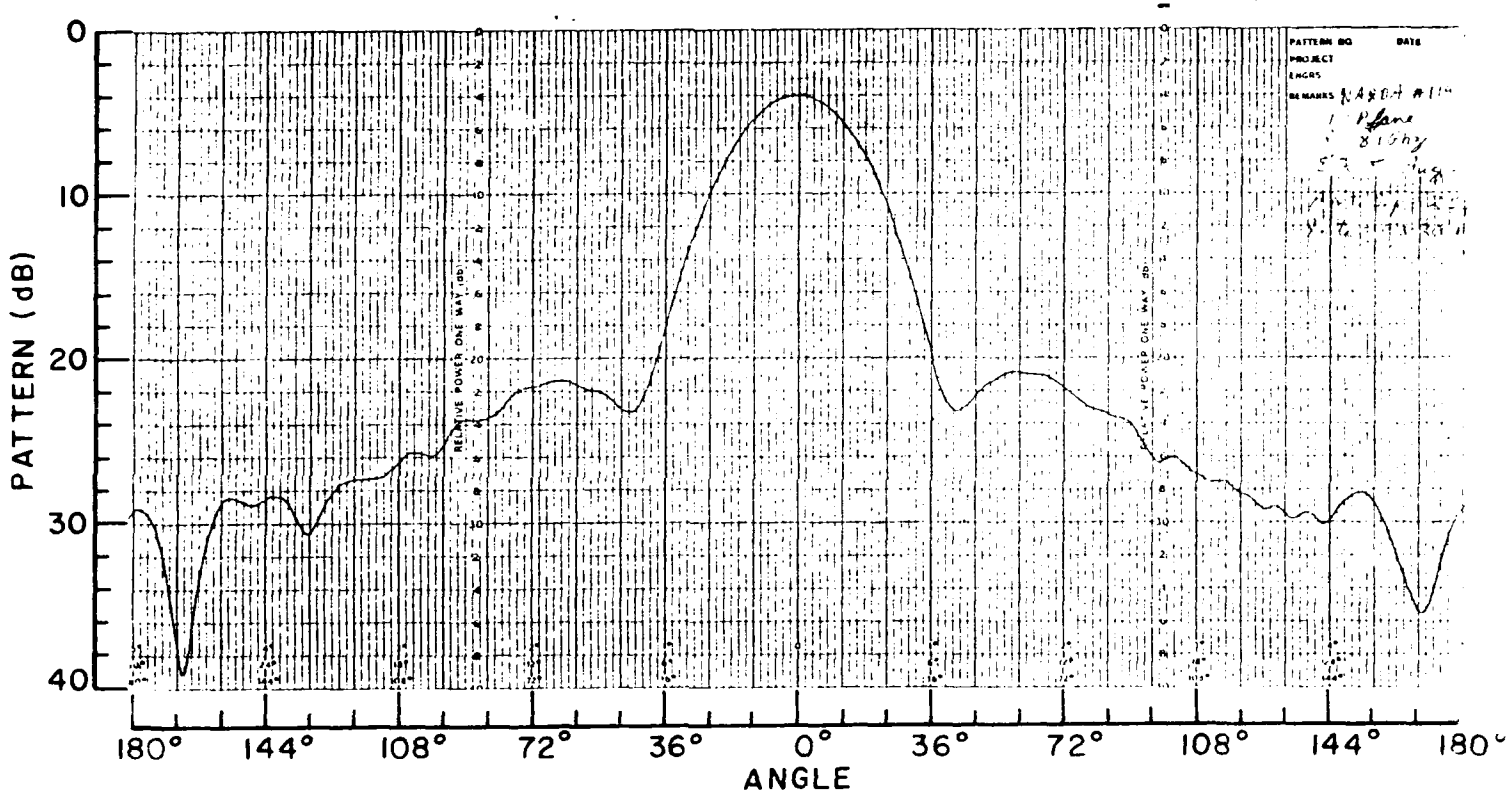

Figure 45. Narda 640.
E-Plane
f = 3.1 GHz

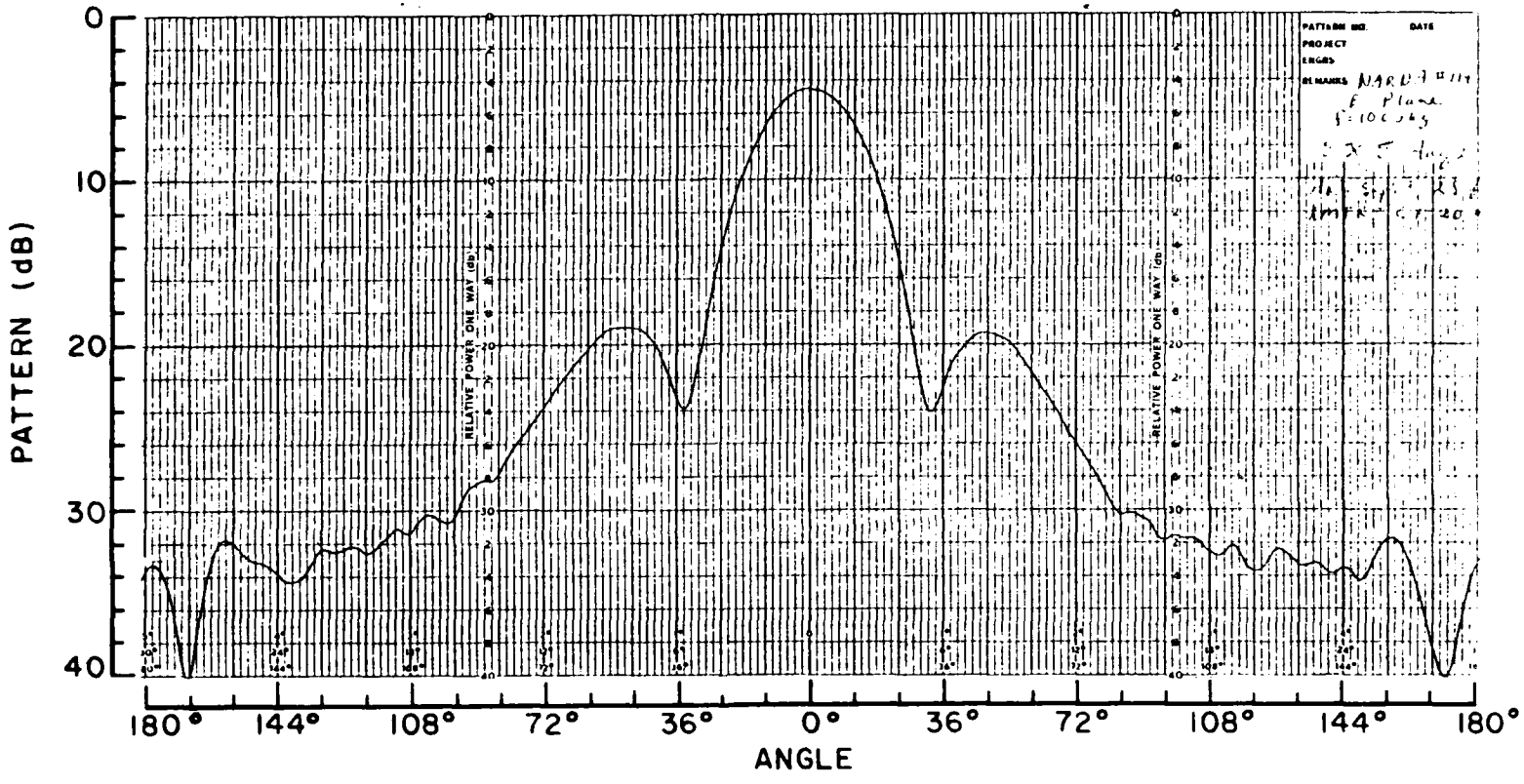

Figure 46. Narda 640.
E-Plane
f = 10.0 GHz

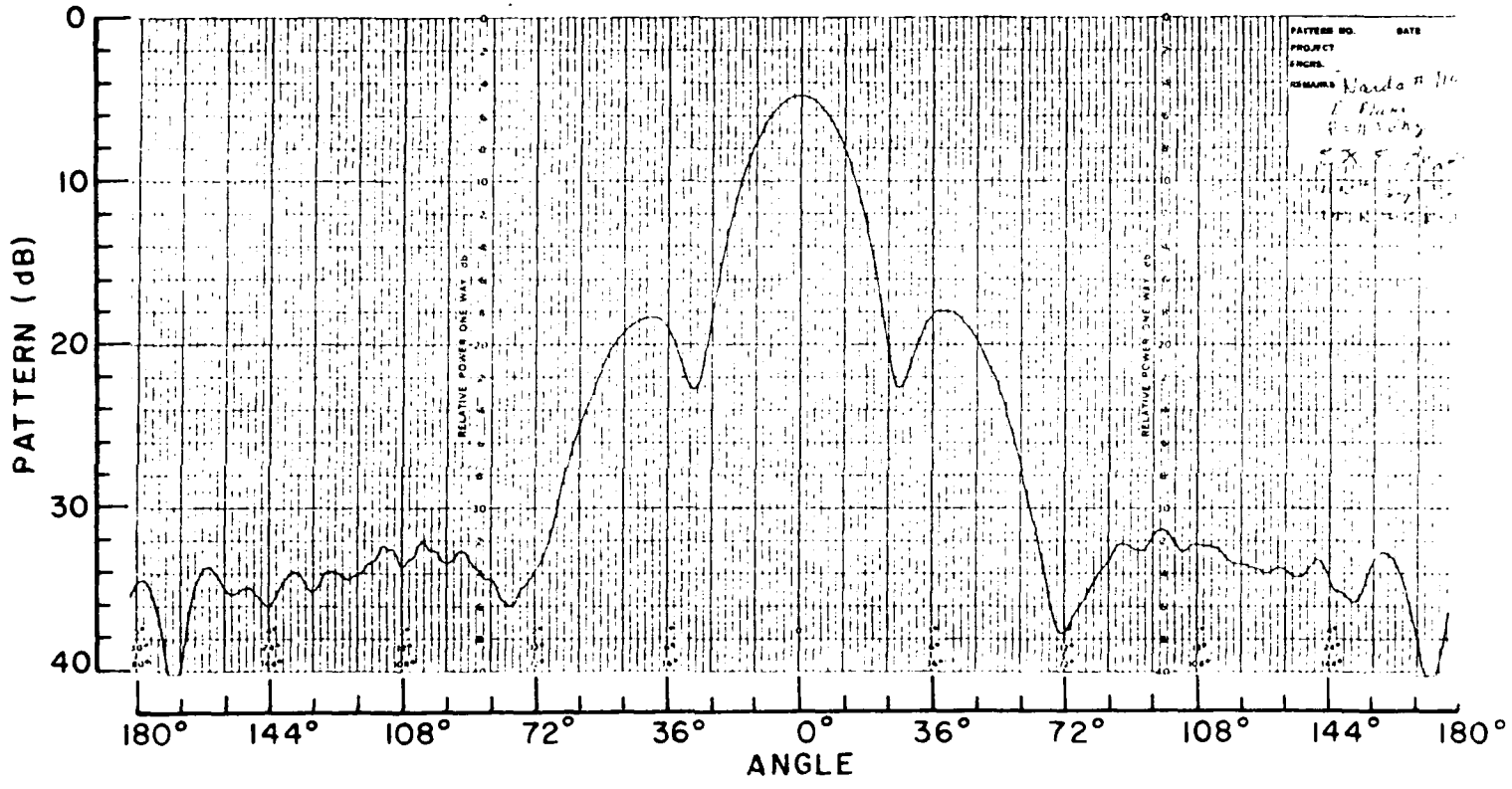

Figure 47. Narda 640.
E-Plane
f = 11.5 GHz

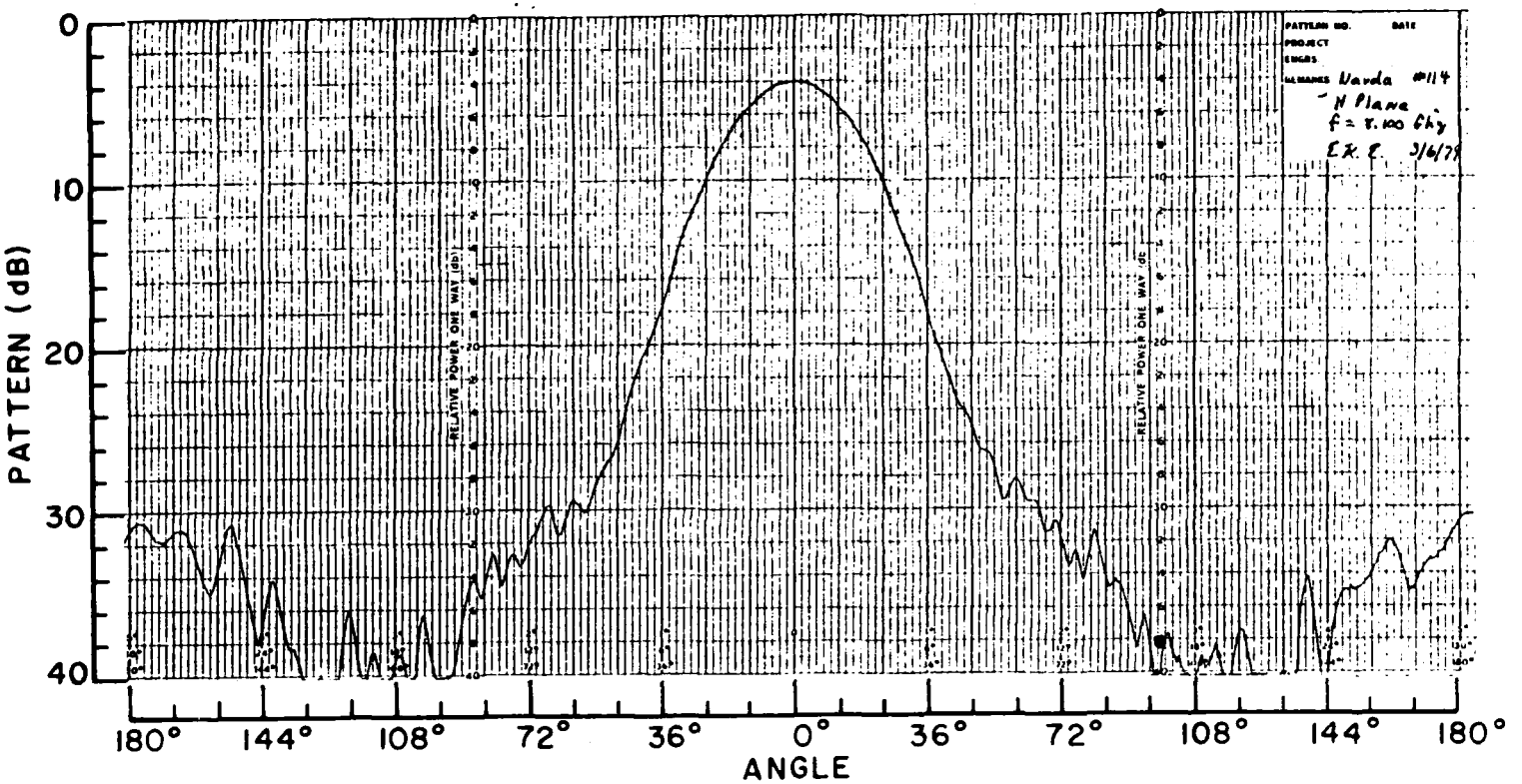

Figure 48. Narda 640.
H-Plane
f = 8.1 GHz

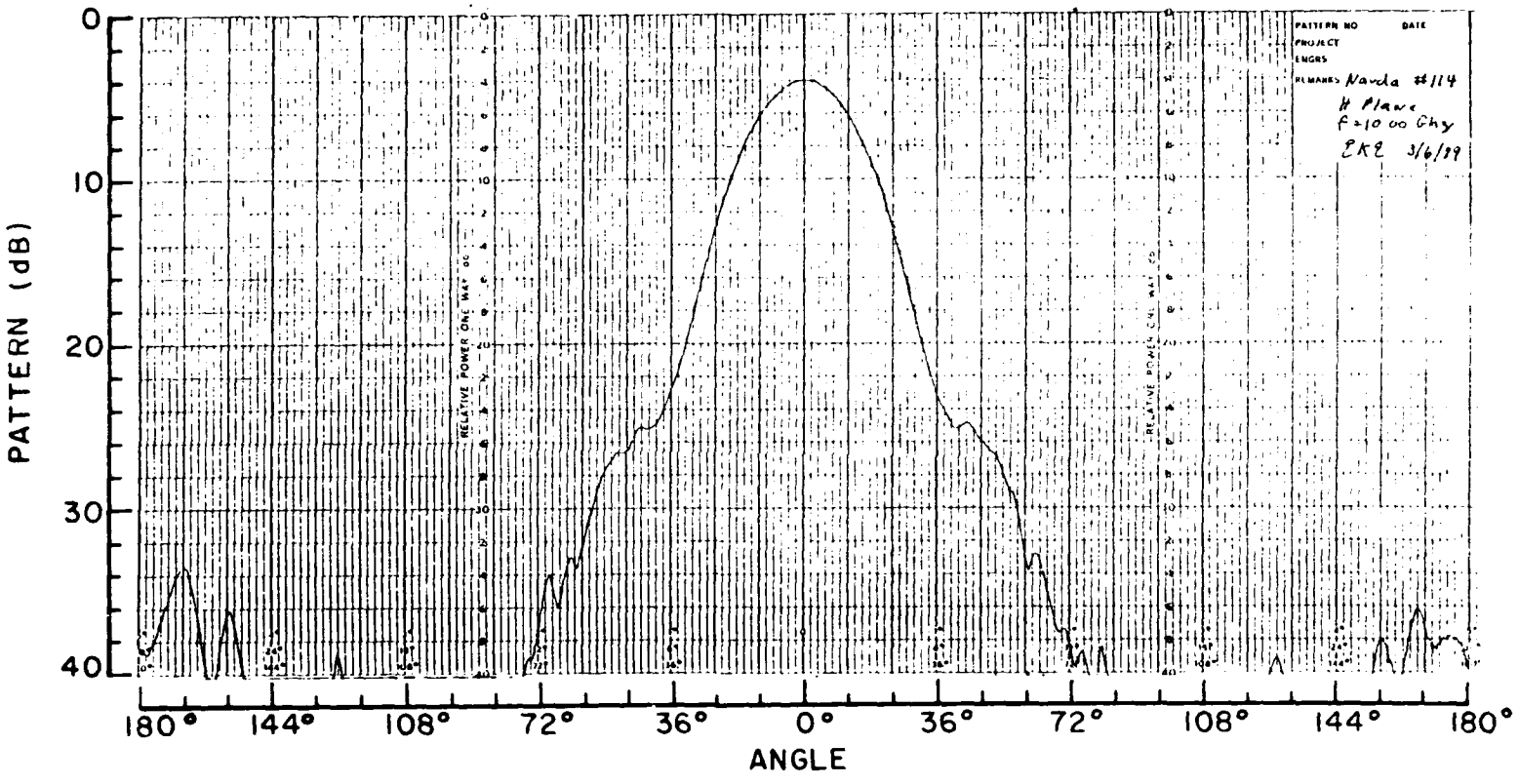

Figure 49. Narda 640.
H-Plane
f = 10.0 GHz

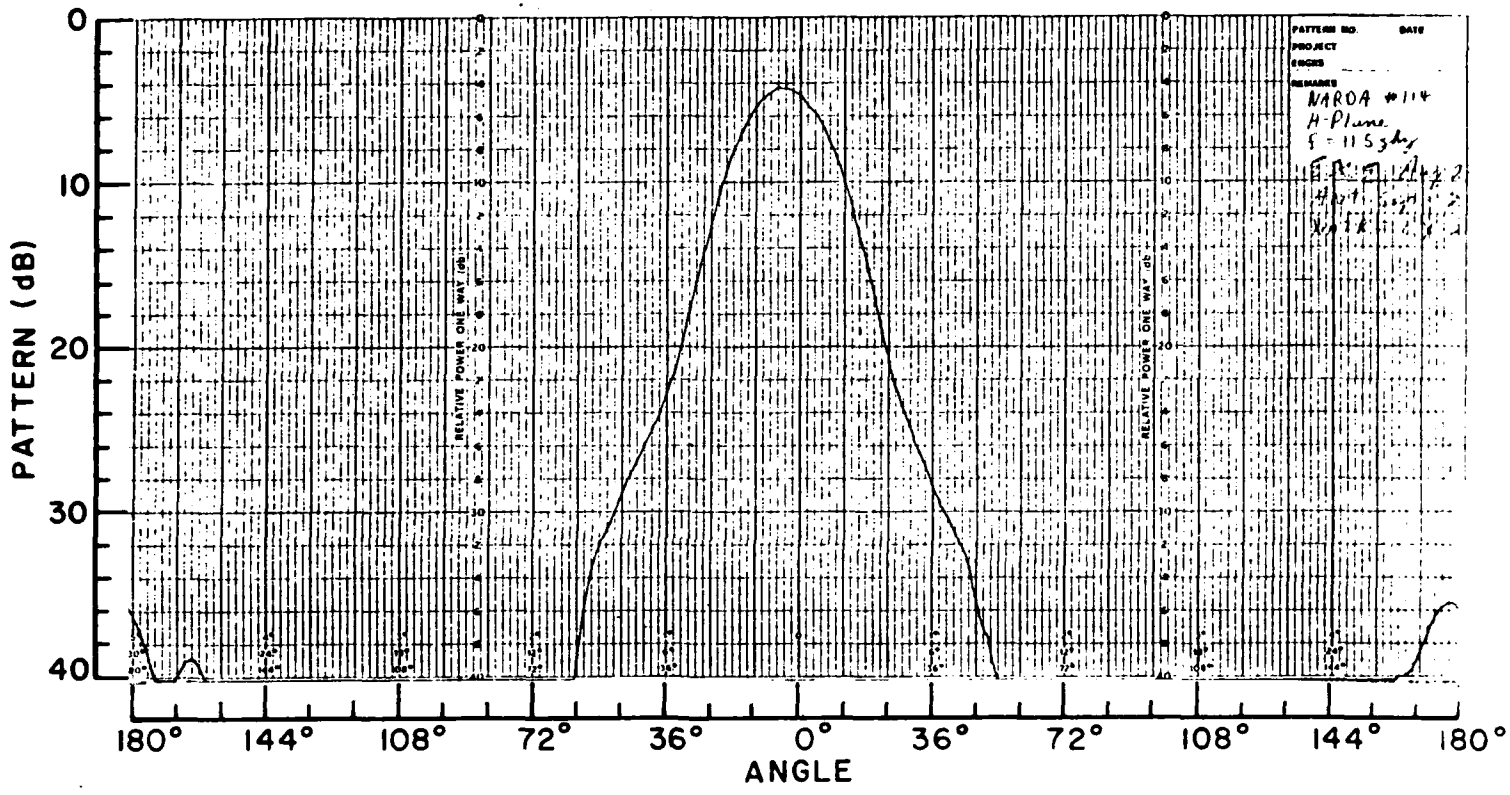

Figure 50. Narda 640.
H-Plane
f = 11.5 GHz

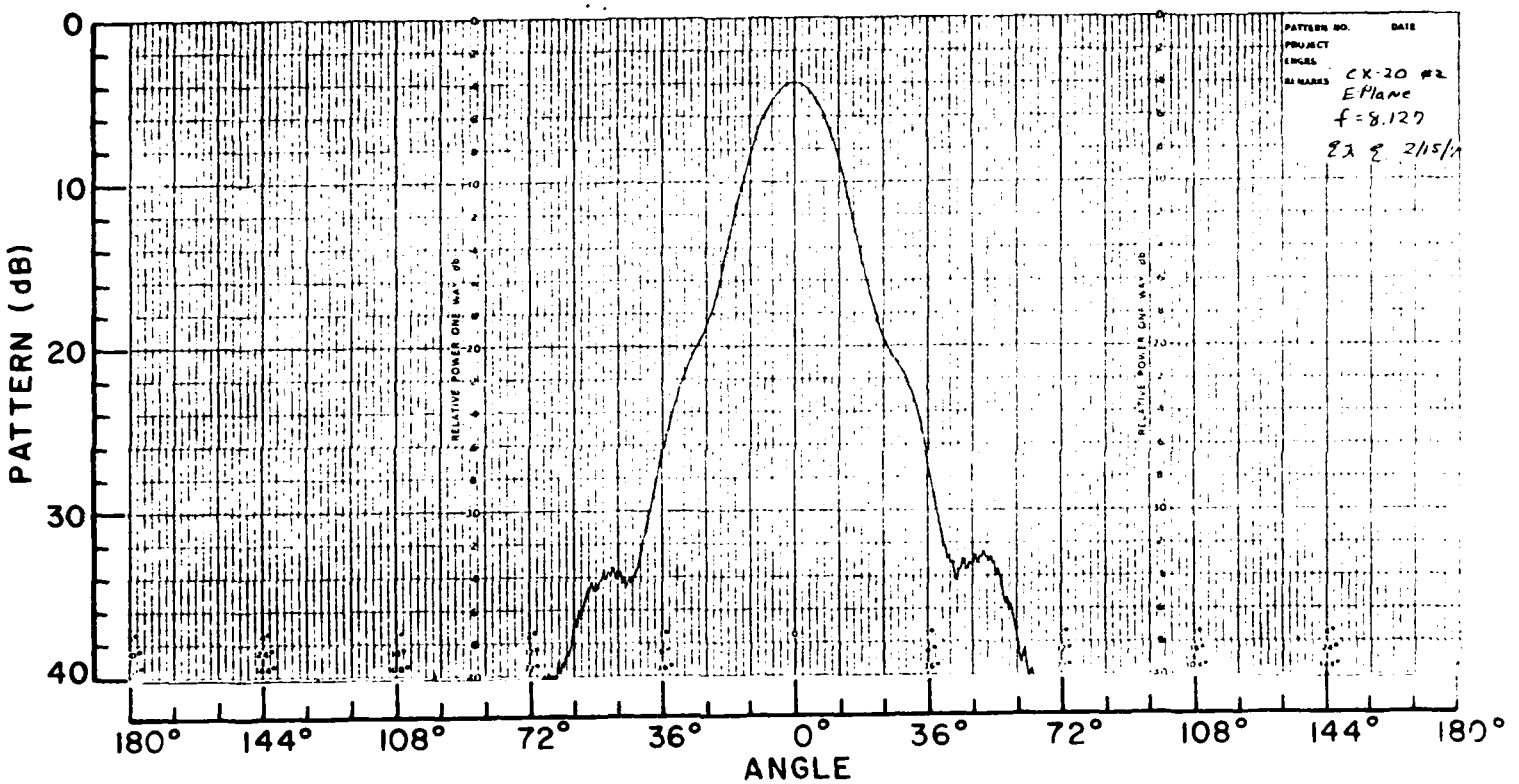

Figure 51. Ladar Systems CX-20
E-Plane
f = 8.1 GHz

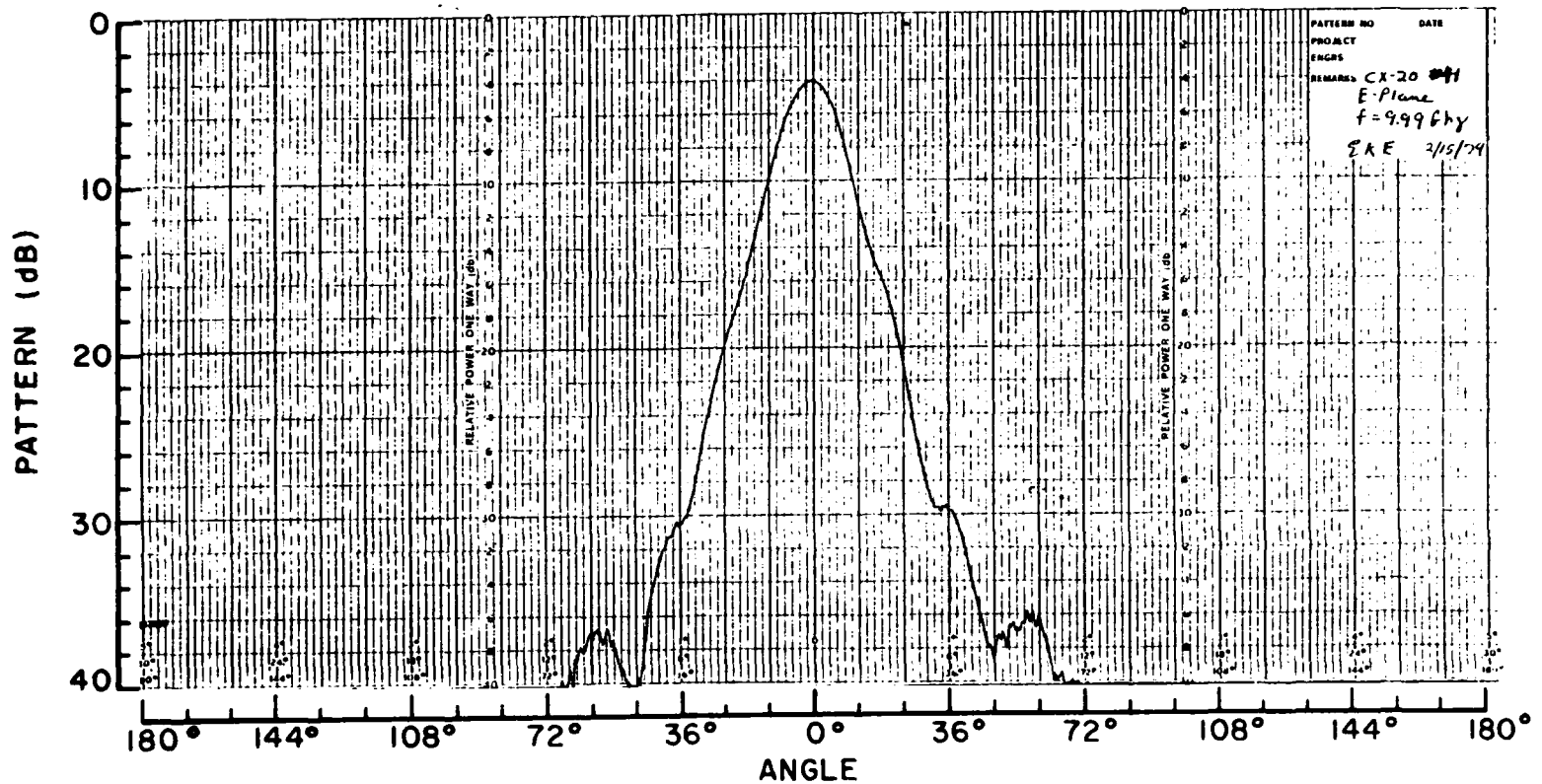

Figure 52. Ladar Systems CX-20
E-Plane
f = 10.0 GHz

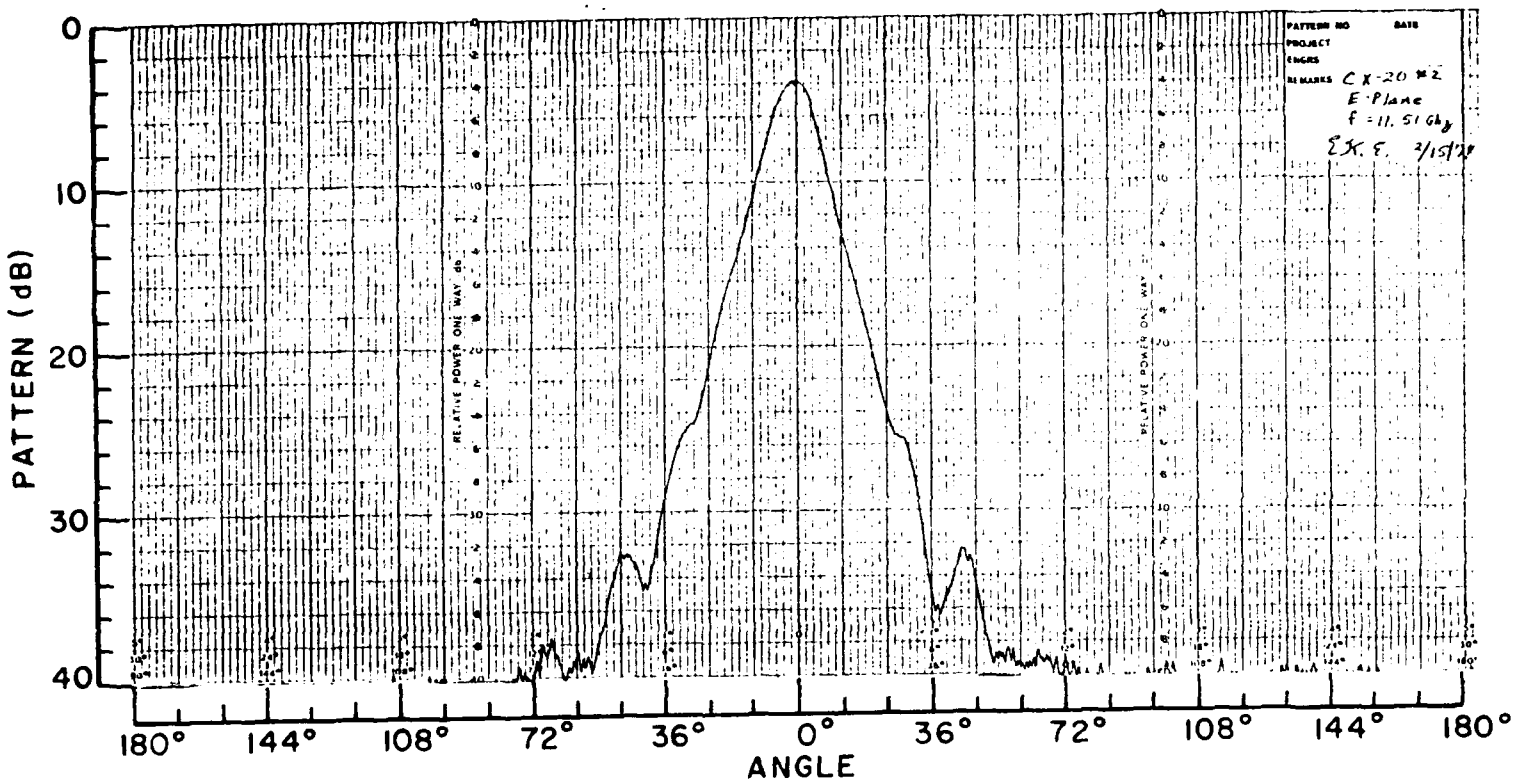

Figure 53. Ladar Systems CX-20
E-Plane
f = 11.5 GHz

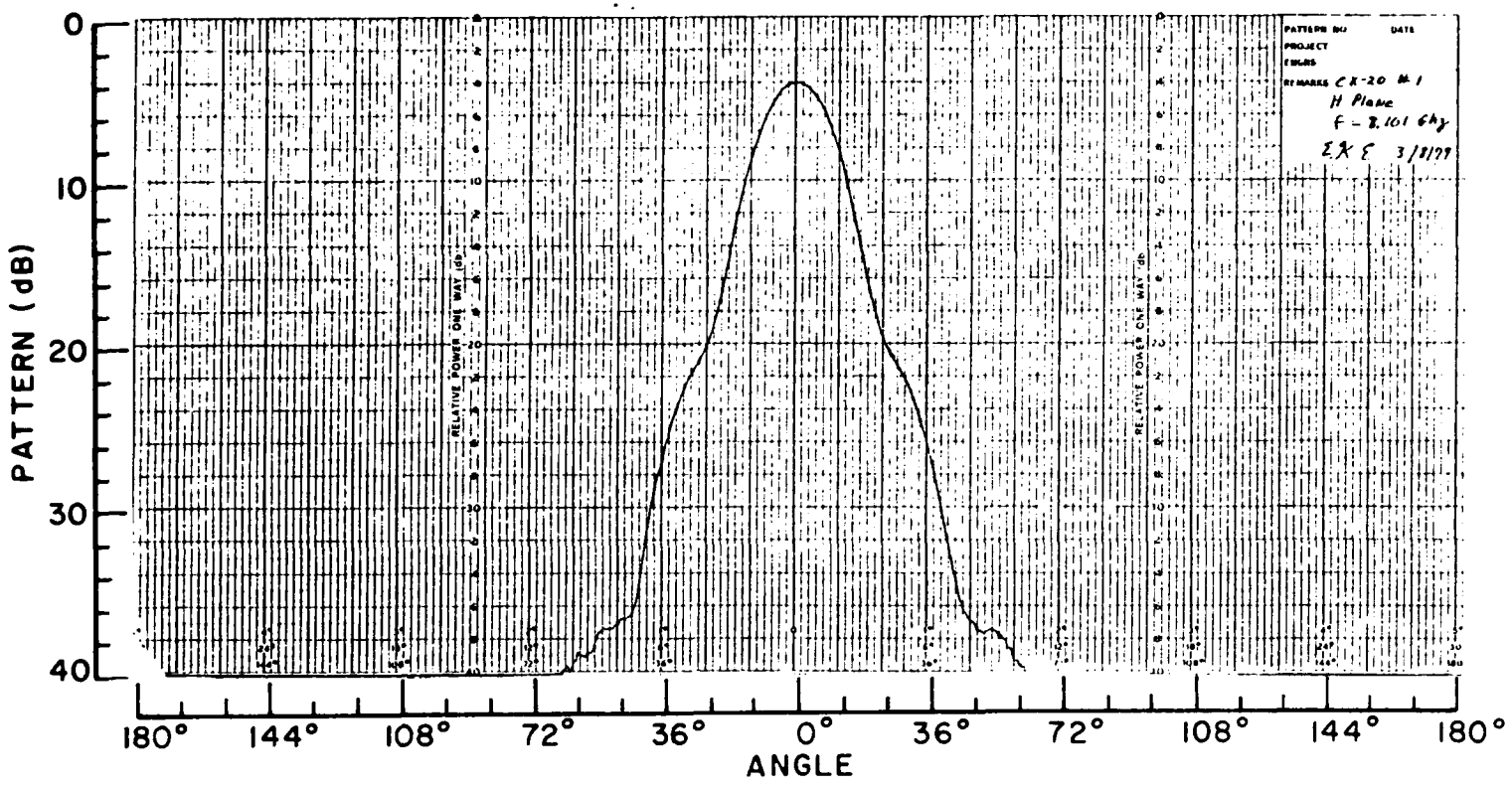

Figure 54. Ladar Systems CX-20
H-Plane
f = 8.1 GHz

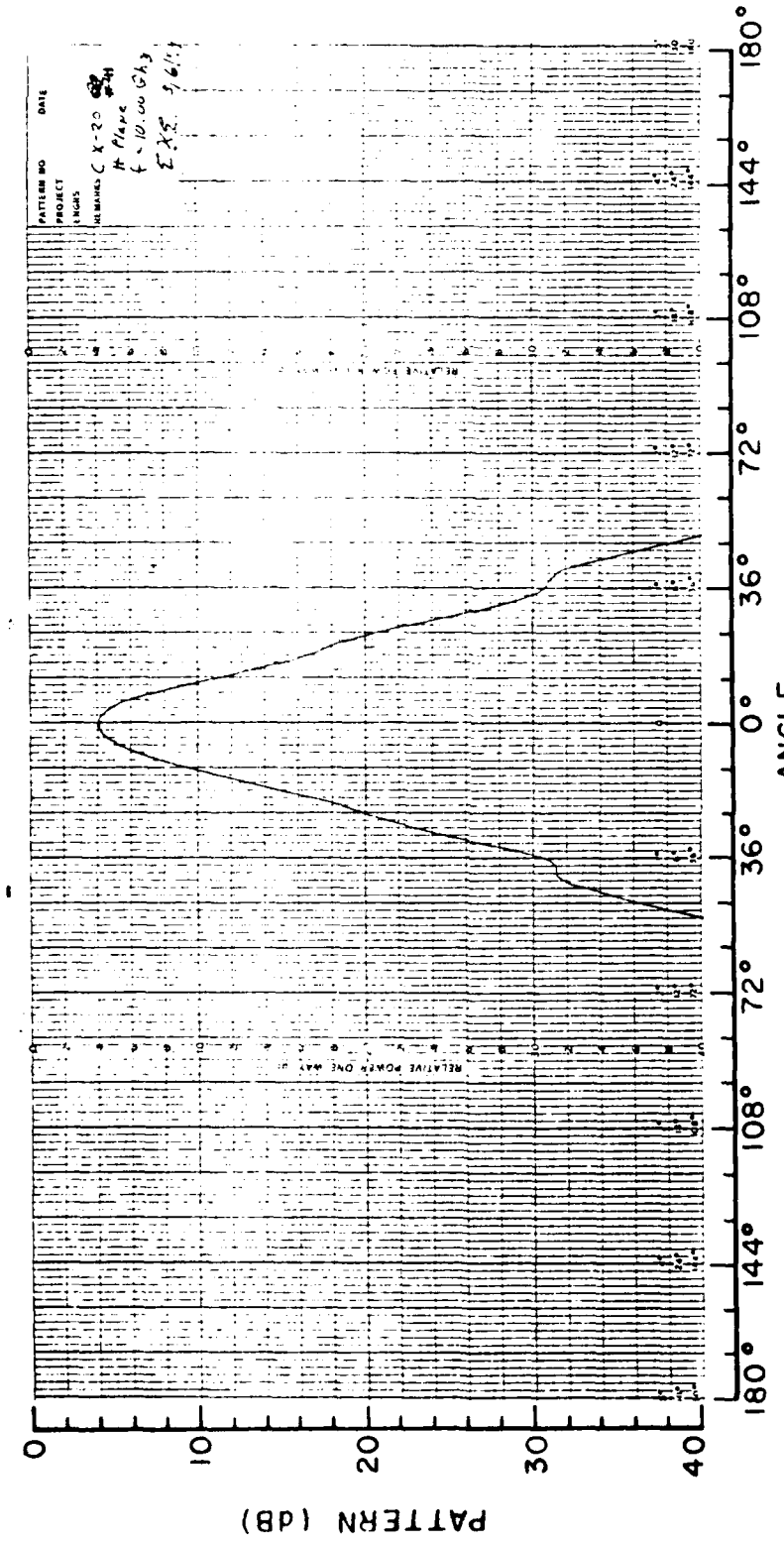

Figure 55. Ladar Systems CX-20
H-Plane
f = 10.0 GHz

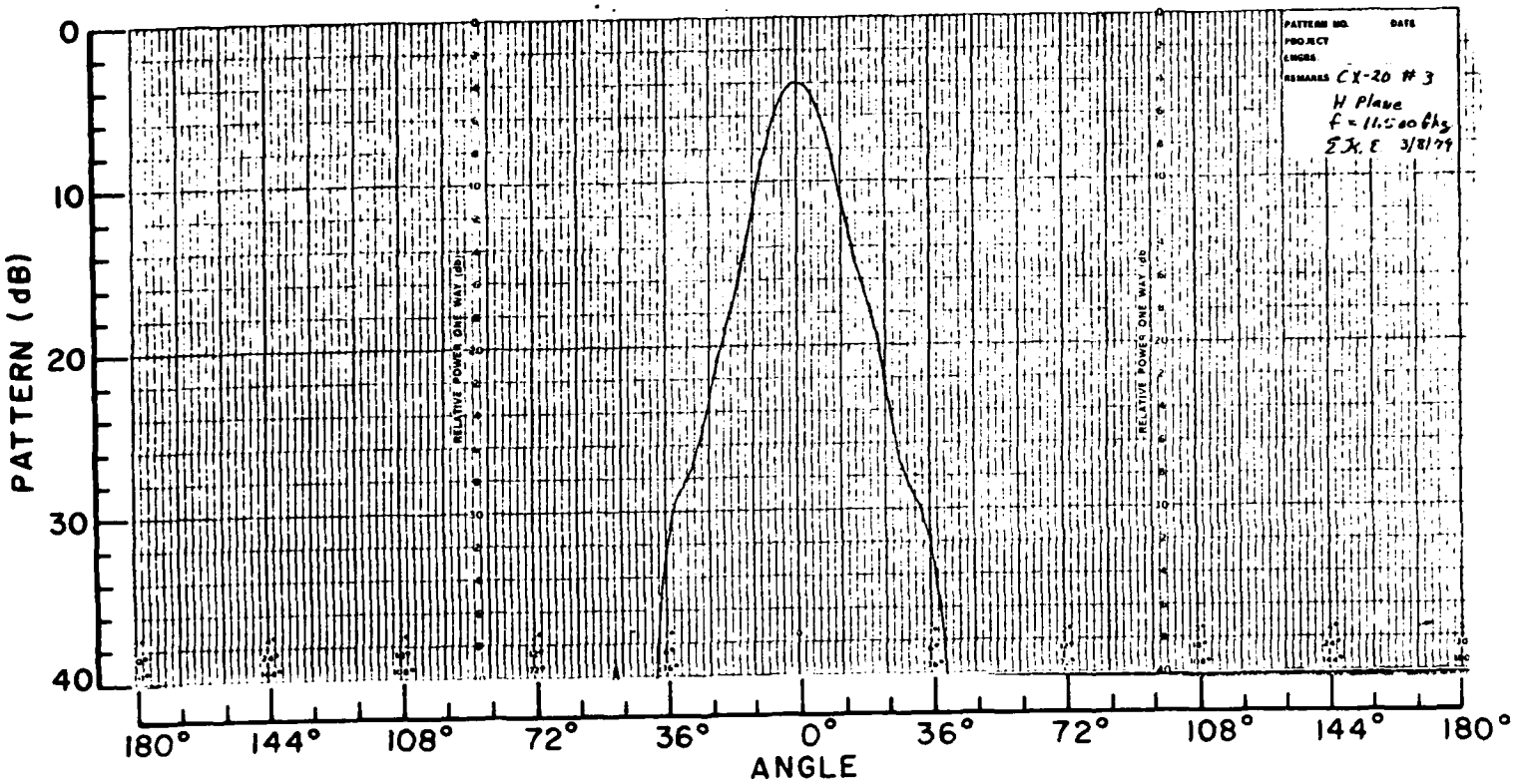

Figure 56. Ladar Systems CX-20
H-Plane
f = 11.5 GHz

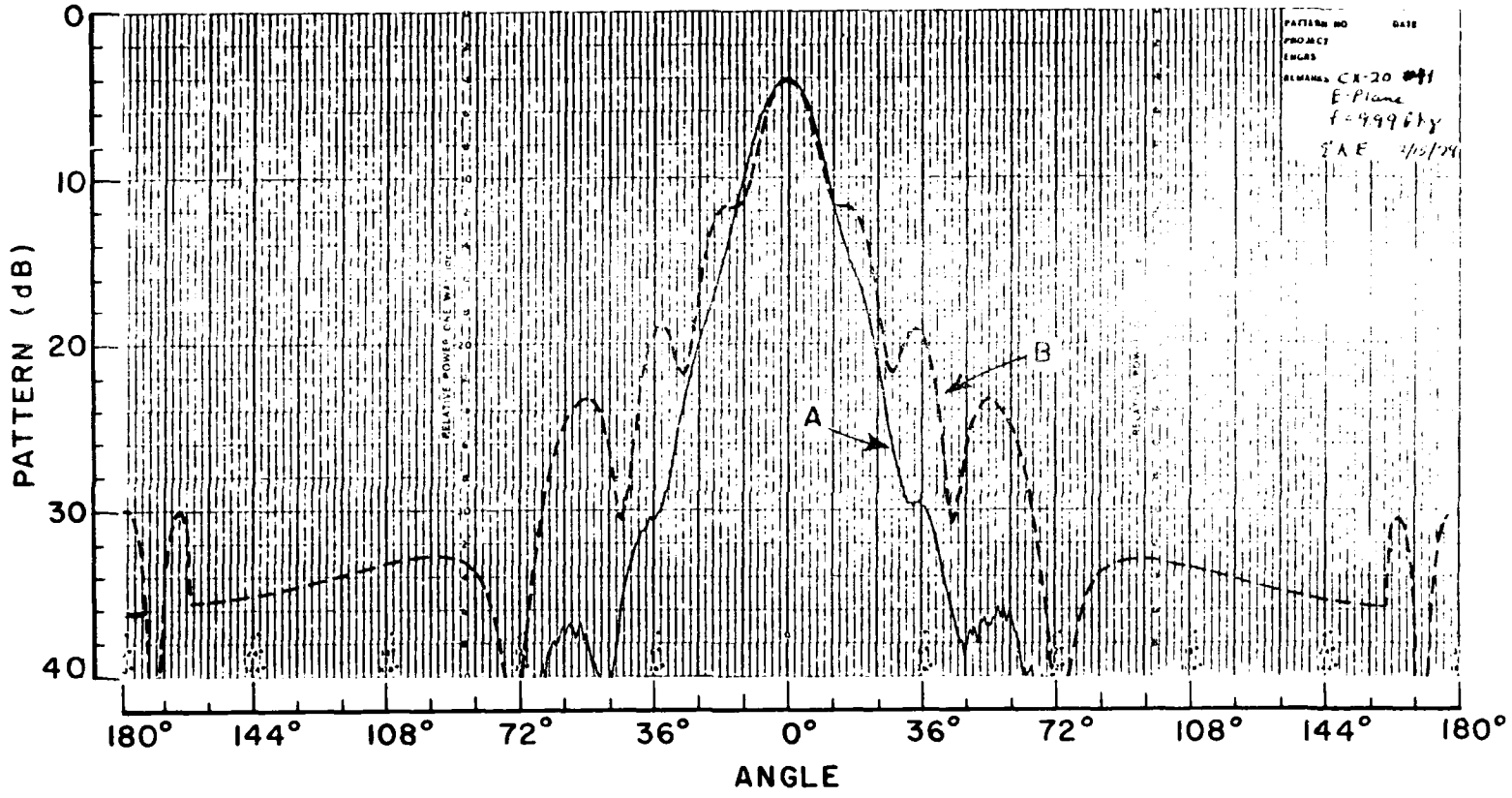

Figure 57. E-Plane Pattern; 10 GHz

a) Ladar Systems CX-20 corrugated horn (measured)
b) Same horn without corrugations (GTD calculation)

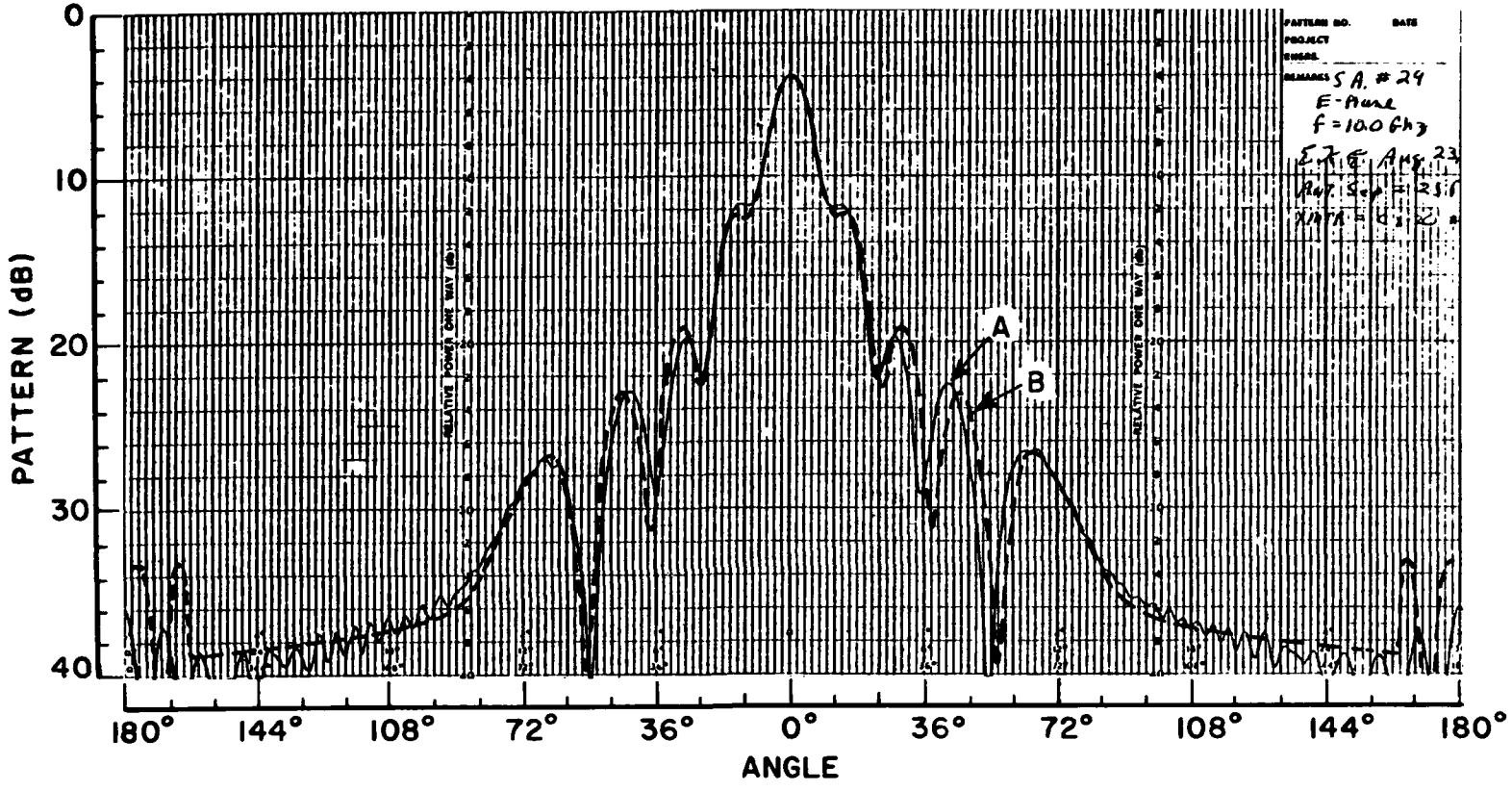

Figure 58. Scientific Atlanta 12-8.2; E-Plane; 10 GHz

a) measured
b) GTD calculation

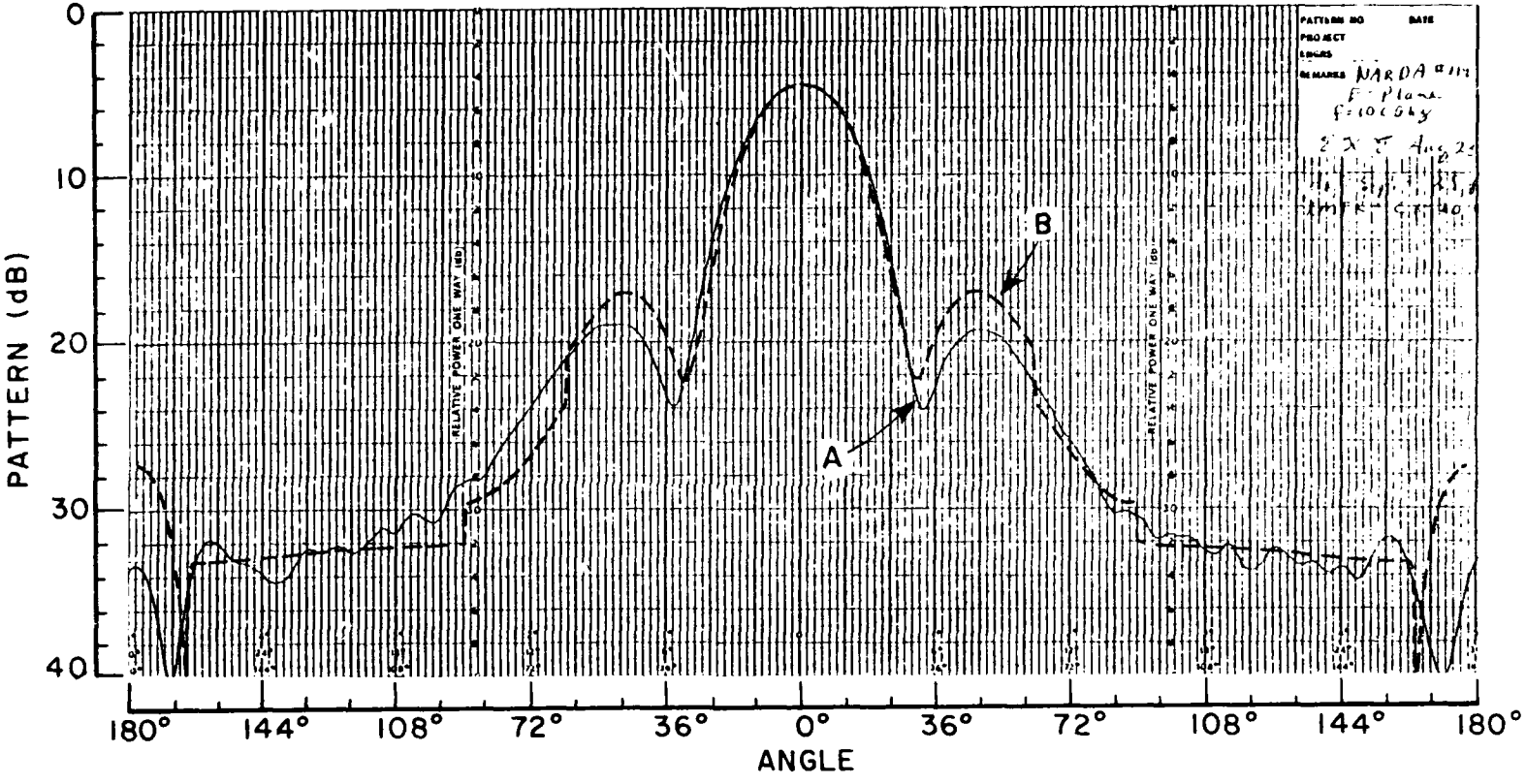

Figure 59. Narda 640; E-Plane; 10 GHz

a) Measured
b) GTD calculation

CHAPTER V
CONCLUSION

There are several factors which contribute to errors in gain measurements for horn antennas. It has been shown that if antenna separation R is taken between apertures instead of the amplitude centers in Friis' transmission formula, rather large errors in gain calculations may be encountered, if near-field corrections are not applied. For example, the Scientific Atlanta model 12-8.2 horn is much more sensitive to this error than is the Narda model 640 horn. This results because the amplitude center of the Scientific Atlanta (at 10 GHz) is approximately 6.58 wavelengths behind the aperture whereas the amplitude center of the Narda is very close to the aperture. Therefore, for many horns (especially long horns), the proper choice of R (separation between amplitude centers) will yield the greatest improvement in gain calculations made from rather close range coupling measurements.

Another problem is horn interaction or standing wave. If antenna coupling is measured only at a few widely separated discrete aperture separations, gain calculations and amplitude center calculations may be widely scattered. This results because some of the coupling points may be at relative maximums, some at relative minimums, and some in between (see Figure 9). This problem is easily resolved by measuring coupling as a continuous function of aperture separation (at least over a few cycles of the ripple) and taking an average as in Figure 9.

Another source of error is that Friis' transmission formula assumes that the transmitting antenna is illuminating the aperture of the receiving antenna with a uniform spherical wave. This is not the case; especially with high-gain horns at rather close separations. This is the reason for introducing the correction factors involving T_E and T_H in Equation (16a) which was developed in Reference [2].

In general, the sources of error presented above are more severe for long, large-aperture, high-gain horns. One advantage of this type of horn is that multipath is less of a problem than it is for low gain (and therefore high side lobe) horns. Obviously, the proper use of absorbing material (preferably cone type) will eliminate most multipath problems. Also, grazing incidence should be avoided. This may be difficult to avoid if coupling measurements are made at large separations when the antennas are only a few feet above

the floor (assuming that the main-beam axes are closer to the floor than the nearest wall). If the floor is closest to the main-beam axes, the use of horizontal polarization will result in less multipath than vertical polarization. This results because there is less radiation to the side in the H-plane (in the direction of the floor) than there is in the E-plane.

Two questions need to be answered: Can the amplitude center of a horn antenna be measured? Can the far-field gain be measured accurately without theoretical corrections? A method of calculating the location of the amplitude center was presented in Chapter III Section A. This method involves only simple calculations suitable for a hand calculator. Using this method, the amplitude centers of three antennas (Scientific Atlanta 12-8.2, Narda 640, and Ladar Systems CX-20) were calculated. The results obtained for the Narda and the Ladar Systems antennas agree very well with theoretical values obtained in [2]. But, the result obtained for the Scientific Atlanta horn did not agree very well with theory until theoretical near-field modifications were applied to the coupling. The reason for this problem is that the Scientific Atlanta model 12-8.2 is a long, large aperture, high-gain horn compared to the other horns tested. Coupling measurements for this type of horn require greater aperture separations to approach far-field conditions. As aperture separations become large, near-field corrections vanish. It would appear that if coupling is measured at sufficiently large horn separations, the amplitude center location could be calculated without any near-field corrections. This is true for the Narda model 640 and Ladar Systems model CX-20 horns. But, this has not been found to be necessarily true for the Scientific Atlanta model 12-8.2 horn. Some of the difficulty here is in controlling coupling measurements at large separations. Therefore, a general rule, applicable to all horns, has not be made concerning a minimum acceptable aperture separation.

Assuming that we have accurate coupling measurements, it has been shown that: 1) with theoretical near-field corrections, very accurate far-field gain calculations may be obtained from relatively close range coupling measurements and 2) without any theoretical near-field corrections, the gain and sometimes the amplitude center of a horn antenna may be accurately and easily computed provided the minimum aperture separation is sufficiently large.

REFERENCES

1. W. C. Jakes, Jr., "Gain of Electromagnetic Horns," Proceedings of the IRE, Vol. 39, February 1951, pp. 160-162.

2. H. H. Chung and R. C. Rudduck, "Near Field Correction Curves for Standard Gain Horn Antennas," Report 711587-1, The Ohio State University ElectroScience Laboratory, Department of Electrical Engineering; being prepared under Contract N00014-76-A-0039-RZ-1 for the 2750'th Air Base Wing/PMR, Specialized Procurement Branch.

3. R. E. Lawrie and L. Peters, Jr. "Modifications of Horn Antennas for Low Sidelobe Levels, IEEE Transactions on Antennas and Propagation, Vol. AP-14, September 1966, pp. 605-610.

4. P. M. Russo, R. C. Rudduck and L. Peters, Jr., "A Method for Computing E-Plane Patterns of Horn Antennas," IEEE Transactions on Antennas and Propagation, Vol. AP-13, March 1965, pp. 219-224.